

INFORMATION TO USERS

This manuscript has been reproduced from the microfilm master. UMI films the text directly from the original or copy submitted. Thus, some thesis and dissertation copies are in typewriter face, while others may be from any type of computer printer.

The quality of this reproduction is dependent upon the quality of the copy submitted. Broken or indistinct print, colored or poor quality illustrations and photographs, print bleedthrough, substandard margins, and improper alignment can adversely affect reproduction.

In the unlikely event that the author did not send UMI a complete manuscript and there are missing pages, these will be noted. Also, if unauthorized copyright material had to be removed, a note will indicate the deletion.

Oversize materials (e.g., maps, drawings, charts) are reproduced by sectioning the original, beginning at the upper left-hand corner and continuing from left to right in equal sections with small overlaps.

Photographs included in the original manuscript have been reproduced xerographically in this copy. Higher quality 6" x 9" black and white photographic prints are available for any photographs or illustrations appearing in this copy for an additional charge. Contact UMI directly to order.

**ProQuest Information and Learning
300 North Zeeb Road, Ann Arbor, MI 48106-1346 USA
800-521-0600**

UMI[®]



Copper Recovery From Wastewater Using an Electrochemical Rotating Barrel Reactor

BY

Abdallah A. Al-Shammari

A Thesis Presented to the
DEANSHIP OF GRADUATE STUDIES

KING FAHD UNIVERSITY OF PETROLEUM & MINERALS

DHAHRAN, SAUDI ARABIA

In Partial Fulfillment of the
Requirements for the Degree of

MASTER OF SCIENCE

In

CHEMICAL ENGINEERING

April 2002

UMI Number: 1409808

UMI[®]

UMI Microform 1409808

**Copyright 2002 by ProQuest Information and Learning Company.
All rights reserved. This microform edition is protected against
unauthorized copying under Title 17, United States Code.**

**ProQuest Information and Learning Company
300 North Zeeb Road
P.O. Box 1346
Ann Arbor, MI 48106-1346**

KING FAHD UNIVERSITY OF PETROLEUM & MINERALS

DHAHRAN 31261, SAUDI ARABIA

DEANSHIP OF GRADUATE STUDIES

This thesis, written by


ABDALLAH A. AL-SHAMMARI


Under the direction of his Thesis Advisor and approved by his Thesis Committee, has been presented to and accepted by the Dean of Graduate Studies, in partial fulfillment of the requirements for the degree of

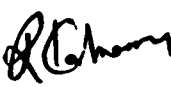
MASTER OF SCIENCE IN CHEMICAL ENGINEERING


Thesis Committee


Prof. Der-Tau Chin (Chairman)


Dr. Saleem-ur-Rahman (Co-Chairman)


Prof. Abdullah A. Shaikh
(Department Chairman)


Dr. Ramazan Kahraman (Member)


Prof. Osama A. Jannadi
(Dean of Graduate Studies)

29/4/2002
Date



Dedicated to
My Loving Parents and Wife

ACKNOWLEDGMENTS

All praise, glory and gratitude be to Allah who said in the Holy Qura'n that "He who taught (the use of) the pen. Taught the man that which he knew not". Acknowledgment is due to King Fahd University of Petroleum & Minerals and Chemical Engineering Department for supporting this research.

I would like to express my extreme appreciation and gratitude to my thesis advisor Prof. Der-Tau Chin for his continuous support and encouragement. It was a great experience working and learning with him. I am also deeply grateful to the other members of my thesis committee, Dr. Saleem ur Rahman and Dr. Ramazan Kahraman for their suggestions and comments.

I would to extend my thanks to Prof. Abdallah Shaikh, Chairman of the Chemical Engineering Department, for his encouragement and help. Thanks are also to Chemical Engineering Department Workshop staff namely, Mr. Kamal Mahgoub, Mr. Mahdi, Mr. Ibrahim and Mr. Romeo for their efforts during the experimental work.

Special and deep thanks to my wonderful parents, wife, brothers and sisters for their invaluable help and motivation. Last, but not least, I extend my thanks and appreciation to my friends, colleagues and everyone who helped directly or indirectly to get this work done.

CONTENTS

	LIST OF TABLES	v
	LIST OF FIGURES	vi
	ABSTRACT (English)	ix
	ABSTRACT (Arabic)	x
Chapter 1	INTRODUCTION	1
Chapter 2	BACKGROUND AND LITERATURE REVIEW	3
2.1	Toxic Metal Sources and Discharge Regulations	3
2.2	Separation Technologies for Metal Removal	4
2.3	Literature Review of Copper Recovery by Electrolysis Process	9
2.4	Rotating Barrel Electrode	12
2.5	Theory of Data Analysis	15
Chapter 3	EXPERIMENTAL	21
3.1	Experimental Setup	21
3.2	Calibration of Copper Ion Selective Electrode	22
3.3	Experimental Procedure	23
3.4	Range of the Control Variables	24
3.5	Difficulty Encountered in the Experiment	24
Chapter 4	RESULTS AND DISCUSSION	34
4.1	General Behavior of Electrolytic Cell for Copper Recovery from Wastewater	34
4.2	Reaction Rate Constant for Copper Deposition at Different Cell Voltages	36
4.3	Effect of Barrel Rotation Speed and Comparison with Mass Transfer Coefficient	37

4.4	Effect of Percent Barrel Loading on Apparent Reaction Rate Constant	40
4.5	Effect of Barrel Tilt Angle and Percent Barrel Immersion on Apparent Reaction Rate Constant	41
4.6	Effect of Anode Surface Area on Cell Performance	41
4.7	Current Efficiency and Energy Consumption for Copper Recovery from Wastewater	42
Chapter 5	CONCLUSIONS AND RECOMMENDATIONS	61
5.1	Conclusions	61
5.2	Recommendations	63
	APPENDIX	64
	NOMENCLATURE	130
	REFERENCES	132

List of Tables

Table No.		Page No.
2.1	Disposal regulation of toxic substances in Saudi Arabia. (ref. Environmental Protection Rules, 1988).	20
3.1	Equipment used in the experiment.	25
3.2	The ranges of variable parameters in the experiment.	26
4.1	Comparison between the apparent reaction rate constant, calculated true reaction rate constant and mass transfer coefficient at different barrel rotating speeds, 4.5 V cell voltage, 50% barrel load and 45° barrel tilt angle.	45
4.2	Current efficiency and energy consumption at different cell voltages.(50% barrel load, 45° barrel tilt angle, 75% barrel immersion and 20 rpm)	46

List of Figures

Figure No.		Page No.
3.1	Photograph of the experimental setup.	27
3.2	Schematic of the electrolytic cell and electric circuit.	28
3.3	Photograph of the electrolytic cell.	29
3.4	Photograph of copper raschig rings used as the cathode.	30
3.5	Photograph showing a stainless steel dangler ball to provide electric contact to copper rings in the electrolysis.	31
3.6	Photograph showing the concentration measurement with copper ion selective electrode and a pH/mV meter.	32
3.7	Sample calibration curve of the selective copper ion electrode.	33
4.1	Copper ion concentration change during the experiment for an experiment run at a cell voltage of 3.5 V, 50 % barrel load, 45° barrel tilt angle and 12 rpm barrel rotational speed. The electrolytic cell contained 14 liter of a simulated wastewater at 24.6 °C.	47
4.2	pH change during the experiment.(The experimental conditions are the same as in Figure 4.1)	48
4.3	Cell current versus experimental time at 3.5V, 50% barrel load, 45° barrel tilt angle and 12 rpm barrel rotational speed.	49
4.4	Effect of cell voltage on the change of copper ion concentration for a series of runs at 50% barrel load, 45° barrel tilt angle and 20 rpm of barrel rotation speed. In all runs, the cell contained 14 liter of a simulated wastewater at 25 °C.	50
4.5	Apparent reaction rate constant versus cell voltage at 50% barrel load, 50% barrel immersion, 45° barrel tilt angle and 12 rpm barrel rotational speed.	51

4.6	Copper particles used as the cathode inside the plating barrel. (a) Particles before electrolysis. (b) Particles after electrolysis with bright deposit under normal operation conditions. (c) Passivated copper particles coated with black $\text{Cu}(\text{OH})_2$ at high applied cell voltages.	51
4.7	A log-log plot of the apparent reaction rate constant versus barrel rotating speed at 3.5 & 4.5 Volts. The other operation conditions are kept constant at 50% barrel load and 45° barrel tilt angle.	53
4.8	Calculated reaction rate constant and the mass transfer coefficient versus barrel rotational speed at 4.5 V, 50% barrel load and 45° barrel tilt angle.	54
4.9	Effect of percent barrel loading on the apparent reaction rate constant at different cell voltages, 45° barrel title angle, 50% barrel immersion and 20 rpm barrel rotational speed.	55
4.10	Effect of percent barrel loading on the effective volumetric reaction rate constant, k_a , at different cell voltages, 45° barrel title angle, 50% barrel immersion and 20 rpm barrel rotational speed.	56
4.11	Effect of barrel immersion angle on the apparent reaction rate constant at a cell voltage of 4.5 V, 50% barrel load, 50% barrel immersion and 18 rpm barrel rotational speed.	57
4.12	Effect of barrel immersion on the apparent reaction rate constant at different barrel loadings, 4.5 V of cell voltage, 30° barrel title angle and 18 rpm barrel rotational speed.	58
4.13	Effect of anode surface area on the apparent reaction rate constant at 4.5 V of cell voltage, 50% barrel load, 30° barrel tilt angle, 50 % barrel immersion and 18 rpm.	59

4.14	Instantaneous current efficiency versus electrolysis time at different cell voltages, 50% barrel load, 45° barrel tilt angle and 20 rpm.	60
-------------	---	-----------

THESIS ABSTRACT

Name: ABDALLAH A. AL-SHAMMARI
Title: COPPER RECOVERY FROM WASTEWATER USING
AN ELECTROCHEMICAL ROTATING BARREL REACTOR
Degree: MASTER OF SCIENCE
Major Field: CHEMICAL ENGINEERING
Date of Degree: *APRIL 2002*

Environmental pollution is a major problem facing us today. The rapid growth and the applications of advanced production technology resulted in high metal contaminants in wastewater streams. This study is concerned with removing toxic heavy metal ions (copper ions) from industrial wastewater prior to its discharge to the waste streams.

In this project, copper ion concentration in a wastewater was reduced from one hundred parts per million (ppm) to less than one part per million and the copper ions were recovered in their metallic form by electrodeposition at the cathode of an electrochemical cell. An oblique rotating barrel, which was partially filled with copper raschig rings, was used as the cathode. The rotating barrel offers a high mass transfer rate and a large cathode surface area for copper electrodeposition.

This thesis presents the experimental measurements of the apparent reaction rate constant of copper deposition reaction at different operation variables. These variables include; cell voltage, barrel rotation speed, percent barrel loading, percent barrel immersion, barrel tilt angle, and anode surface area. The experimental results showed that rate of copper deposition reaction inside the rotating barrel was mass transfer and kinetically controlled. With an operating cell voltage of 2.5 to 5.0 V, the overall current efficiency for copper recovery was 20 to 53 %, and the electric energy requirement was in the range of 4 to 21 kWh per kilogram of copper recovered from the wastewater. These results indicate that the present electrolytic process is economically feasible for large scale industrial wastewater treatment operations.

Master of Science Degree

King Fahd University of Petroleum & Minerals

Dhahran, Saudi Arabia

ملخص الرسالة

الإسم:	عبدالله بن عبدالعزيز الشمري
العنوان:	إسترجاع النحاس من مياه التصريف الصناعي باستخدام مفاعل كهروكيميائي أسطواني نوو.
الدرجة:	ماجستير
التخصص:	هندسة كيميائية
التاريخ:	صفر ١٤٣٣هـ

يعتبر التلوث البيئي من أهم المشاكل التي تواجهنا في هذا العصر. فالزيادة الكبيرة في أعداد السكان و التطبيق المتصاعد لتكنولوجيا التصنيع المتقدمة أسهما في زيادة المواد الملوثة في المياه. هذه الدراسة تركز على إزالة أيونات المعادن الثقيلة (أيونات النحاس) من مياه التصريف الصناعية. حيث يتم إسترجاع أيونات النحاس الموجودة في مياه التصريف عن طريق الترسيب الكهربائي عند القطب الموجب (الكاثود) من الخلية الكهروكيميائية بانقاص تركيزها من مائة جزء لكل مليون جزء من السائل إلى أقل من جزء واحد. القطب الموجب في هذه الخلية مصمم على شكل أسطوانة تدور داخل السائل و مملؤه جزئياً بقطع نحاسية ذات شكل أسطواني مفرغ يمكنها توفير أعلى نسبة انتقال للمادة و كذلك مساحة أكبر للتفاعل الكيميائي.

هذه الدراسة أيضاً تبين القيم التجريبية لثابت معدل تفاعل ترسيب النحاس تحت عدة متغيرات في الخلية الكهروكيميائية. هذه المتغيرات هي : جهد الخلية الكهربائي و سرعة دوران الأسطوانة و نسبة تحميل الأسطوانة و نسبة غمر الأسطوانة و درجة إمالة الأسطوانة و مساحة القطب السالب (الأنود). و كذلك تشير إلى أن تفاعل ترسيب النحاس كهربائياً يتأثر بكيفية انتقال السائل داخل الأسطوانة و بالخواص الكيميائية الحركية للتفاعل ذاته. و أن فعالية التيار الكهربائي خلال الخلية الكهروكيميائية المستخدمة لأسترجاع النحاس تتراوح بين ٢٠ و ٥٣ بالمانه بينما الطاقة الكهربائية اللازمة لتراوح بين ٤ و ٢١ كيلو واط في الساعة لكل كيلو جرام من النحاس المسترجع من مياه التصريف عند جهد كهربائي بين ٢,٥ و ٥ فولت. هذه النتائج تشير إلى أن هذه العملية الكهروكيميائية مجدية اقتصادياً لعمليات معالجة مياه التصريف الصناعي عندما تكون نسبة الملوثات المعدنية كبيرة.

درجة الماجستير في العلوم

جامعة الملك فهد للبترول و المعادن

CHAPTER 1

INTRODUCTION

The presence of metallic contaminants in wastewater streams has been a main source of concern to many process industries. Wastewater containing toxic metal ions, like cadmium, chromium, copper, gold, lead, nickel, and zinc, is generated in large quantities during electroplating, manufacturing of microelectronic parts, mining, and processing of photographic films. In this project, copper ions were recovered from the wastewater in their metallic form by electrodeposition at the cathode of an electrochemical cell. An oblique rotating barrel, which was partially filled with copper raschig rings, was used as the cathode. The rotating barrel offers a high mass transfer rate and a large cathode surface area for the copper electrodeposition.

In this work, experiments were carried out to evaluate if the electrolysis method was able to reduce the copper ion concentration in the wastewater to less than one part per million (ppm) as required by the discharge regulations of wastewater in the Kingdom of Saudi Arabia. Copper electrodeposition reaction is a first order reaction with respect to the copper ion concentration in the electrolyte. The rate constant of copper deposition reaction was calculated by measuring the concentration change of copper ion versus the time at different operation variables, like cell voltage, barrel rotation speed, percent barrel loading, percent barrel immersion, barrel tilt angle, and anode surface area. The current efficiency and the energy consumption of the copper recovery process were calculated by measuring the amount of copper recovered at the cathode and the total electric charges

used in the electrolysis. The results obtained in the present study were compared to the values of a different electrolytic system reported in the open literature.

This thesis report consists of five chapters. Chapter 2 describes the background of wastewater treatment technologies and the literature review of metal recovery by the electrolysis process. The experimental setup and procedures are described in Chapter 3. Chapter 4 discusses the results of copper recovery from wastewater using an electrochemical rotating barrel reactor. Chapter 5 presents the conclusions of this study and the recommendations for future studies. Finally, the appendix shows the tabulated experimental data.

CHAPTER 2

BACKGROUND AND LITERATURE REVIEW

This chapter describes the background and literature review of metal recovery by electrolysis process. First, the wastewater sources that generate large quantities of toxic metal ions are presented. Then, it discusses the separation technologies for metal removal and their advantages and disadvantages. The chapter contains a literature survey of the electrolysis process for recovering copper from the wastewater. The important research done in this field, and its positive and negative aspects are described. This chapter also presents the work done on the rotating barrel as the cathode of electrochemical cell and the method of data analysis.

2.1 Toxic Metal Sources and Discharge Regulations

Wastewater contains toxic metals ions such as cadmium, chromium, copper, gold, lead, nickel, silver, and zinc are generated in large quantities by many chemical and manufacturing processes. The main sources of these toxic metals are:

- Electroplating industries;
- Microelectronic parts manufacturing;
- Mining and metal surface treatment;
- Petroleum refinery;
- Photographic films processes;
- Printing industries;
- Wood preservative industries.

These toxic metals should be removed from the wastewater before discharging to protect the people and the environment. In Saudi Arabia, the discharge regulations have been determined and controlled since 1980. The maximum metal concentrations allowed in industrial effluent are shown in Table 2.1.

2.2 Separation Technologies for Metal Removal

Membrane Separation Technologies

The membrane processes used to remove metals from the wastewater are ultrafiltration, reverse osmosis, and electrodialysis processes. Reverse osmosis and electrodialysis are used to recover plating compounds from rinse water while ultrafiltration needs to be combined with other process to recover metals.

Reverse osmosis involves passing wastewater through a semi-permeable membrane at a pressure greater than the osmotic pressure of dissolved materials in the solvent. Due to this applied pressure, water flows from the concentrated solution to the diluted solution. This process provides a concentrated metal ion solution which needs to be further treated and this is the main disadvantage of the process.

Electrodialysis is a recent technology for the recovery of plating chemicals from rinse solution. Electrodialysis uses an electric field as the driving force to remove charged ionic species from the feed stream. Anion and cation exchange membranes allow anions and cations, respectively, to pass from the feed stream to a concentrated ionic solution. A significant advantage of electrodialysis over reverse osmosis is its ability to

concentrate solutions up to their solubility limit without the need for auxiliary equipment such as evaporators. Its drawback is that it can not be used for metal removal from high concentration solutions.

Extraction

Liquid-liquid extraction involves the separation of a component from waste solution by transferring it to a second liquid. The extractant is immiscible in the wastewater, but exhibits a preferential affinity for the constituent to be removed. Although the liquid extraction is not widely applied in wastewater treatment, it has potential for removing many toxic metals from wastewater. Liquid extraction is particularly attractive in the cases where solutes are present at high concentration levels or when other treatment methods are less effective. The hydrometallurgical copper industry has applied selective extractants that have a high affinity for copper in weak acidic and ammoniacal solutions, while simultaneously rejecting ferric iron.

Adsorption

Adsorption involves the interphase accumulation or concentration of a substance at the surface of a solid adsorbent. The most widely used adsorption methods are carbon adsorption and ion exchange. Activated carbon adsorption involves separation of a substance from one phase (an aqueous solution) and concentrate it at the surface of an activated carbon particles. Activated carbon is widely used for the removal of organic contaminants and it can be successfully achieved for removing many metallic compounds.

Ion exchange has been used commercially to recover metals from wastewater of the metal finishing, electroplating, and fertilizer manufacturing industries. In ion exchange, metal ions from dilute solution are exchanged for ions which are held by electrostatic forces on the surface of an ion-exchange resin. The major applications of ion exchange are water purification and selective removal of toxic heavy metal and metal-cyanide complexes from dilute wastewater streams. The major advantages of this method are:

- i) it enables recycling of process water; and**
- ii) it enables recovery of process chemicals.**

Its disadvantages are:

- i) it provides a concentrated solution which needs to be further treated;**
- ii) it is usually run as a batch process; and**
- iii) it is difficult to find a suitable ion-exchange resin for treatment of a waste solution containing mixed metal ions .**

Electrolytic Processes

An electrolytic cell is the basic device used in electroplating operations. The cell consists of an anode and a cathode immersed in an electrolyte. When the electric current is applied, dissolved metal ions in the electrolyte are reduced and deposited on the cathode. This process is attractive for pollution control because of its ability to remove specific contaminants from the waste stream without the addition of chemicals, which produce large quantities of sludge. In addition, it is possible to reuse the metal which is removed from the solution. Electrolytic treatment is not effective in remove all contaminants. It is most effective in removing the noble metals such as gold and silver

because these metals have positive electrode potentials and they are easily reduced and deposited on the cathode. Other metals like aluminum and magnesium cannot be removed by this process, because their electrode potentials are negative, which favor oxidation rather than reduction. Metals such as copper, tin, lead, nickel, zinc, and cadmium can be removed, but a great amount of current is required especially when the metal concentration is low. Many electrolytic reactors have been designed with electrodes that either enhance mass transfer or have large surface area. Some of the electrode designs are:

- Concentric cylinder;
- Porous plates;
- Rotating cylinder;
- Packed bed;
- Fluidized-bed;

The electrodes used in these reactors may be effective in removing metals from solution but their design may also make it difficult to remove the metal once it has been plated to the cathode. A literature review of the electrolytic process for wastewater treatment is given in section 2.3.

Chemical/ Physical Treatment

The main chemical / physical methods of removal of metallic contaminants from the wastewater are:

- Precipitation (metal hydroxide precipitation)
- Coagulation and flocculation
- Chemical reduction

- Flotation

Metal hydroxide precipitation is the most effective method of removing metals from wastewater by neutralizing the wastewater by adding either NaOH or Ca(OH)₂. This reduces the solubility of metal ions in water and then the metal hydroxide particles settle under gravity in a settling pond where they are removed by filtration . The main advantages of this method are;

- i) it can be applied to many waste streams;
- ii) relatively low energy consumption;

Its disadvantages are :

- i) metals are lost (cannot be recovered in a usable form);
- ii) not applicable to waste with strongly complexed metal ions without pretreatment;
- iii) the filtration sludge is hazardous.

Thermal Treatment

Evaporation and crystallization are the thermal methods of metal removal. Evaporation is a common method used in the chemical process industry to separate materials on the basis of their relative volatilities. In the metal finishing and electroplating industry, evaporation is used to concentrate and recover metals by removing the more volatile and nonmetallic component in the waste which is usually the water. In general, evaporation is not economical for recovery of plating chemicals from dilute rinse water due to the high energy and operation costs. Crystallization is also a recovery technique in

which metal contaminants are precipitated through evaporation, cooling and then removed by settling or centrifugation .

Biological Treatment

Biological treatment includes sulfide precipitation, adsorption, and bioflocculation. The main biological treatment technologies are activated sludge, anaerobic digestion, and algal treatment. The main problem in biological system is the high concentration of heavy metals which are toxic to many micro-organisms and cause serious upsets in the system operation .

2.3 Literature Review of Copper Recovery by Electrolysis Process

As discussed in previous section, metal ion solutions are generally treated by chemical-physical processes such as chemical precipitation and ion exchange. The most utilized treatment is to precipitate heavy metals as hydroxide sludge. This process is simple to operate and its capital and operation costs are low. However, a large quantity of sludge is formed and it has no reuse value and can cause other environmental problems. For these reasons the electrochemical recovery of metal from dilute solution offers several advantages. The most attractive features of this technology are high efficiency, amenability to automation, and the lack of sludge although it needs high energy when the concentration of metals is low in the wastewater.

Different types of electrochemical cell design have been described in the literature for metal recovery since 1930s. Hickman et al. (1933) used the electrolysis for the

recovery of heavy metals from the wastewater of the photographic industries. Cedrone (1956) used a sliver tower to recover silver from photographic fixing solution. In recent years, many publications discussed the effect of shapes and materials of the electrode in addition to the operation variables on metal recovery process (from Zhou 1993).

Bisang (1966) investigated the effect of side reaction, such as reduction of oxygen, on copper deposition on packed-bed electrodes. Fleischmann et al. (1971) used solid copper and copper coated glass spheres as the cathode in a fluidized bed to plate copper onto particles. In 1976, he used a rotating disk electrode to achieve high mass transfer rate and small energy consumption. A flow-through porous electrode was investigated to remove copper ions from the dilute solution theoretically and experimentally by Bennion and Newman (1972). Newman and Trainham estimated the minimum metal concentration attainable with this device in the same year (from Carlo, et al. 1999).

Holland (1978) described an ECO-cell which consisted of concentric cylinders. It had an inner rotating cylinder cathode with a diaphragm and an outer cylinder as the anode. Schore and George (1980) developed a rotating cathode to recover copper and EDTA from electroless copper plating baths. In 1981, Scott described an experimental study of a moving bed of solid metal particles which were used for the electrolytic recovery of copper and other metals (from Carlo, et al. 1999). In the same year, Tison (1981) described the effectiveness for wastewater treatment of a tumbled-bed electrochemical reactor. Copper recovery from a dilute acid copper system was used as the test case for removing toxic heavy metal ions from industrial wastewater. He

presented the overall reactor performance and how it was affected by cathode potential, flow-through rate, and metal ion concentration.

Robertson et al. (1983) studied the removal of copper, silver and gold from the rinse water using electrolysis and compared the results to the ion exchange system. They found that 99 percent of metal can be removed by electrolysis cell and it was less costly to install and maintain than the ion exchange system. Stankovic and Zvonimiv (1983) used a rotary drum electrode to extract copper. Tyson (1984) studied copper recovery and cyanide destruction using fluidized bed electrode (from Zhou, 1993). Howie and Tison (1984) studied the copper recovery rate of a rotating barrel plater when the barrel load was 50 to 70 percent of the barrel volume. This barrel plater combined the desirable features of a tumbled-bed reactor and achieved a threefold increase in volumetric recovery rates. Hinatsu and Foulhes (1991) used the linear-sweep voltammetry and chronopotentiometry for the determination of kinetic parameters for the electrolytic recovery of copper from a simulated acid copper electroplating waste solution. Pletcher et al. (1991-1993) studied mass transport and removal of copper from dilute solution in acidic sulfate media using a reticulated vitreous carbon cathode (from Carlo, et al 1999). Wiaux (1991) carried out an experimental study to recover copper and destroy cyanide using a RETEC-50 cell which used metal mesh as the cathode (from Zhou, 1993). Chin and Zhou (1993, 1994) used a batch and a continuous electrochemical systems consisting of a rotating plating barrel cathode and a packed-bed anode to recover copper and simultaneously destroy cyanide in a waste copper cyanide solution. The cyanide destruction experiments were carried out with and without the addition of NaCl.

Campbell et al. (1994) used a fluidized bed cell and a packed graphite particle cathode to improve the mass transfer for the removal of copper (from Carlo, et al 1999). Szpyrkowicz et al. (1998) carried out a study to optimize the operating conditions for the simultaneous electrooxidation of cyanide and recovery of copper in a dilute rinse wastewater using stainless steel plate electrodes. Carlo et al. (1999) studied the influence of flow rate and initial copper concentration on the removal efficiency and yield for cathodic deposition of copper from an industrial effluent by using titanium and stainless steel plate as cathode materials. Lidia et al.(2000) studied the simultaneous electrooxidation of cyanides and the effect of pH and chloride ion on recovery of copper using a Ti/Pt anode . Chin (2000) used a flow-through electrolytic cell to remove copper from wastewater. The electrolytic cell was in the form of two concentric cylinders. The inner cylinder was a ruthenium oxide coated titanium mesh anode and the outer cylinder was a porous carbon felt cathode pre-coated with a thin layer of copper. Grau and Bisang (2001) examined the performance of an undivided electrochemical batch reactor with a rotating cylinder electrode under potentiostatic control for the removal of cadmium from a sodium sulfate solution.

2.4 Rotating Barrel Electrode

The rotating barrel electrode is a perforated cylindrical basket partially loaded with metal particles to be used as a cathode. In the present work, an oblique barrel was used to remove copper from a dilute waste solution. It was a perforated polypropylene basket having 3 fins along its circumferential direction and 8 fins along its axial direction

on the exterior surface. The barrel was partially immersed in wastewater at an oblique angle from the horizontal position. During barrel rotation, the barrel lifted the metal particles to the top surface, and then they rolled down to the bottom of the barrel causing a series of lift-up and roll-down movements. The fins worked as rotating bucket and provided electrolyte recirculation. The rotating barrel had many advantages. It provided compact and uniformly distributed deposits of recovered metal. It had low energy consumption at high metal concentrated solution and it had low maintenance costs in industrial application. The major disadvantage of the plating barrel was the low recovery rates for a given reactor volume compared to other reactor designs like the packed-bed reactor.

Since 1900, the plating barrel has been used in the metal finishing industry for plating small parts of metals. Many publications were concerned with the design of the apparatus and the preparation for cleaning and pickling of work load. An important research was done by Crawford (from Zhou 1993). He discussed the factors affecting the metal deposition rate like the current density and plated parts geometry. Krejcik (from Zhou 1993) studied the same matter and found that the deposition rate can be increased by the following factors;

- Increasing the terminal voltage in the plating solution.
- Increasing the current to the cathode.
- Enlarging the area of the anode.
- Decreasing the distance between the anode and the cathode.
- Increasing the perforation area on the barrel wall.

Tison (1981) studied copper removal from wastewater using a tumbled-bed electrochemical reactor. He examined the effect of barrel loading, cathodic potential, and the initial copper concentration on the copper recovery rate. Howie and Tison (1984) presented the effect of percent barrel loading and compared the performance of the barrel plater with that of the tumbled-bed and the packed-bed electrode. Chin and Zhou (1993-1994) used a rotating barrel as the cathode to recover copper ions and a packed-bed anode to simultaneously oxidize cyanide from wastewater for batch and continuous systems. They studied the effect of operation conditions, such as cell current, solution temperature, solution feed rate, solution recirculation rate, NaCl concentration, barrel speed and loading on the removal rate of copper and cyanide destruction rate. They found that the effluent total cyanide and metal concentrations decreased with :

- Increasing cell temperature.
- Increasing cell current.
- Increasing NaCl concentration.
- Increasing barrel rotating speed.
- Increasing solution recirculation rate.

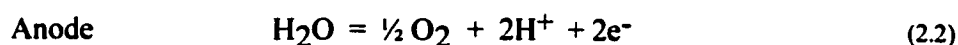
They also found that the energy consumption decreased with increasing cell temperature and decreasing cell current. The optimal barrel loading was 50 percent of the barrel volume. In 1995, Chin and Zhou studied the mass transfer process and particle motion in a plating barrel at different barrel immersed angles and rotation speeds. They observed three kinds of particle motion including slumping, falling, and cascading motion

and described empirical mass transfer correlations that are to be presented in the next section.

Finally, most of the work done in copper removal by electrolysis process were mainly concentrated on the shape of the cathode like fluidized bed, rotating disk, tumbled bed, and metal mesh cathode to get high mass transfer area. Many works were done on a horizontal rotating barrel cathode and they were concentrated on the effect of operating parameters, like solution recirculation rate, solution temperature, cell current, and barrel rotating speed. This study is concentrated on copper removal using an oblique rotating barrel which has not been commonly examined before. The reaction rate constant for copper electrodeposition is measured at different operation parameters like cell voltage, barrel rotating speed, and barrel immersion angles. The present study also evaluated the current efficiency and energy consumption for copper removal from wastewater.

2.5 Theory of Data Analysis

The copper electrodeposition is a first order reaction with respect to copper ion concentration in the wastewater. The cathodic and anodic reactions in the cell are:



By assuming a uniform concentration throughout the solution tank and electrolytic cell,

the following equation is obtained for batch operation:

$$V_{sol} \frac{dC}{dt} = -kAC \quad (2.3)$$

The initial condition is

$$\text{at } t=0, \quad C=C_0$$

The solution of the above equation by integration is:

$$\frac{C}{C_0} = \exp\left(-\frac{kAt}{V_{sol}}\right) \quad (2.4)$$

where C is the concentration of copper ion in the solution (wastewater) at the time t ; C_0 is the initial concentration of copper ion; k is the first order reaction rate constant for the deposition of copper at the cathode; A is the total cathode area (surface area of all copper balls); and V_{sol} is the volume of the solution. However, the actual process is not only kinetic as suggested by Equation (2.3). The copper ions have to diffuse through bulk solution of CuSO_4 to reach the electrode surface where they react to produce metallic copper. The experiment data for copper concentration versus time when plotted as $\ln C$ versus time will allow estimation of k , which will be an overall transfer coefficient, a resultant of mass transfer coefficient and kinetic constant. This is termed as apparent reaction rate constant.

The true reaction rate constant (k_t) is obtained by considering the overall resistance to the reaction rate as the sum of the mass transfer resistance and the true kinetic resistance:

$$\frac{1}{k} = \frac{1}{k_m} + \frac{1}{k_t} \quad (2.5)$$

and

$$k_t = \frac{k_m k}{k_m - k} \quad (2.6)$$

where k_m is the mass transfer coefficient of copper ion at the cathode surface.

The instantaneous current efficiency of the copper electrodeposition reaction at a given electrolysis time can be evaluated by calculating the rate of the change of copper ion concentration (dC/dt) from equation (2.4) and by comparing the value to the cell current (I) at the same electrolysis time according to Faraday's law:

$$\text{Current Efficiency (\%)} = \frac{V_{sol} \frac{dC}{dt}}{\frac{I}{nF}} * 100 \quad (2.7)$$

where F is the Faraday constant (96,500 C/equiv); and n is the number of electrons transferred in the cathode deposition reaction (2 equiv/mol). The average current efficiency is obtained by comparing the mass of copper recovered at the end of the run to the total charge passed during the run according to:

$$\text{Average Current Efficiency (\%)} = \frac{W}{\frac{M}{nF} \int_0^t I dt} * 100 \quad (2.8)$$

where θ is the total electrolysis time during the run; W is the mass of copper deposited at the cathode; and M is the atomic mass of copper (63.5 g/mol).

The energy consumption per kilogram of copper removed from wastewater is calculated by integrating the experimental cell current and voltage curve with respect to the time according to :

$$\text{Energy (kWh/kg-metal)} = \frac{\int_0^{\theta} I E_{\text{cell}} dt}{3600 * 1000W} \quad (2.9)$$

where E_{cell} is the anode-cathode cell voltage; θ is the total electrolysis time in seconds; and W is the mass of copper in kilograms removed from the wastewater.

The rate of copper recovery is either mass transfer or kinetically controlled. It can be examined by comparing the apparent reaction rate constant, k (m/s) to the mass transfer coefficient, k_m (m/s). The mass-transfer coefficient is a function of barrel geometry, barrel operating conditions, and solution properties. It can be calculated according to:

$$Sh = \frac{k_m d_p}{D} = \alpha Re^{\beta} (ScGr)^{\gamma} \quad (2.10)$$

here Sh is Sherwood number and it is a function of Reynolds number (Re) and the product of Schmidt and Grashof numbers ($ScGr$). Reynolds number (Re) is the ratio of inertial force to viscous force, representing the influence of barrel rotational speed on mass transfer :

$$Re = \frac{d_p (d_b \Omega) \rho_l}{\mu} \quad (2.11)$$

The product of Schmidt and Grashof numbers represents the ratio of buoyant force to viscous force:

$$ScGr = \frac{g(\rho_p - \rho_l)d_p^3}{\mu D} \quad (2.12)$$

where D is diffusivity of the copper ions (m^2/s), μ is solution viscosity (kg/ms), Ω is barrel rotational speed (rad/s), d_p is copper particle diameter (m), d_b is barrel diameter (m), ρ_p is copper particle density(kg/m^3), ρ_l is solution density (kg/m^3). The quantities α, β , and γ are empirical coefficients depending on barrel loading, barrel immersion, and barrel tilt angle. Chin and Zhou (1995) obtained empirical correlations for mass transfer to solid cylindrical particles in a rotating barrel.

**Table 2.1. Disposal regulation of toxic substances in Saudi Arabia.
(Environmental Protection Rules,1988)**

Substance		Max. ppm* per Day	Monthly Average of ppm.
Cadmium	Cd	0.5	0.02
chlorine	Cl	---	0.5
Chromium	Cr	2	0.1
Copper	Cu	1	0.2
Cyanide	CN	2	0.5
Lead	Pb	1	0.05
Mercury	Hg	0.01	0.1
Nickel	Ni	2	0.001
Phosphorous	P	---	0.2
Zinc	Zn	10	1

ppm : parts per million.

CHAPTER 3

EXPERIMENTAL

This chapter describes the experiment setup and the construction of the main equipment such as rotating barrel, solution tank, and electrolytic cell. In addition, this chapter describes the experimental procedures, including the preparation of test solution, measurement of copper ion concentration and the range of control variables used in the experiment.

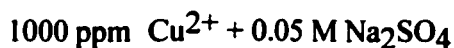
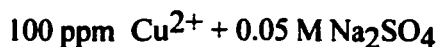
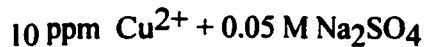
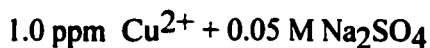
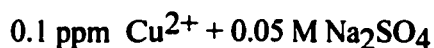
3.1 Experimental Setup

The experimental setup is shown in Figure 3.1. It consisted of an oblique rotating barrel, a rotating motor, a direct current power supply, an ammeter, and a solution tank. The solution tank was a 20 liter rectangular container. It was made of plexiglass with 40 cm in length, 20 cm in width, 25 cm in height, and 1.0 cm in wall thickness. The solution tank functioned as the electrolytic cell as shown schematically in Figure 3.2. Figure 3.3 is a photograph of the electrolytic cell. The cathode in this cell was the oblique rotating barrel that could rotate at different speeds and at different immersion angles. The oblique barrel was 15 cm in diameter and 15 cm in height. It was a perforated polypropylene basket having 3 fins along its circumferential direction and 8 fins along its axial direction on the exterior surface. The barrel was partially filled with copper particles in the shape of Raschig rings as the cell cathode. The copper rings, as shown in Figure 3.4, were 1.0 cm in height, 6.35 mm in outer diameter, and 0.76 mm in wall thickness. They were used to provide a large surface area for the electrodeposition of copper ions from the test solution.

The barrel was driven by a variable speed electric motor and have a speed range of 0-20 rpm. In addition, the electrolytic cell contained 3 graphite plates as the anode. Each plate was 28.5 cm in length, 7.0 cm in width, and 1.0 cm in thickness. The copper rings (the cathode) and the graphite plates (the anode) were connected to the DC power supply as shown in Figure 3.2. The electric contact to the copper rings was made by a stainless steel dangler ball as shown in Figure 3.5. A built in voltmeter in the DC power supply was used to measure the anode-to-cathode cell voltage. An external ammeter as shown in Figure 3.2 was used to measure the electric current to the cell. The experimental equipment specifications are presented in Table 3.1.

3.2 Calibration of Copper Ion Selective Electrode

During the experiment, the concentration of copper ion in wastewater was measured by a copper ion selective electrode and its reading shown as mV on a pH/mV meter (not as ppm Cu). A calibration curve relating the electrode potential (mV) to the concentration of copper (ppm) was needed. This was done by preparing the standard copper solutions whose copper ion concentration differed by a factor of 10 as shown below:



The calibration procedure involved the insertion of the copper ion selective electrode in 50 ml of a standard solution, addition of one milliliter of an ionic strength adjuster (5.0 M NaNO_3) and reading of the electrode potential on the digital pH/mV meter as shown in Figure 3.6. A sample calibration curve showing the concentration of copper ion versus mV reading is given in Figure 3.7.

3.3 Experimental Procedure

First, the holder of the rotating barrel was fixed to a desired angle and the barrel was partially filled with copper rings. The solution tank was filled with 14 liters of distilled water. The motor driving the barrel was switched on and the rotating speed of the barrel inside the water was measured with a stop watch. A simulated wastewater containing about 100 ppm copper ions and 0.05 M Na_2SO_4 was prepared in the solution tank by adding 5.28 grams of copper sulfate ($\text{CuSO}_4 \cdot \text{H}_2\text{O}$) and 85.44 grams of sodium sulfate (Na_2SO_4) into 14 liters of water. The solution was mixed well by using a plastic stirring rod. A 50 ml sample was taken from the solution and the initial copper ion concentration and solution pH were measured with the copper ion selective electrode and a combination pH electrode on the pH/mV meter. Subsequently, the barrel was immersed into the solution and electrolysis was started by applying a constant cell voltage (3-7 V) from DC power supply. At specified time intervals, the cell current, pH and copper ion concentration were measured by using a 50 ml of the solution sample. One milliliter of an ionic strength adjuster (5.0 M NaNO_3) was added to all samples taken for the concentration measurement. The experiment kept running until the copper ion

concentration reduced to less than 1.0 ppm to permit the discharge of the wastewater into the drain system.

3.4 Range of the Control Variables

The main variables and parameters that were changed in the experiments were:

- Cell voltage – anode to cathode voltage (V).
- Barrel loading percent of barrel volume occupied by copper rings (%).
- Barrel rotating speed- in number of revolution per minute (rpm).
- Barrel immersion angle- angle of barrel axis from the horizontal position (degree).
- Barrel immersion – percent of barrel basket volume immersed in water (%).
- Anode surface area, (cm²).

The range of these controlled variables used in the present work are shown in Table 3.2. All experiments were carried out at the room temperature of 25 ± 1 °C.

3.5 Difficulty Encountered in the Experiment

In some experiments, we observed that the copper Raschig rings color changed to black, especially at high cell voltages, when there was excessive hydrogen evolution at the barrel cathode. Also, at low voltages some copper rings located at the bottom edge of the barrel changed to black because they did not move. This issue will be discussed in details in Chapter 4.

Table 3.1. Equipment used in the experiment.

Equipment	Specifications	Model
Rotating Barrel	15 cm diameter, & 15 cm height	Model 60 Sterling system St. Charles, IL., USA
Rotating Motor	0 - 20 rpm	
Rectangular Solution Tank	20 Liter	
DC Power Supply	0-36 V & 0 - 20 A	EA-3033 Elektronisk Labor-Netzgerat, Germany
pH/mV Meter		Cole Parmer #59002-30 Vernon Hills, IL., USA
Selective Metal Ion Electrode	For copper	Cole Parmer 27502-14 Oka Park Avenue, Niles Illinois, USA
Animeter	0-5 A	MR 21 France

Table 3.2. The ranges of variable parameters in the experiment.

Variable Parameters	Values
Cell Voltage (V)	2.5, 3, 4, 5, 6 & 7
Barrel Loading Percentage	15, 25, 50 & 70
Barrel Rotating Speed (rpm)	4, 8, 12, 16, 18 & 20
Barrel Immersion Angle from the Horizontal Position (degree)	15, 30, 45, 60, 75 & 90
Barrel Immersion Percentage	25, 50, 75 & 100
Anode Surface Area (cm ²)	450-1350 for five different anode areas

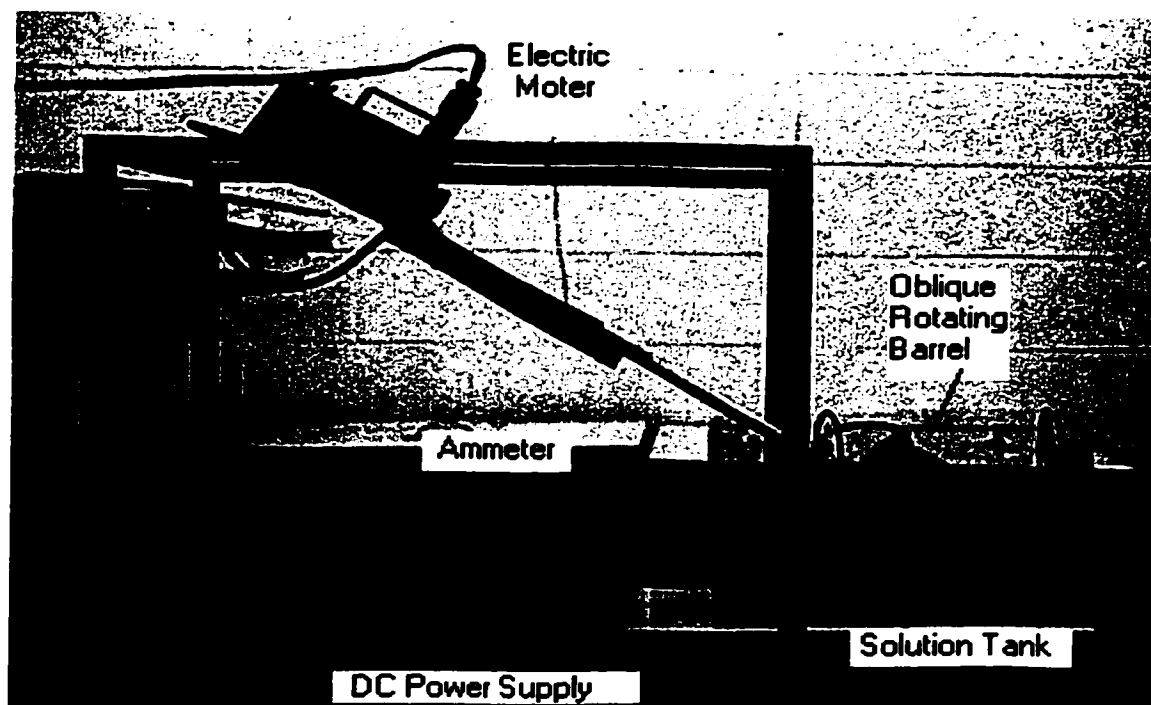


Figure 3.1. Photograph of the experimental setup.

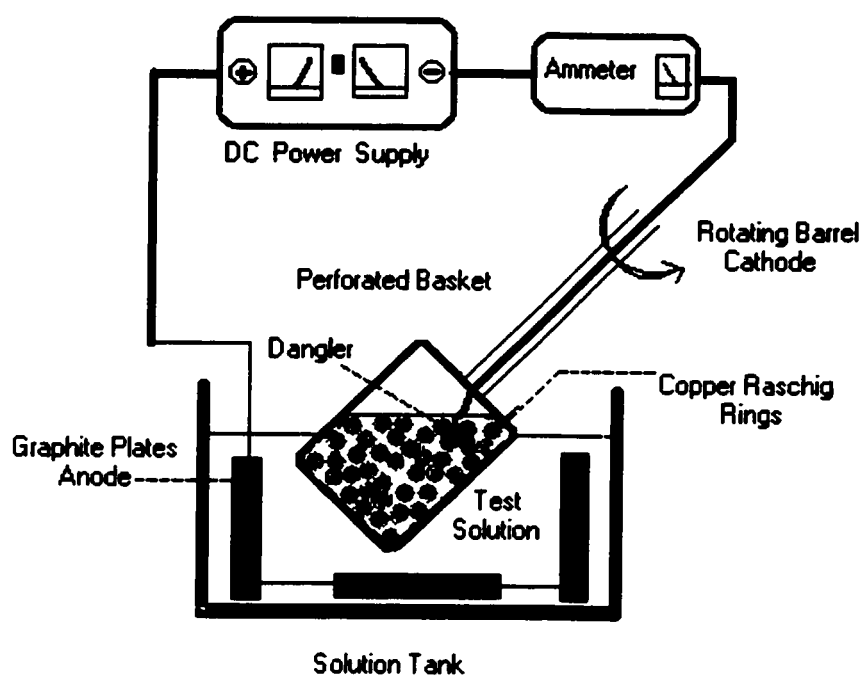


Figure 3.2. Schematic of the electrolytic cell and electric circuit.

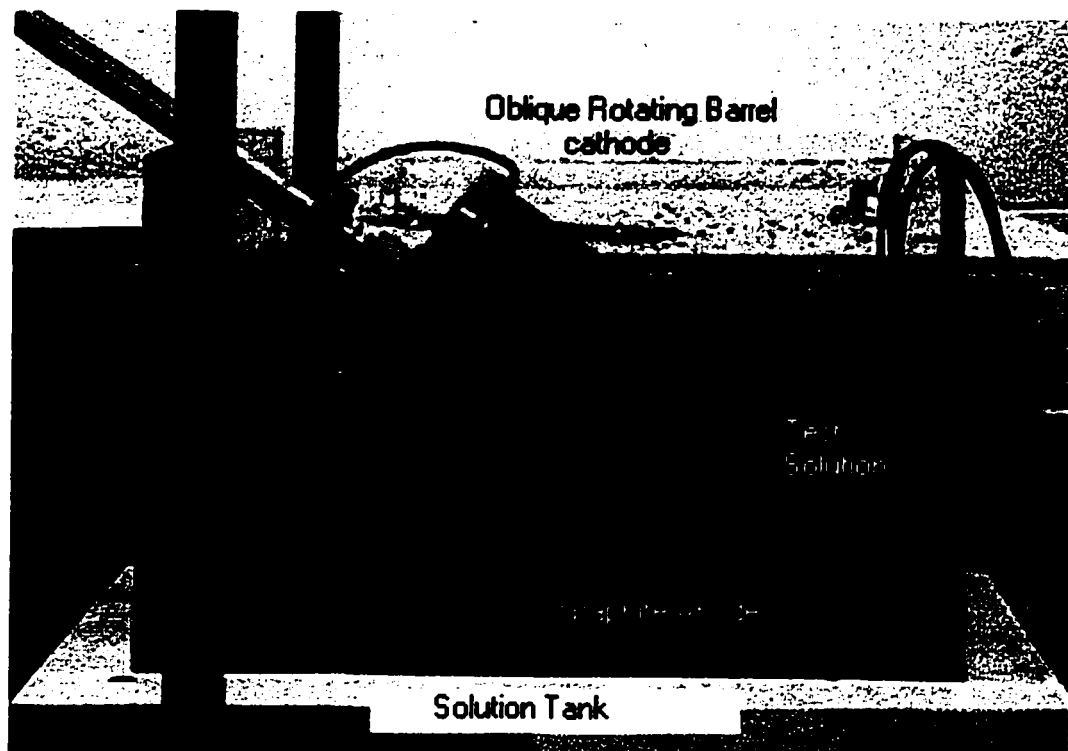


Figure 3.3. Photograph of the electrolytic cell.

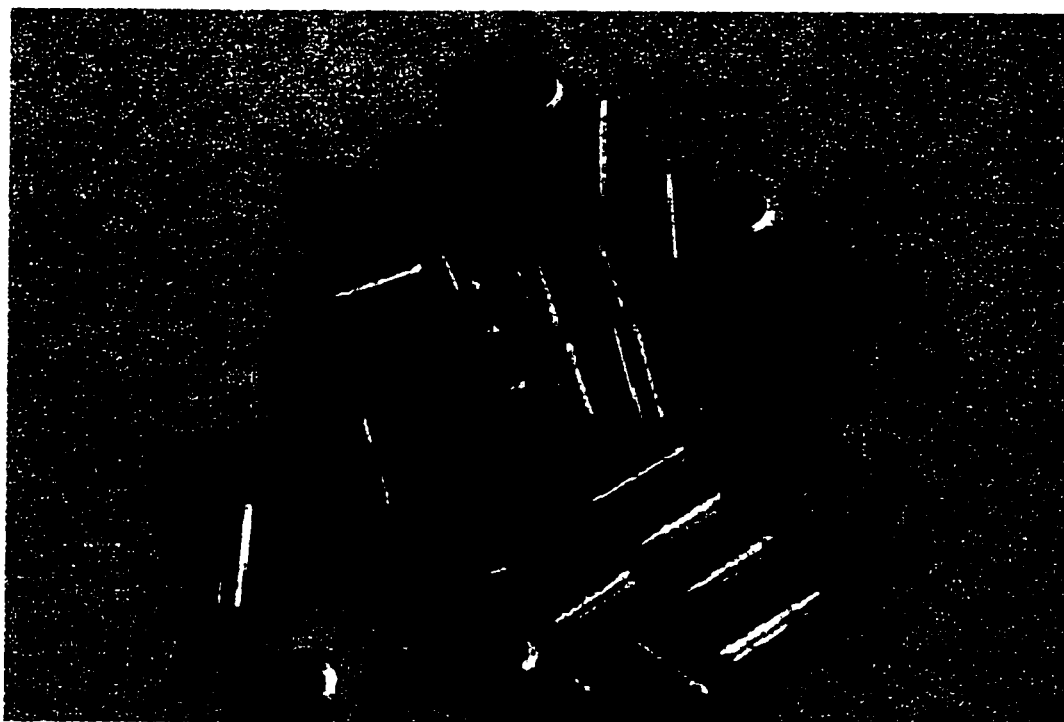


Figure 3.4. Photograph of copper Raschig rings used as the cathode.

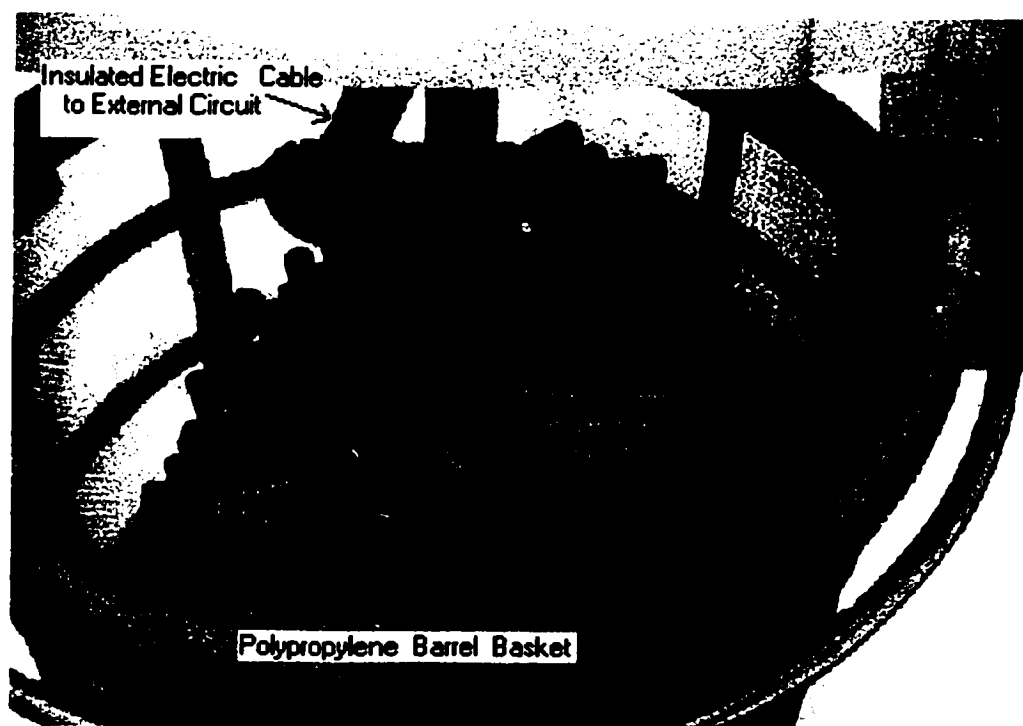


Figure 3.5. Photograph showing a stainless steel dangler ball to provide electric contact to copper rings in the electrolysis.



Figure 3.6. Photograph showing the concentration measurement with copper ion selective electrode and a pH/mV meter.

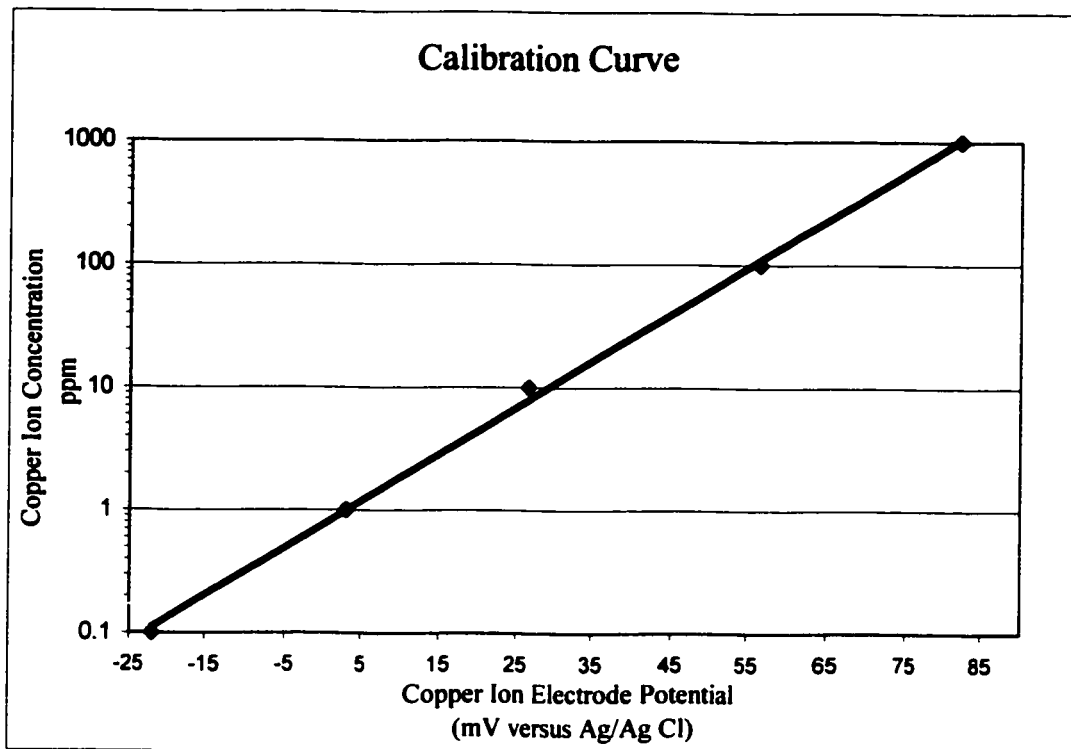


Figure 3.7. Sample calibration curve of the selective copper ion electrode.

CHAPTER 4

RESULTS AND DISCUSSION

This chapter discusses the results of copper recovery from wastewater using an electrochemical rotating barrel loaded with Rasching rings. First, it presents the general behavior of electrolytic cell for copper recovery including the change of copper ion concentration, pH, and cell current during the experiment. Then, it discusses the effect of operation variables on the apparent reaction rate constant. These variables are cell voltage, barrel rotation speed, percent barrel loading, percent barrel immersion, barrel tilt angle, and anode surface area. The reaction rate constant presented in this chapter is mainly the apparent reaction rate constant. The cathode passivation phenomenon is observed at high applied cell voltages and the possible side reactions that caused this passivation are discussed. In addition, this chapter presents the calculated values of instantaneous current efficiency, average current efficiency, and electric energy consumption. The results obtained in this project are compared to the values of a different electrolytic system reported in the open literature.

4.1 General Behavior of Electrolytic Cell for Copper Recovery from Wastewater

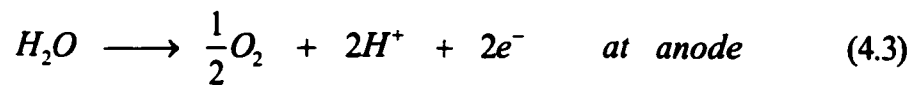
Figure 4.1 is a semi-logarithmic plot describing the experimental relation between copper ion concentration change and the electrolysis time at a cell voltage of 3.5 V, 50 percent barrel loading, 45° barrel tilt angle, and 12 rpm of barrel rotating speed. The initial concentration of the copper ion in the wastewater was 125 ppm. It was reduced to less than 1 ppm after 190 minute of electrolysis to permit the discharge of wastewater into the drain system as required by Saudi government

discharge regulations (Environment Protection Rules,1988). The Figure shows the logarithmic decrease of copper ion concentration in wastewater with the time:

$$\ln C = \ln C_0 - \frac{kA}{V_{sol}}t \quad (4.1)$$

where k is the first order apparent reaction rate constant in m/s for electrode deposition of copper ion at the cathode, A is the cathode surface area in m^2 , V_{sol} is the wastewater volume in m^3 , t is the electrolysis time, C_0 is the initial copper ion concentration in ppm and C is copper ion concentration at any electrolysis time.

Figure 4.2 shows the pH value of wastewater versus the time during the experiment at the same operation conditions of Figure 4.1. At the beginning of the run, the pH value was 5.6 and it started to decrease at a fast rate due to a high copper electrodeposition rate at the cathode, Equation (4.2), and a high rate of water decomposition to O_2 gas and H^+ ions at the anode, Equation (4.3):



The anode reaction of Equation (4.3) released H^+ ions and increased the solution acidity. However, as the electrolysis proceeded, the rate of copper deposition decreased at the cathode due to decreasing copper ion concentration in wastewater.

A main side reaction at the cathode started to occur when the copper deposition rate became small. This side reaction was the reduction of water molecules to H_2 gas and OH^- ions:



The OH^- ions, generated from the above reaction, neutralized H^+ ions produced at the anode, and thus decreased the rate of pH change. The pH became constant, around 3, at the end of the run.

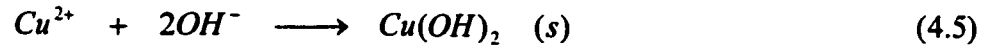
Figure 4.3 shows the cell current change during the experiment at a cell voltage of 3.5 V, 50 percent barrel loading, 45° barrel tilt angle, and 12 rpm barrel rotational speed. The electrolytic cell current decreased from 0.95 to 0.78 A. The current change was small and was linear with time. The cell current increased with increasing the cell voltage.

4.2 Reaction Rate Constant for Copper Deposition at Different Cell Voltages

Figure 4.4 shows the effect of cell voltage on the copper ion concentration in the wastewater at 50 percent barrel loading, 45° barrel tilt angle, and 20 rpm. The rate of decrease of copper concentration increased and the electrolysis time needed to decrease copper concentration to less than 1 ppm decreased with increasing the cell voltage. The apparent reaction rate constant (k) was calculated from the slope of the linear plot of $\ln(C)$ versus time as described in Equation (4.1).

Figure 4.5 is a plot of apparent reaction rate constant versus cell voltage at the same operation conditions as in Figure 4.4. The reaction rate constant increased initially with increasing the cell voltage. However, when the applied voltage was greater than 5V, the reaction rate constant started to decrease due to the formation of black $\text{Cu}(\text{OH})_2$ coating on the cathode surface as shown in Figure 4.6.c. Figure 4.6.a shows copper particles before the electrolysis experiment and Figure 4.6.b shows the

bright deposit on the copper particles after electrolysis with a low cell voltage of less than 5V. At high cell voltage, the side reaction of hydrogen evolution of Equation (4.4) became excessively high and produced a high concentration of OH⁻ ions at the cathode surface. The generated OH⁻ ions reacted with copper ions (Cu²⁺) to form a black layer of Cu(OH)₂ on the copper particles as shown in Figure 4.6.c.



This phenomenon is called cathode passivation. Cathode passivation caused a decrease of the rate of copper deposition in the present cell.

4.3 Effect of Barrel Rotation Speed and Comparison with Mass Transfer Coefficient

The apparent reaction rate constant was affected by barrel rotation speed. Figure 4.7 is a log-log plot of the apparent reaction rate constant versus barrel rotating speed at two cell voltages of 3.5 and 4.5 V, with a 50 percent barrel loading, 50 percent barrel immersion and 45° barrel tilt angle. The apparent reaction rate constant increased with increasing the rotational speed. This indicates that the rate of copper deposition reaction was strongly affected by fluid convection.

The true reaction rate constant (k_t) is obtained by considering the overall resistance to the reaction rate as the sum of the mass transfer resistance and the true kinetic resistance:

$$\frac{1}{k} = \frac{1}{k_m} + \frac{1}{k_t} \quad (4.6)$$

$$k_i = \frac{k_m k}{k_m - k} \quad (4.7)$$

Mass transfer coefficient, k_m , in a plating barrel is related to the Reynolds, Schmidt and Grashof numbers by (Chin and Zhou 1995):

$$Sh = \frac{k_m d_p}{D} = \alpha Re^{0.32} (ScGr)^{0.5} \quad (4.8)$$

$$Re = \frac{d_p (d_b \Omega) \rho_l}{\mu} \quad (4.9)$$

$$ScGr = \frac{g(\rho_p - \rho_l) d_p^3}{\mu D} \quad (4.10)$$

where d_p is the particle diameter, d_b is the diameter of the plating barrel, D is the diffusion coefficient of an active diffusion species, Ω is the barrel rotational speed in rad/s, ρ_p is the density of the particles, and ρ_l and μ are the solution density and viscosity. The quantity α in Equation (4.8) is an empirical coefficient depending on the particle geometry, the percent barrel loading and the barrel tilt angle, θ (in degree). For a 50 percent barrel immersion, Chin and Zhou (1995) obtained α for a barrel with solid cylindrical particles:

for 13 % barrel load,

$$\alpha = 3.5 \times 10^{-4} - 2.89 \times 10^{-4} \sin^{1.43} \theta \quad (4.11)$$

for 25 % barrel load,

$$\alpha = 2.4 \times 10^{-4} - 1.79 \times 10^{-4} \sin^{2.16} \theta \quad (4.12)$$

for 50 % barrel load,

$$\alpha = 1.3 \times 10^{-4} - 6.39 \times 10^{-5} \sin^{1.51} \theta \quad (4.13)$$

At a 50 % barrel load and 45° barrel tilt angle, the value of α as calculated from Equation (4.13), is 8.9×10^{-5} . Equations (4.8) and (4.9) imply a log-log correlation between the mass transfer coefficient k_m and the barrel rotation speed Ω , for a given electrolytic system.

In the present work, the copper particle was in the shape of Raschig ring of 10 mm in height, 6.35 mm in outer diameter, and 0.76 mm in wall thickness. We assume that Equations (4.8)-(4.13) are valid for estimating the mass transfer coefficient on the Rasching rings. The equivalent diameter, as calculated from the following equation, was 6.30 mm:

$$d_p = \left(\frac{6 V_{particle}}{\pi} \right)^{1/3} = \left(\frac{6 \times 133.5 \text{ mm}^3}{\pi} \right)^{1/3} = 6.30 \text{ mm} \quad (4.12)$$

The diffusivity of the copper ion D was taken as $7.2 \times 10^{-10} \text{ m}^2/\text{s}$ (Lobo 1989), the solution viscosity μ was taken as $9.0 \times 10^{-4} \text{ kg/m.s}$ at 25 °C (Lobo 1989), the barrel diameter d_b was 0.15 m, the copper particle density ρ_p was 8954 kg/m^3 , and the solution density ρ_l was 1000 kg/m^3

Figure 4.8 shows a comparison among the apparent reaction rate constant, k , and calculated mass transfer coefficient, k_m , and true reaction rate constant, k_t , at 4.5 V

cell voltage, 50 percent barrel loading, and 45° barrel tilt angle. The numerical values of the calculated true reaction rate constant and the mass transfer coefficient are listed in Table 4.1. The ratio of k/k_m (fraction of mass transfer resistance) varied from 0.69 to 0.54 with an average of 0.59 while the ratio of k/k_t (fraction of true kinetic resistance) varied from 0.31 to 0.46 with an average of 0.41 as shown in Table 4.1. These results imply that the copper electrodeposition in the present cell was mass transfer and kinetically controlled.

4.4 Effect of Percent Barrel Loading on Apparent Reaction Rate Constant

Percent barrel loading was an important factor affecting the copper recovery rate. Figure 4.9 shows the change of the apparent reaction rate constant with percent barrel loading and cell voltages at a 45° barrel tilt angle, 50 percent barrel immersion, and 20 rpm of barrel rotating speed. The reaction rate constant decreased with increasing percent barrel load primarily due to an increase in cathode surface area at large barrel loadings. To avoid this effect of cathode surface area, an effective volumetric reaction rate constant was calculated:

$$ka = k \frac{A}{V_{sol}} \quad (4.15)$$

where A is the total cathode surface area and V_{sol} is the solution volume in the electrolytic cell. The results are plotted against cell voltage in Figure 4.10. The value of ka increased with increasing the percent barrel loading. Both figures show that cathode passivation occurred at high applied cell voltages causing a decrease in the value of the reaction rate constants. This cathode passivation occurred at different cell

voltages depending on percent barrel loading. It was particularly serious at a low barrel loading of 15 percent.

4.5 Effect of Barrel Tilt Angle and Percent Barrel Immersion on Apparent Reaction Rate Constant

Figure 4.11 shows the effect of barrel tilt angle on the apparent reaction rate constant at a cell voltage of 4.5 V, 18 rpm, 50 percent barrel loading, and 50 percent barrel immersion. The reaction rate constant decreased with increasing barrel tilt angle from the horizontal position. The lowest value of reaction rate constant was obtained when the barrel was at a vertical position of 90° due to small mass transfer rate. At the vertical position, there was no tumbling motion of copper particles and poor fluid recirculation inside the barrel, causing a decrease in mass transfer rate.

Figure 4.12 shows the effect of percent barrel immersion on the apparent reaction rate constant at several barrel loadings, 4.5 V cell voltage, 30° barrel tilt angle, and 18 rpm. The rate constant increased with increasing barrel immersion up to 75 % of barrel volume. Then it became constant with further increase in immersion level at 50 % and 70 % of barrel loading. At 25 % barrel loading, the reaction rate constant decreased at high immersion levels due to poor solution circulation inside the barrel.

4.6 Effect of Anode Surface Area on Cell Performance

The effect of anode surface area on the apparent reaction rate constant at constant cathode surface area is presented in Figure 4.13. All the data points shown in the figure were obtained at constant cathode surface area of 5900 cm^2 , 4.5 V cell

voltage, 30° barrel tilt angle, 50 % barrel loading, 50 % barrel immersion, and 18 rpm. It shows an initial increase in reaction rate constant with increasing anode area. The reaction rate constant became nearly constant when the anode area was larger than 1100 cm². The overall cell reaction rate could be controlled either by the surface area of the anode or the cathode. At small anode surface area, the anode controlled the overall cell reaction and thus reduced the reaction rate constant for copper electrodeposition reaction. When the anode area became more than 1100 cm² the anode was not the limiting factor for the overall cell reaction and the reaction rate constant value became constant at the cathode for a given set of operating conditions.

4.7 Current Efficiency and Energy Consumption for Copper Recovery from Wastewater

The instantaneous current efficiency for copper electrodeposition reaction at different cell voltages is shown in Figure 4.14 for a set of runs at 50 percent barrel loading, 50 percent barrel immersion, 45° barrel tilt angle, and 20 rpm. The instantaneous current efficiency was calculated from the rate of copper ion concentration change $\left(\frac{dC}{dt}\right)$ at a given electrolysis time, t , according to:

$$\text{Instantaneous Current Efficiency \%} = - \frac{V_{sol}}{I} \frac{dC}{dt} \times 100 \quad (4.16)$$

The quantity $\left(\frac{dC}{dt}\right)$ was evaluated by differentiating Equation (4.1):

$$\frac{dC}{dt} = \frac{-kAC}{V_{sol}} \quad (4.17)$$

At the beginning of the experiment, the instantaneous current efficiency was around 100 percent due to a high copper ion concentration (around 100 ppm). As the

electrolysis proceeded, the current efficiency decreased logarithmically due to decreasing copper ion concentration in the cell. At the end of the experiment, the current efficiency was reduced to around 1 percent. Figure 4.14 also shows that the instantaneous current efficiency decreased with increasing cell voltage.

The average current efficiency was obtained by comparing the mass of copper recovered from wastewater at the end of the run to the total charge passed during the run as:

$$\text{Average Current Efficiency (\%)} = \frac{W}{\frac{M}{nF} \int_0^{\theta} Idt} \times 100 \quad (4.18)$$

The quantity W is the mass of copper (kg) recovered at the cathode according to:

$$W = \frac{m_{sol}(C_o - C_f)}{10^6} \quad (4.19)$$

where m_{sol} is the total mass (kg) of wastewater in cell; C_o and C_f are the initial and the final copper ion concentrations in ppm. Table 4.2 summarizes the results of average current efficiency at four different cell voltages. The average current efficiency decreased with increasing cell voltage.

The table also shows the energy consumption per kilogram of copper removed from wastewater. This was calculated by integrating the experimental cell current and voltage with respect to the time according to:

$$\text{Energy ((kWh / kg - copper))} = \frac{\int_0^{\theta} IE_{cell} dt}{3600 \times 1000 \times W} \quad (4.18)$$

The electric energy consumption increased with increasing cell voltage and it varied from 4.0 kWh/kg-Cu at 2.5 V cell voltage to 20.7 kWh/kg-Cu at 5 V. These results are close to reported values of 11.3 kWh/kg-Cu at 3 V to 17.7 kWh/kg-Cu at 5 V using flow through porous carbon cathode (Chin 2000).

Table 4.1. Comparison between the apparent reaction rate constant, calculated true reaction rate constant and mass transfer coefficient at different barrel rotating speeds, 4.5 V cell voltage, 50% barrel load and 45° barrel tilt angle.

Barrel Rotating Speed (rpm)	Apparent Reaction Rate Constant k (m/s)	True Reaction Rate Constant k_t (m/s)	Mass Transfer Coefficient k_m (m/s)	k/k_t	k/k_m
20	1.12×10^{-5}	2.43×10^{-5}	2.08×10^{-5}	0.46	0.54
18	1.38×10^{-5}	4.40×10^{-5}	2.01×10^{-5}	0.31	0.69
16	1.15×10^{-5}	2.82×10^{-5}	1.94×10^{-5}	0.41	0.59
12	9.92×10^{-6}	2.26×10^{-5}	1.77×10^{-5}	0.44	0.56
8	8.97×10^{-6}	2.13×10^{-5}	1.55×10^{-5}	0.42	0.58
4	7.07×10^{-6}	1.64×10^{-5}	1.24×10^{-5}	0.43	0.57
Average					
				0.41	0.59

Table 4.2. Current efficiency and energy consumption at different cell voltages.(50% barrel load, 45° barrel tilt angle, 75% barrel immersion and 20 rpm)

Cell Voltage (V)	Average Cell Current (A)	Total Time of Experiment (min)	Initial Copper Concentration (ppm)	Final Copper Concentration (ppm)	Mass of Copper Recovered (g)	Average Current Efficiency (%)	Consumed Electric Energy (kWh/kg-Cu)
2.5	0.55	175	95	2.6	1.29	53.0	4.0
3	0.85	225	97	1	1.34	35.7	7.1
4	1.45	200	113	0.9	1.5	27.6	13.3
5	1.84	180	113	0.7	1.5	20.0	21.4

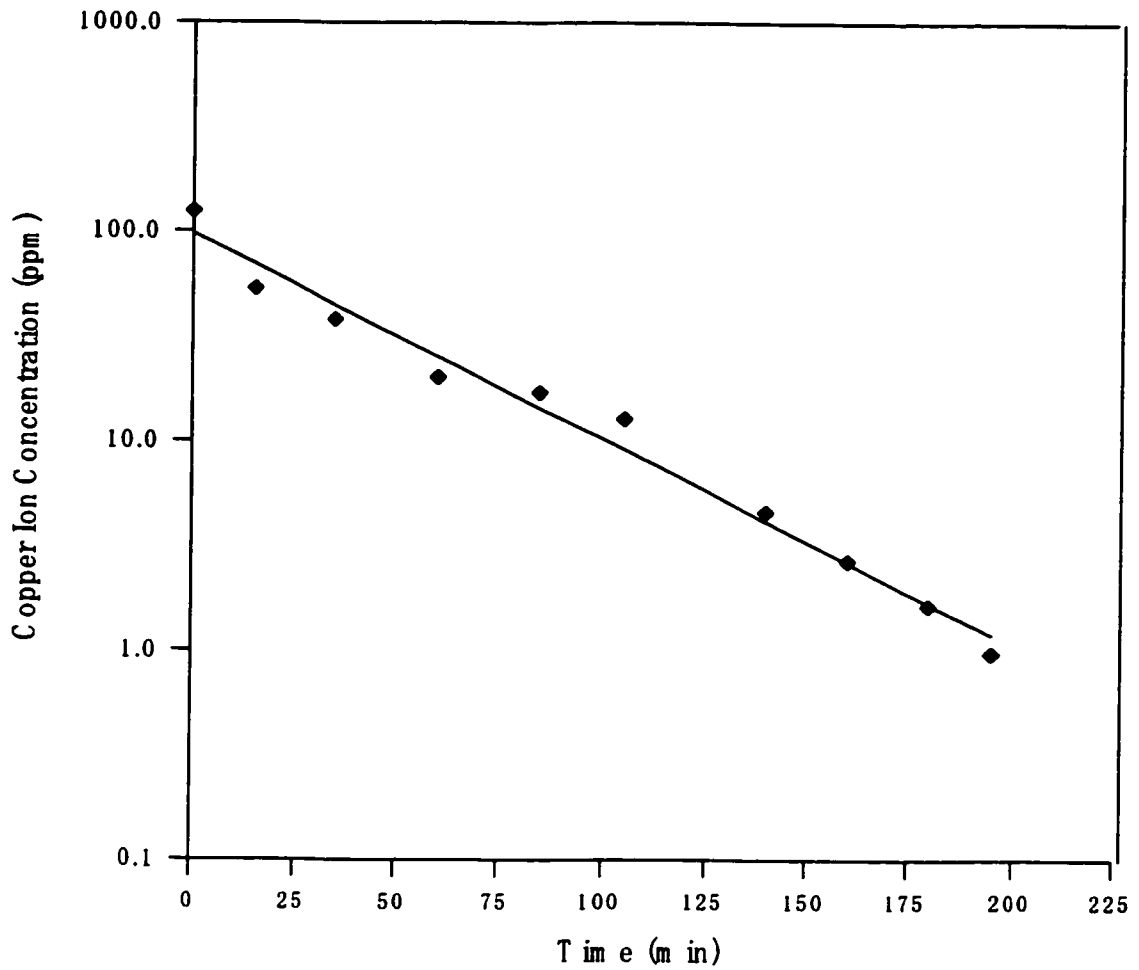


Figure 4.1. Copper ion concentration change during the experiment for an experiment run at a cell voltage of 3.5V, 50% barrel load, 45° barrel tilt angle and 12 rpm barrel rotational speed. The electrolytic cell contained 14 liter of a simulated wastewater at 24.6 °C.

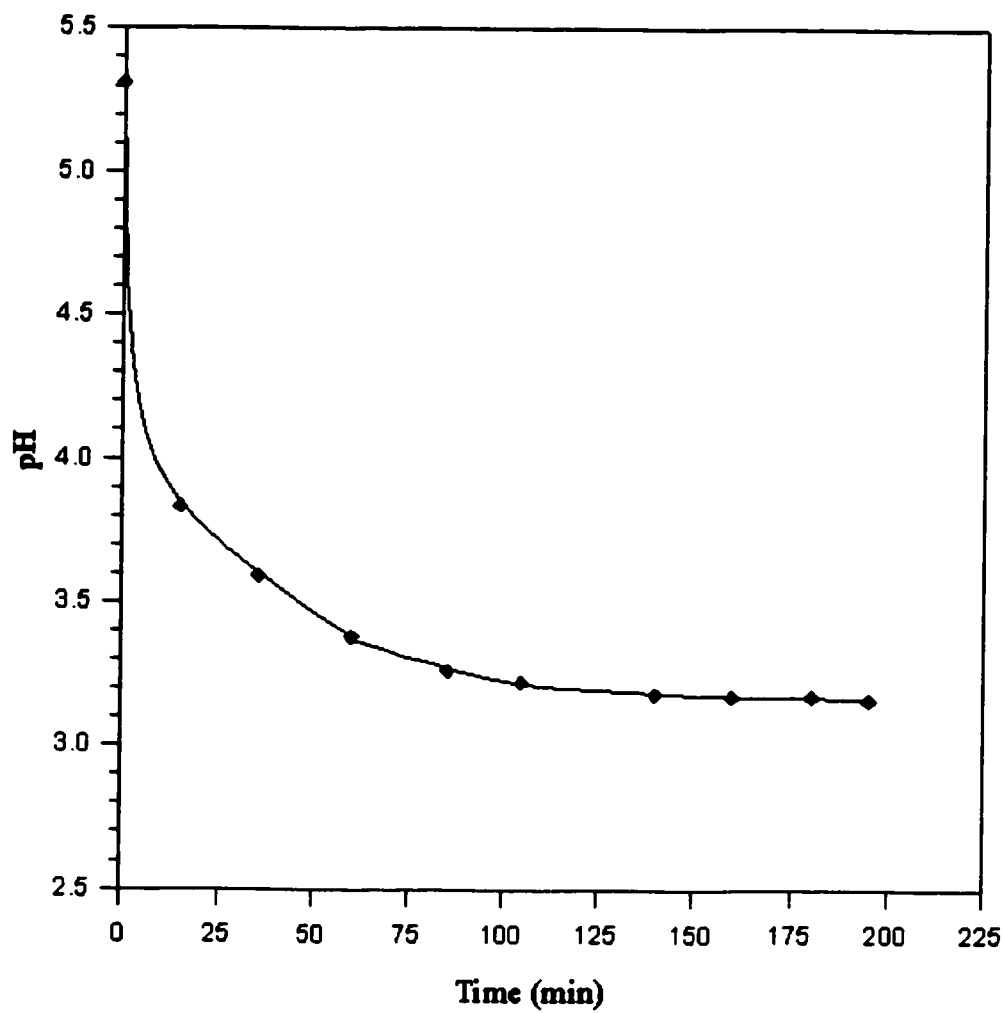


Figure 4.2. pH change during the experiment. (The experimental conditions are the same as in Figure 4.1)

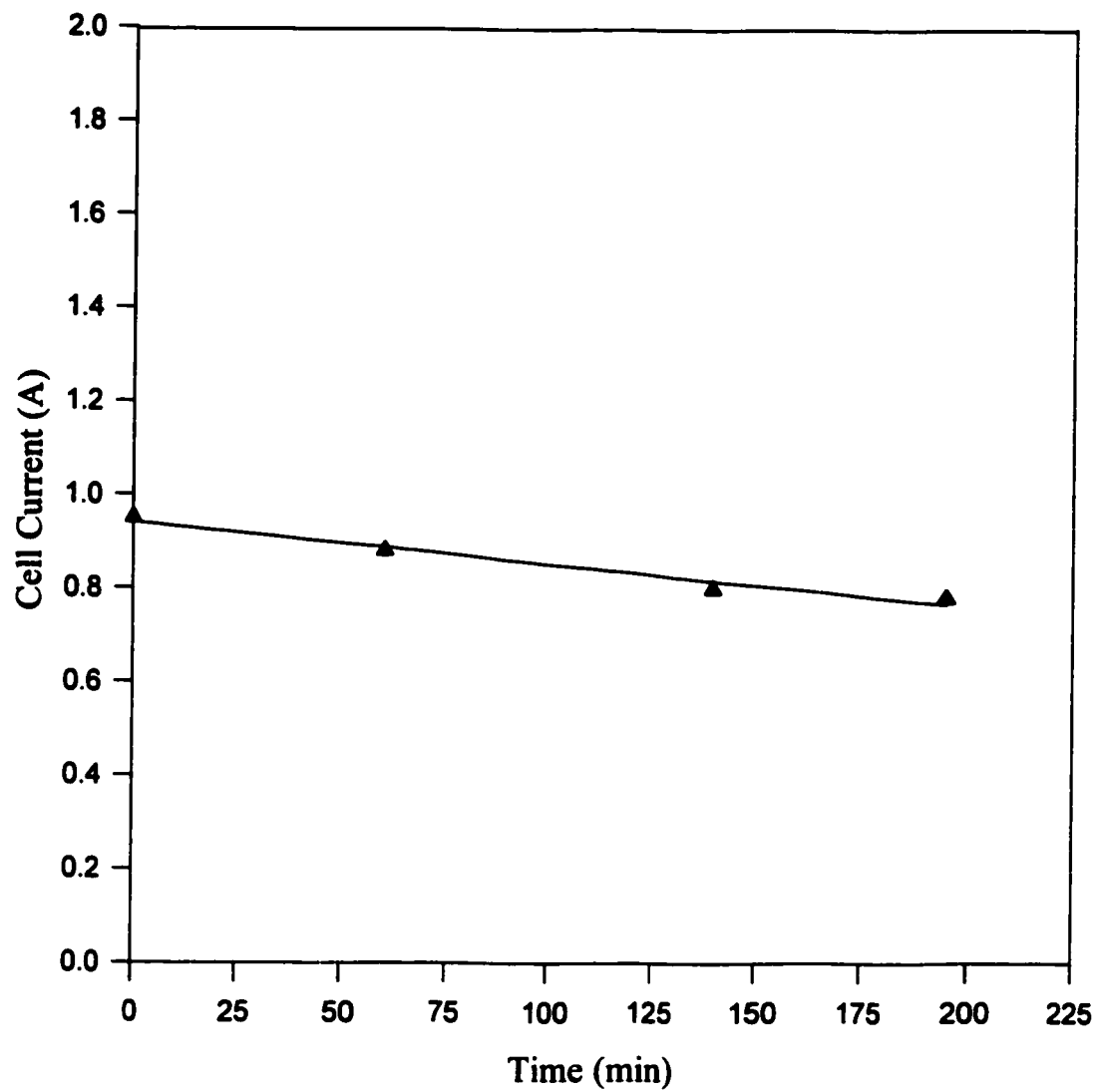


Figure 4.3. Cell current versus experimental time at 3.5V, 50% barrel load, 45° barrel tilt angle and 12 rpm barrel rotational speed.

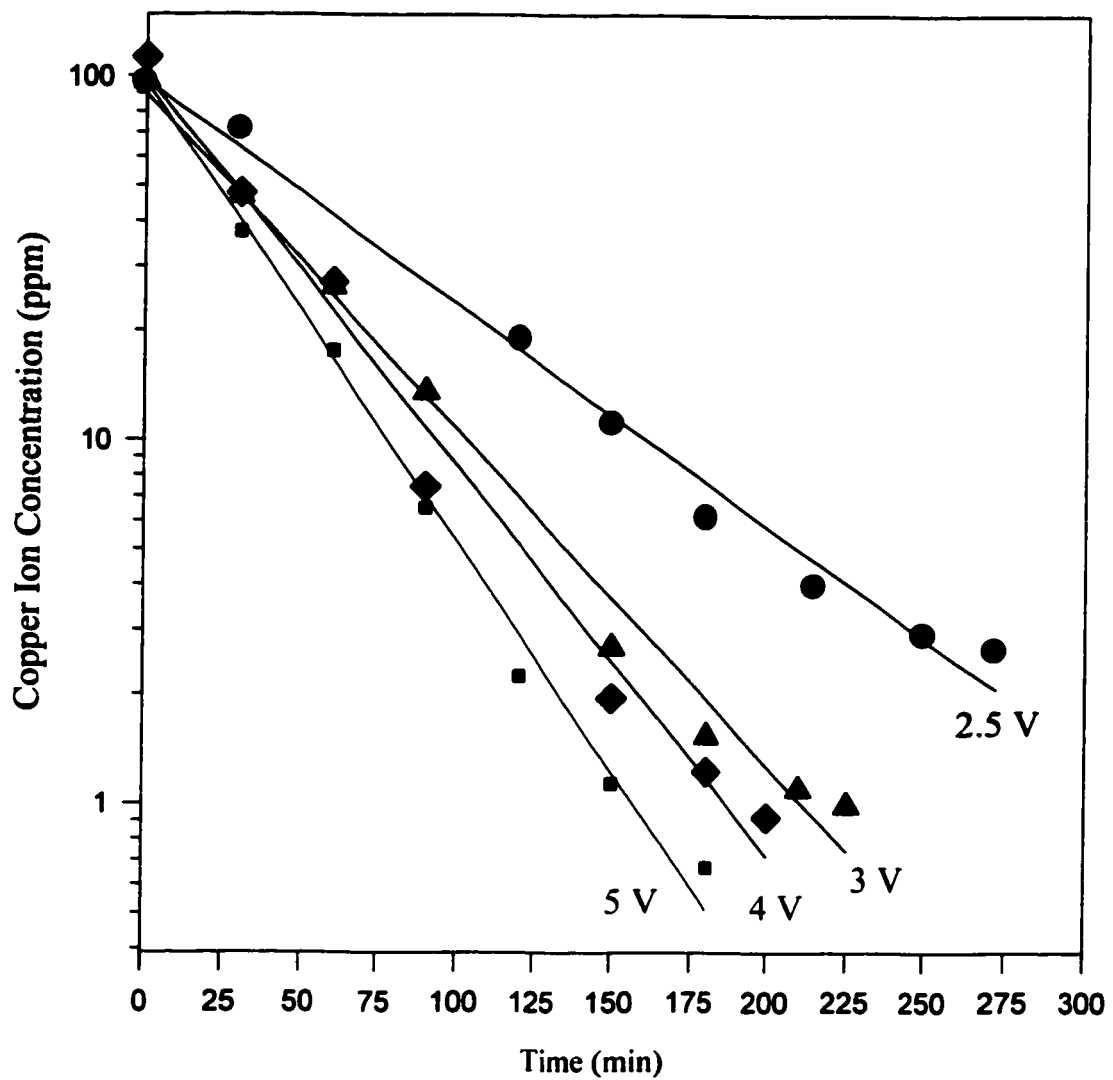


Figure 4.4. Effect of cell voltage on the change of copper ion concentration for a series of runs at 50% barrel load, 45° barrel tilt angle and 20 rpm of barrel rotation speed. In all runs, the cell contained 14 liter of a simulated wastewater at 25 °C

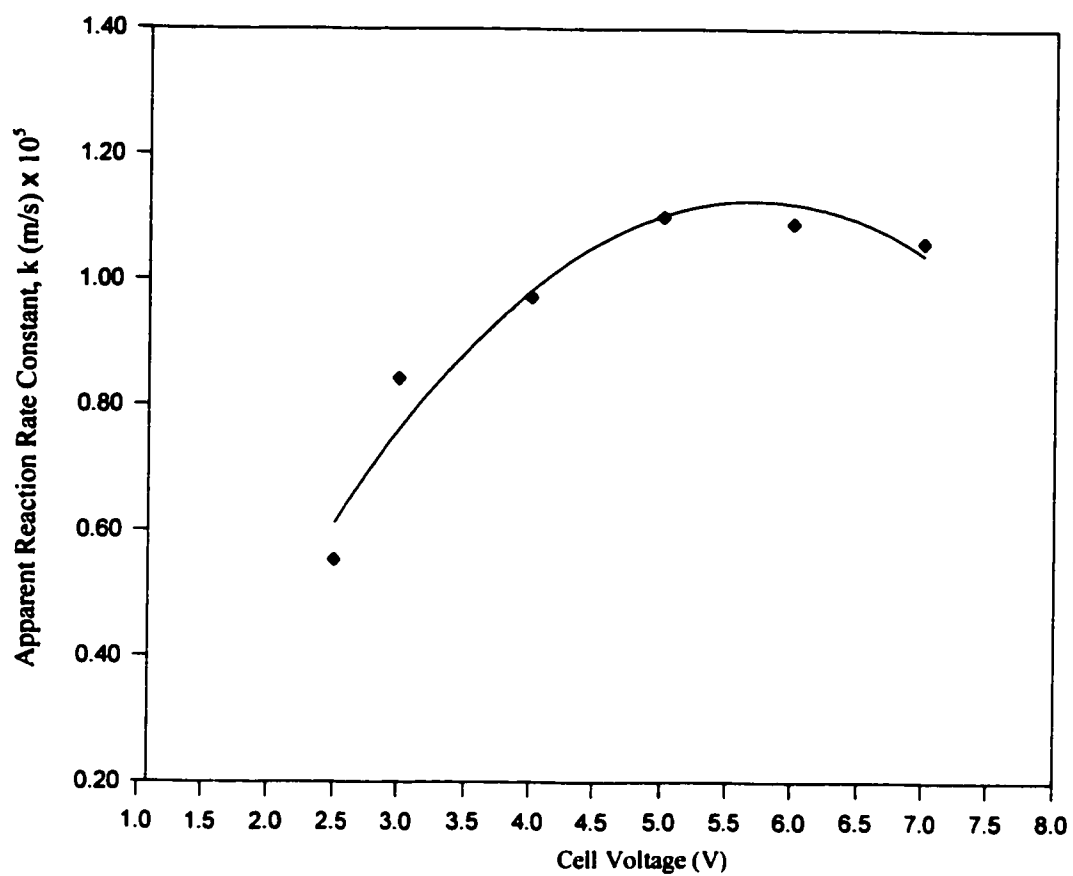


Figure 4.5. Apparent reaction rate constant versus cell voltage at 50% barrel load, 50% barrel immersion, 45° barrel tilt angle and 12 rpm barrel rotational speed.

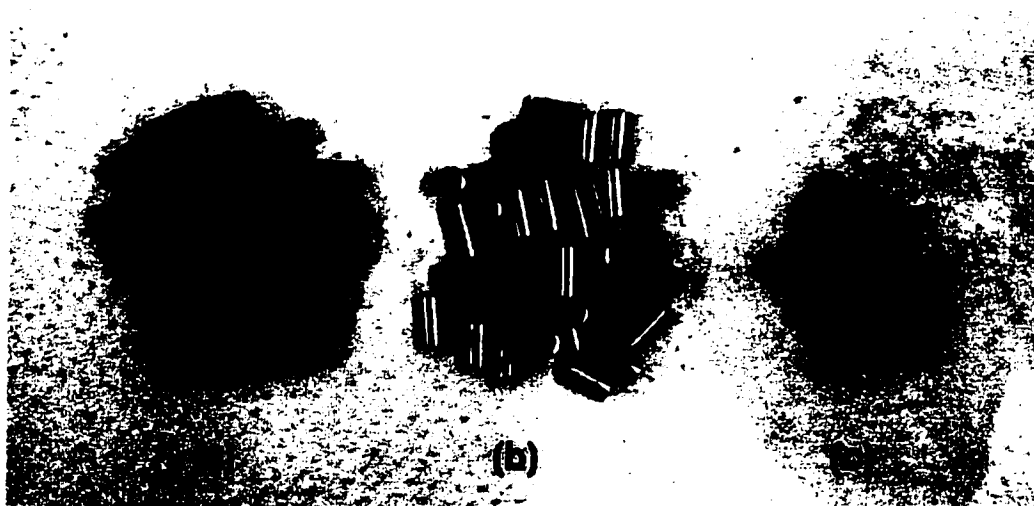


Figure 4.6. Copper particles used as the cathode inside the plating barrel. (a) Particles before electrolysis. (b) Particles after electrolysis with bright deposit under normal operation conditions. (c) Passivated copper particles coated with black $\text{Cu}(\text{OH})_2$ at high applied cell voltages.

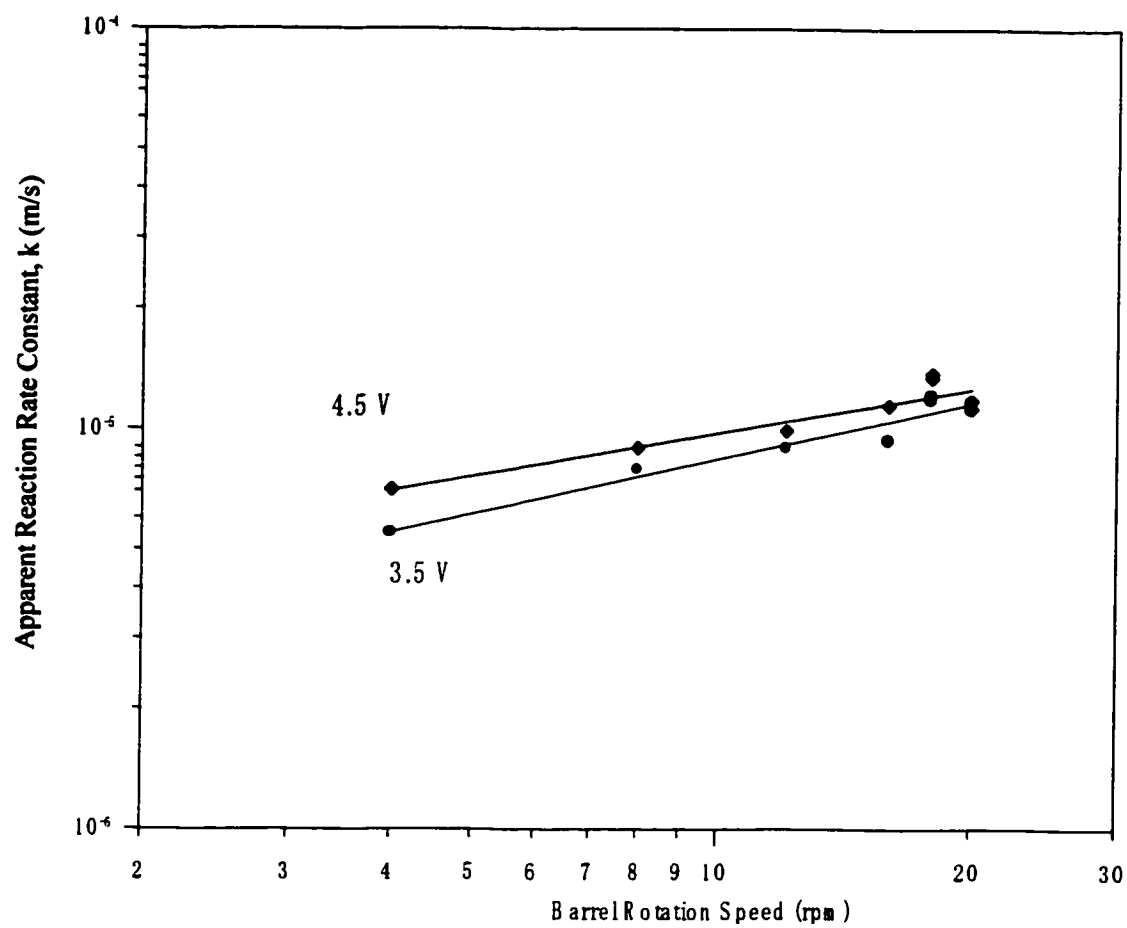


Figure 4.7. A log-log plot of the apparent reaction rate constant versus barrel rotating speed at 3.5 & 4.5 volts. The other operation condition were kept constant 50% barrel load and 45° barrel tilt angle.

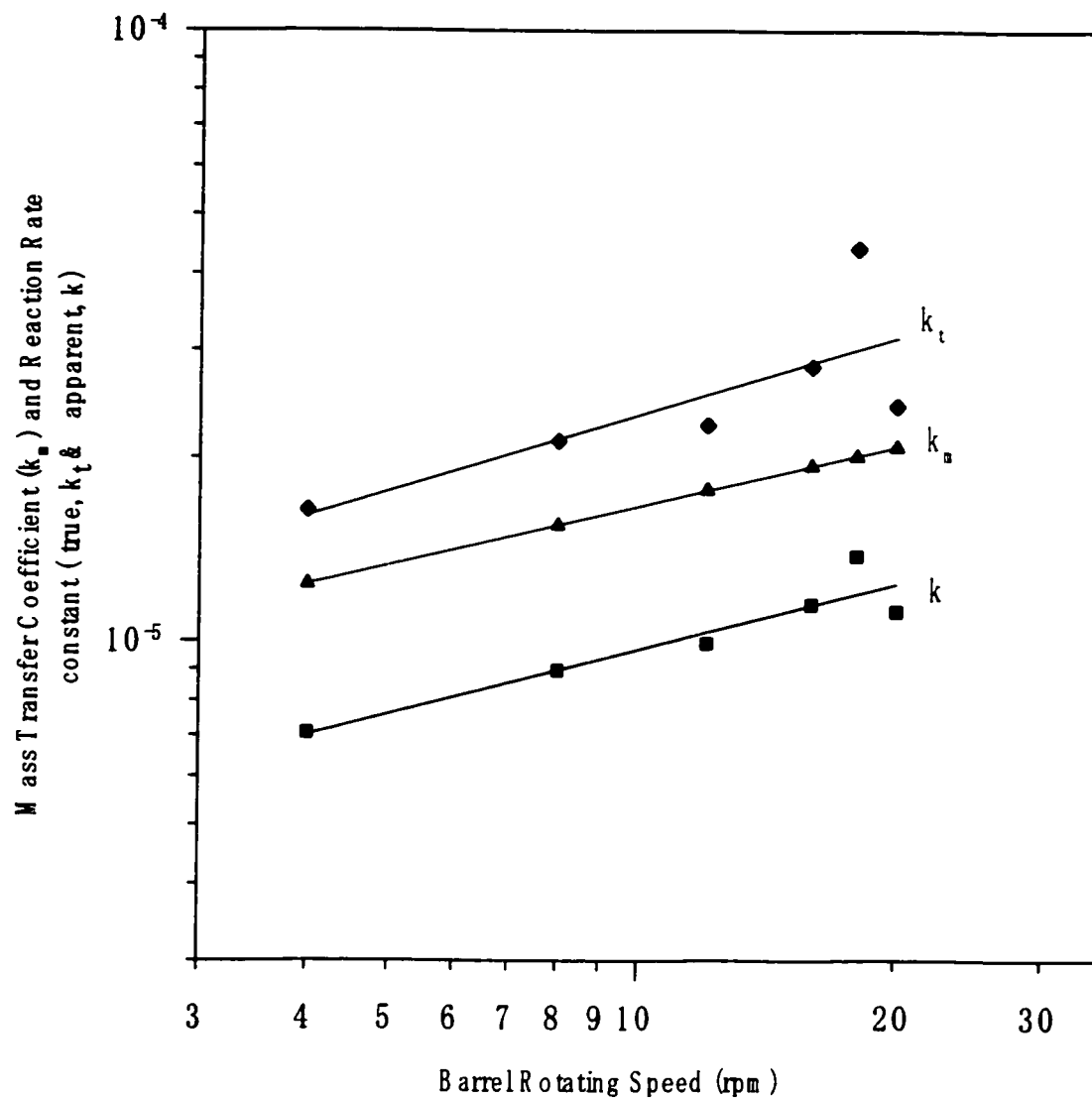


Figure 4.8. Calculated true reaction rate constant and the mass transfer coefficient versus barrel rotational speed at 4.5V, 50% barrel load and 45° barrel tilt angle.

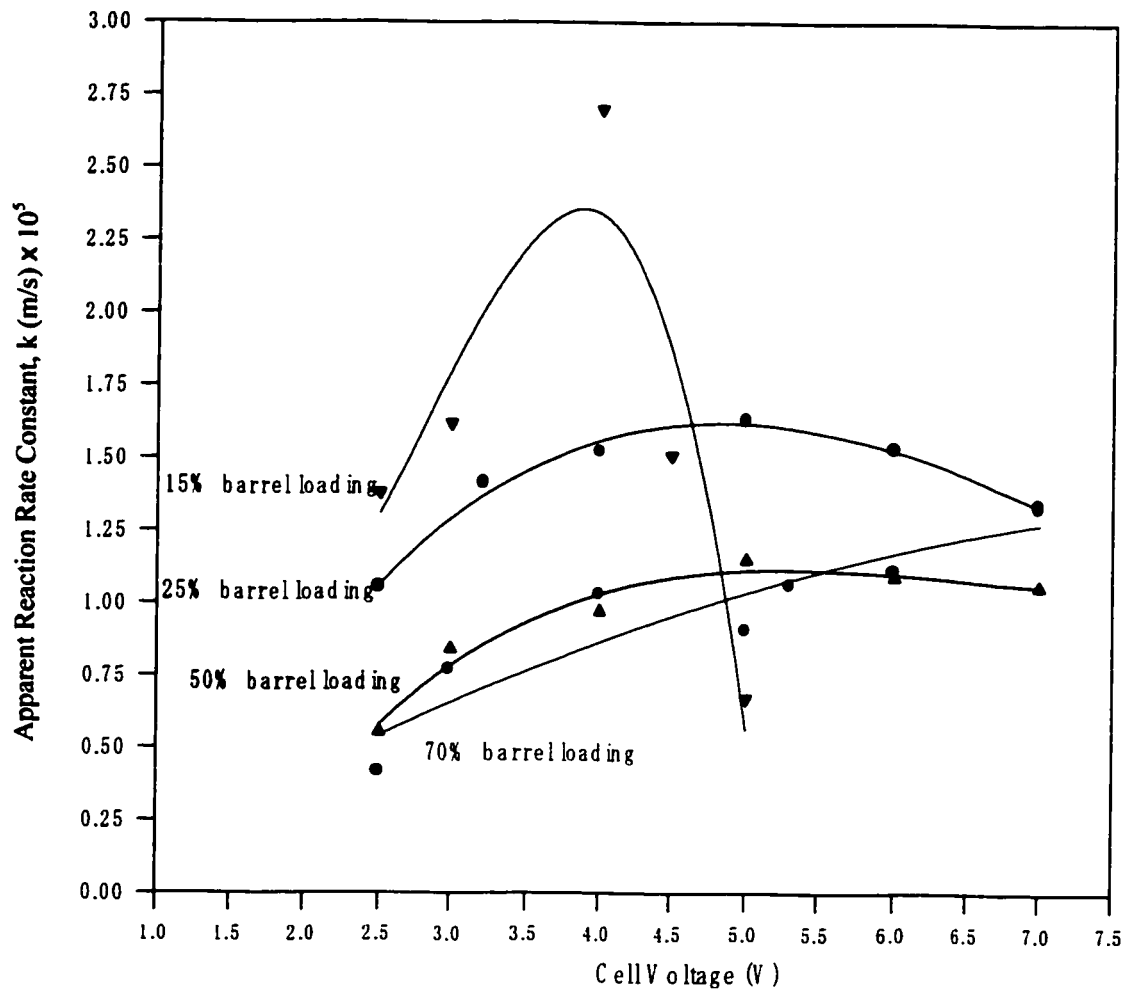


Figure 4.9. Effect of percent barrel loading on the apparent reaction rate constant at different cell voltages, 45° barrel tilt angle, 50% barrel immersion and 20 rpm barrel rotational speed.

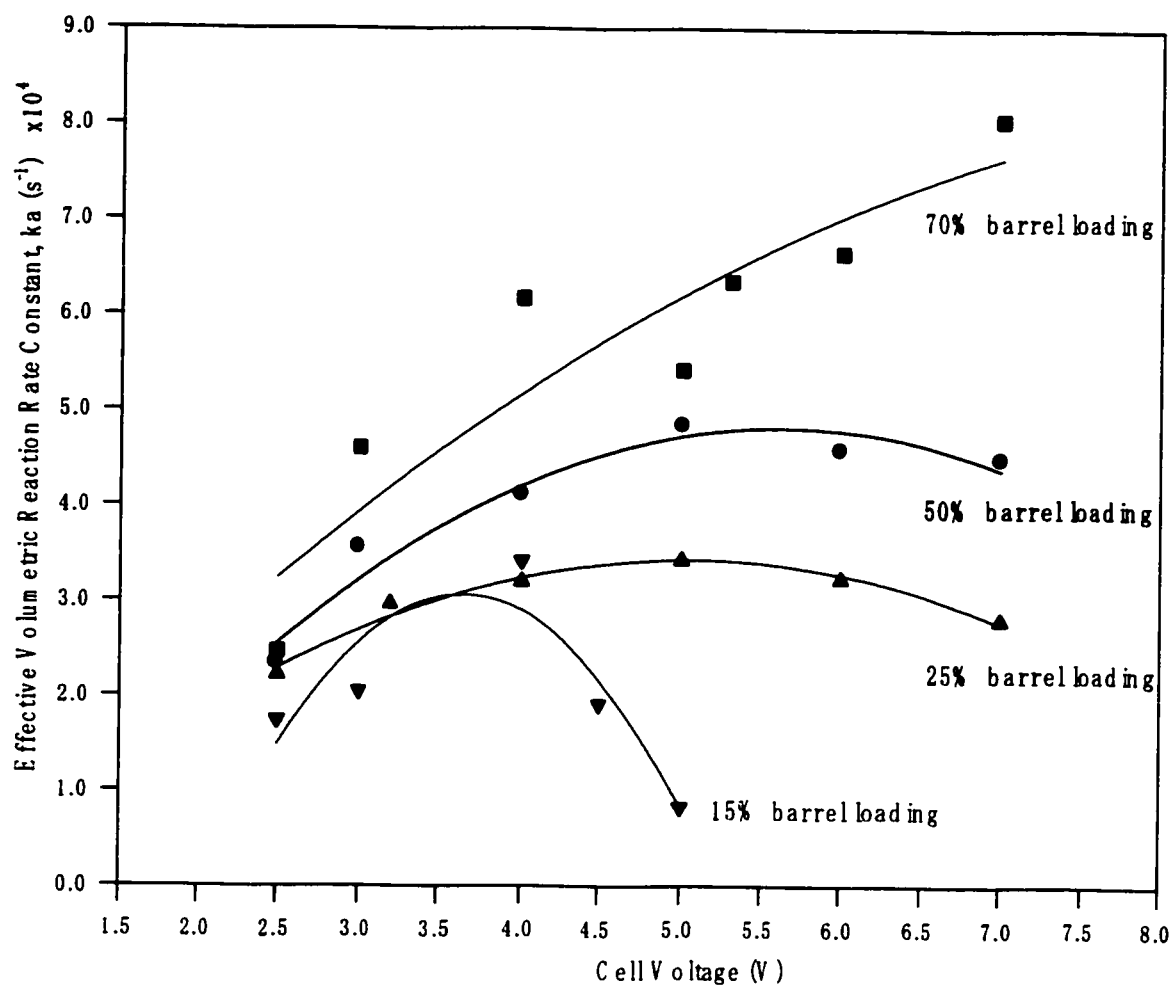


Figure 4.10. Effect of percent barrel loading on the effective volumetric reaction rate constant at different cell voltages, 45° barrel tilt angle, 50% barrel immersion and 20 rpm barrel rotational speed

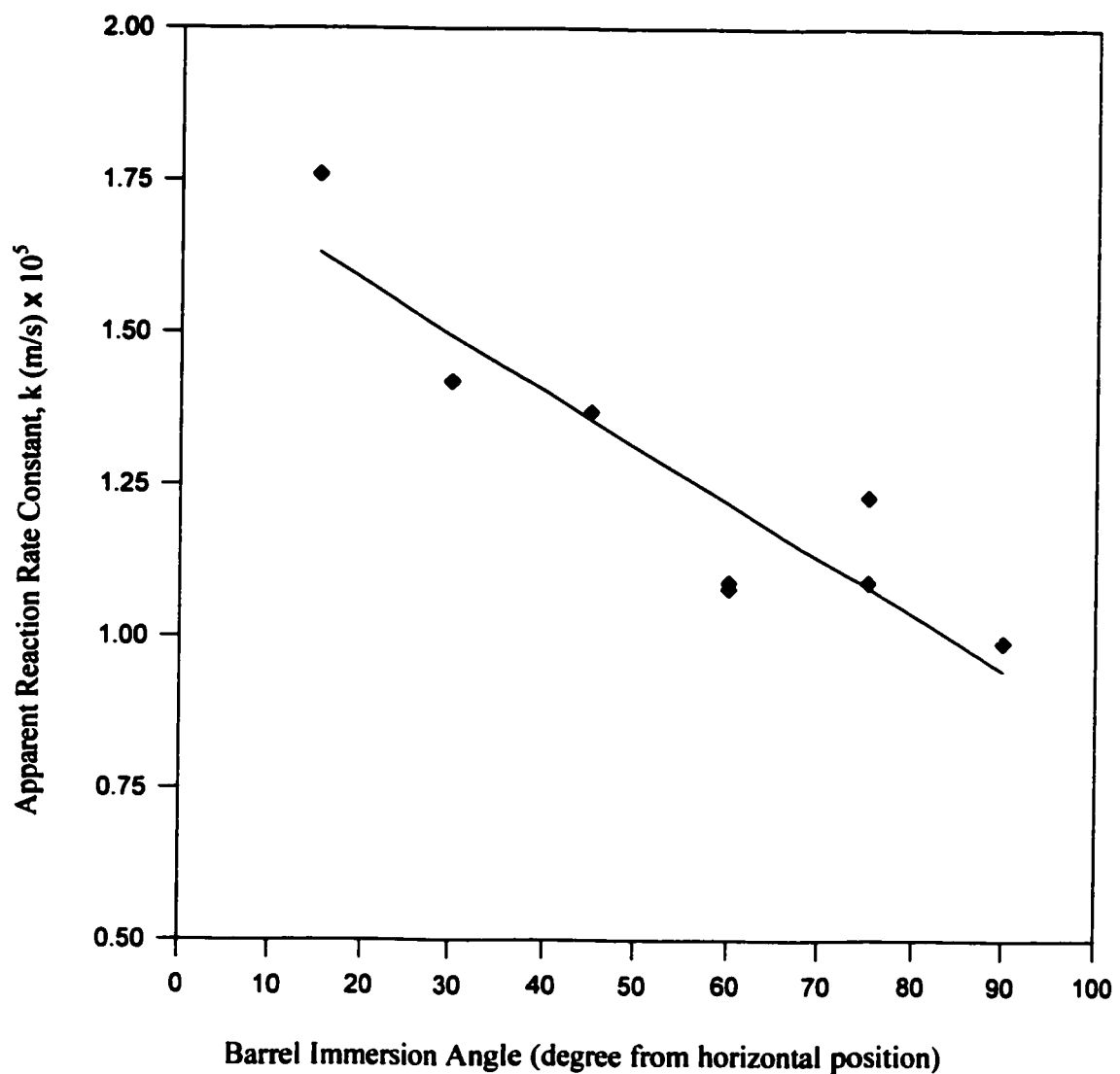


Figure 4.11. Effect of barrel immersion angle on the apparent reaction rate constant at a cell voltage of 4.5 V, 50% barrel load, 50% barrel immersion and 18 rpm barrel rotational speed.

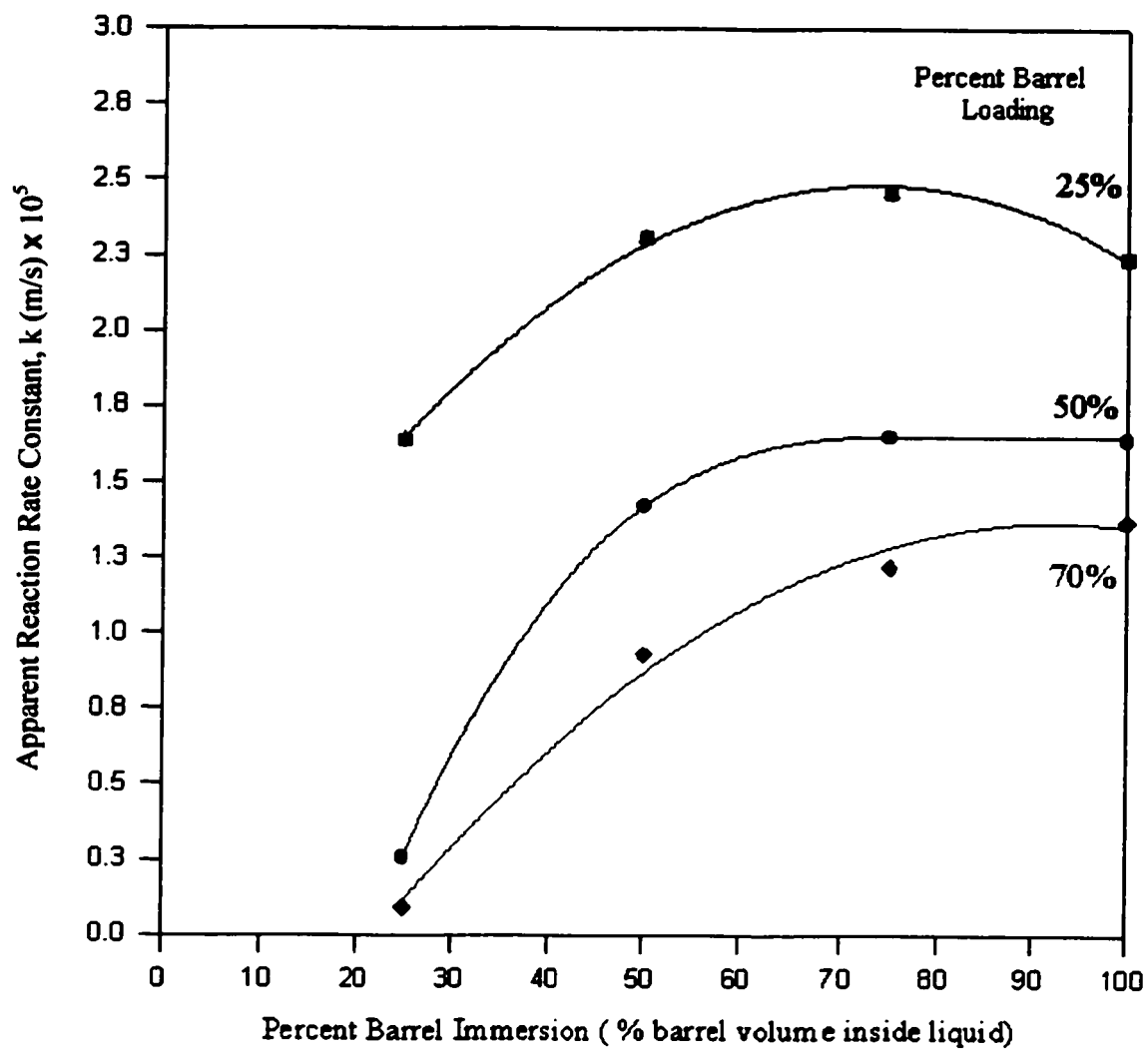


Figure 4.12. Effect of barrel immersion on the apparent reaction rate constant at different barrel loadings, 4.5V of cell voltage, 30° barrel tilt angle, and 18 rpm barrel rotation speed.

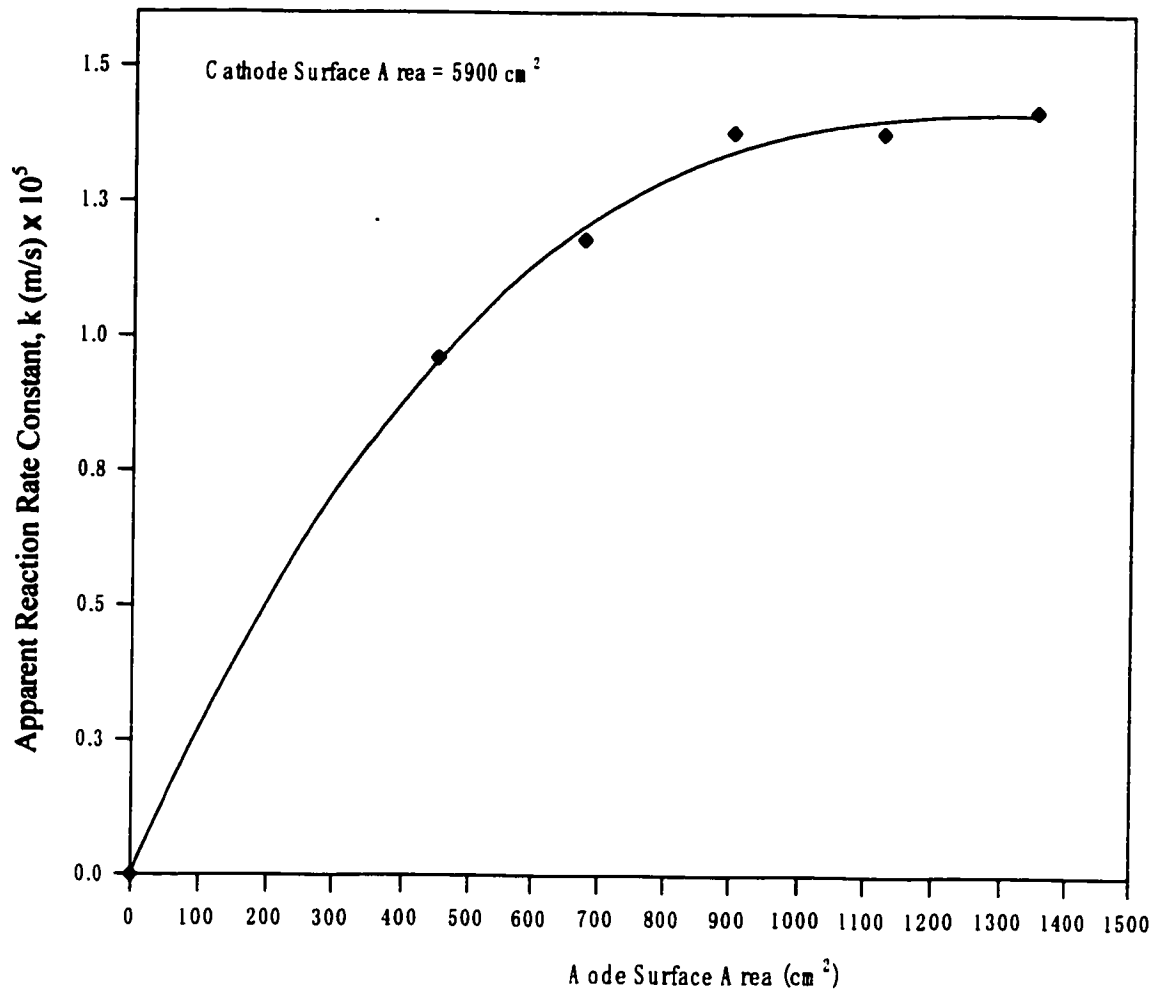


Figure 4.13. Effect of anode surface area on the apparent reaction rate constant at 4.5V cell voltage, 50% barrel load, 30° barrel tilt angle, 50% barrel immersion and 18 rpm.

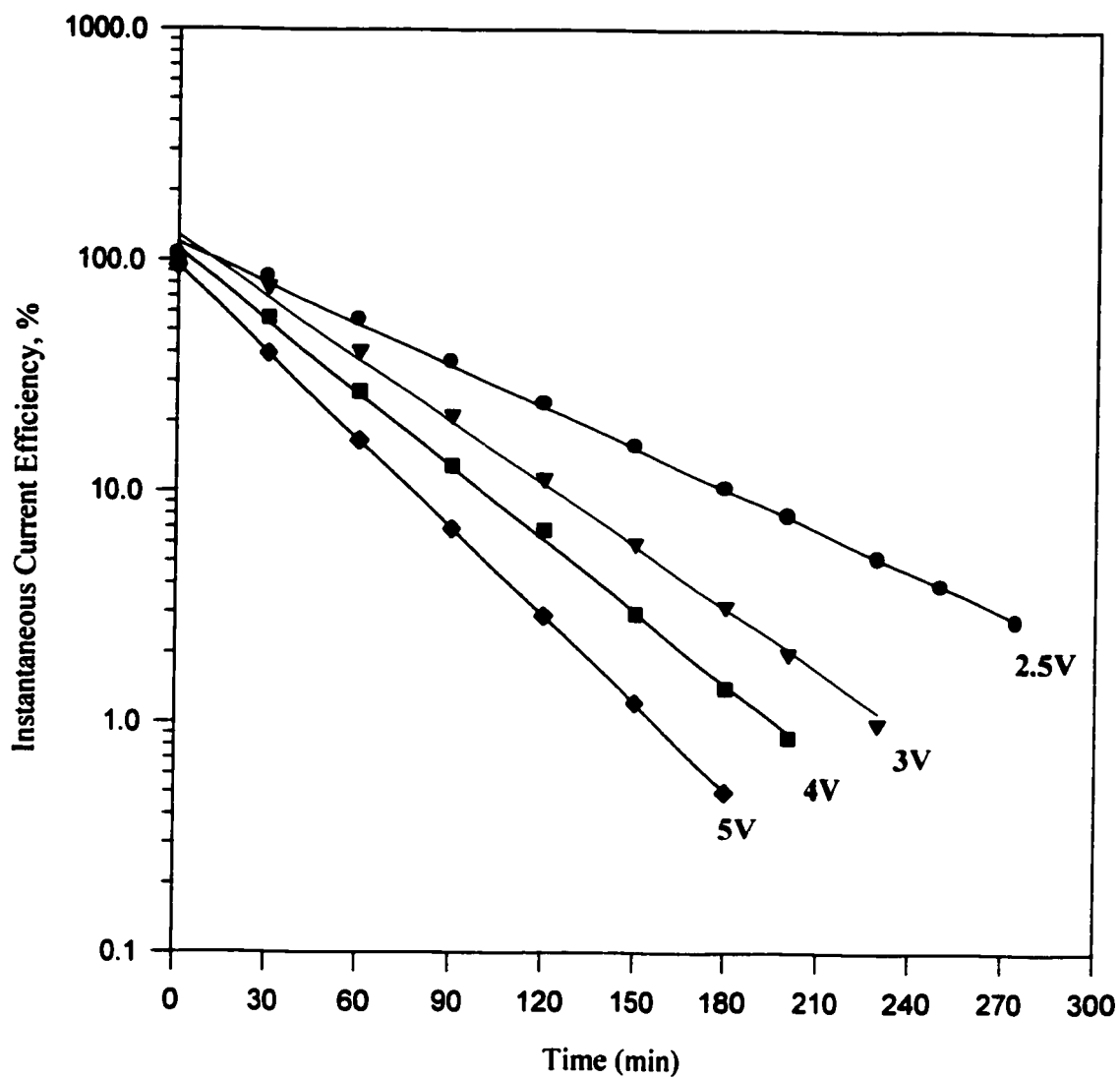


Figure 4.14. Instantaneous current efficiency versus electrolysis time at different voltages, 50% barrel load, 45° barrel tilt angle and 20 rpm.

CHAPTER 5

CONCLUSIONS AND RECOMMENDATIONS

5.1 Conclusions

This study exhibits that the electrolytic process using an oblique barrel cathode offers a high efficiency in removing toxic metals from wastewater. The copper Raschig rings inside the rotating barrel enhanced the metal electrodeposition reaction by providing a high mass transfer rate and a large cathode surface area. The copper ion concentration in the simulated wastewater was reduced from 100 ppm to less than 1 ppm to permit the discharge of the wastewater into the drain system. The effect of the process operation variables on the apparent reaction rate constant of copper electrodeposition at the cathode was investigated. The current efficiency and the energy consumption of copper recovery process were evaluated. The main conclusions of the present study can be summarized as:

1. The copper ion concentration in wastewater decreased logarithmically with the electrolysis time. It was reduced to less than 1 ppm by using the oblique barrel cathode at 4 to 20 rpm and at applied cell voltage of 3 to 5V.
2. At the beginning of the experiment, the pH value of the wastewater decreased with the time due to the production of H^+ ions at the anode. However, at the end of the experiment, the pH change became small and eventually stabilized at a constant value of pH 3.2 due to production of OH^- ions by the hydrogen gas evolution side-reaction at the cathode.
3. The apparent reaction rate constant of copper electrodeposition reaction increased with increasing the cell voltage. However, when the applied voltage was greater

than 5 V, the reaction rate constant started to decrease due to the formation of black layer of $\text{Cu}(\text{OH})_2$ coating on the cathode surface. This phenomenon is called the cathode passivation and it was caused by the high hydrogen evolution as a side reaction at the cathode.

4. The apparent reaction rate constant for copper deposition reaction increased with increasing the barrel rotational speed. This implied that the copper electro-deposition in the present cell was under a mixed mass transfer and kinetic control. Using the values of the mass transfer coefficients calculated from a literature correlation, it was found that the fraction of mass transfer and kinetic resistances were about 0.6 and 0.4 respectively.
5. The apparent reaction rate constant for copper deposition reaction decreased with increasing barrel tilt angle from the horizontal position. The lowest reaction rate constant was obtained when the barrel was at a vertical position of 90° due to a small mass transfer rate.
6. The apparent reaction rate constant for copper deposition increased with increasing percent immersion up to 75 % of barrel volume. Then it became constant with further increase in immersion level.
7. The apparent reaction rate constant for copper deposition at the cathode initially increased with increasing the anode surface area and became nearly constant when the anode area was larger than 1100 cm^2 .
8. The cathodic instantaneous current efficiency decreased logarithmically with time from 100 percent at the beginning of the electrolysis to less than 1 percent near the end of the electrolysis due to decreasing copper ion concentration in the

wastewater. The average current efficiency of the process decreased with increasing cell voltage from 53 percent at 2.5 volt to 20 percent at 5 volt. The electric energy consumption varied from 4 to 21.4 kWh/kg per kilogram of copper recovered.

5.2 Recommendations

For future studies, it is recommended to combine the present electrolytic cell with another metal recovery technology like the electro dialysis, which has high efficiency at low metal ion concentration. The present electrolytic cell has a high current efficiency at high metal concentration while the electro dialysis technology is economical to recover metals from a low concentration solution. This integrated electrolysis and electro dialytic cell may offer a high overall current efficiency and a low energy consumption for recovering heavy metals from wastewater.

Also, a specific study on cathode passivation and hydrogen evolution side reaction at the cathode is recommended. This phenomenon strongly reduces the rate of metal electrodeposition reaction at high cell voltages. The mechanism of these side reactions and the prevention of this cathode passivation phenomenon need to be investigated.

APPENDIX

During the electrolysis process, copper ion concentration in the wastewater decreased with the time at fixed operation variables. One of these variables was changed in each experimental run to study its effect on copper recovery process. This appendix contains the experimental raw data in a tabulated form for all electrolytic experiments at various operation variables:

Control Variable	Page No.
Cell Voltage Effect	65 - 73
Percent Barrel Loading Effect	74 - 91
Barrel Rotation Speed Effect	92 - 107
Barrel Tilt Angle Effect	108 - 114
Percent Barrel Immersion Effect	115 - 125
Anode Surface Area Effect	126 - 129

Cell Voltage Effect

Table. A-1. Fixed operation parameters

Voltage (V)	5
Current (A)	1.36
Barrel load	50%
Barrel Immersion angle	45
Barrel Immersion percent	50%
Rotating speed (rpm)	20
Water Volume (lit.)	14
Na ₂ SO ₄ weight (g)	86.71
CuSO ₄ weight (g)	5.337
Temperature (C)	25.3

$$(\text{ppm})=0.677e^{0.0843*(\text{mV})}$$

$$\text{area (50\%)}=0.5905 \text{ m}^2$$

$$V/A=0.02371 \text{ m}$$

$$k= 0.000524 \text{ m/min}$$

$$8.73E-06 \text{ m/s}$$

Table. A-2. Experimental measurements

Time (min)	ppm	mV	pH
0	85.52	57.4	4.9
30	43.57	49.4	3.66
95	8.71	30.3	3.36
130	3.56	19.7	3.37
155	1.97	12.7	3.36
185	1.13	6.1	3.36
210	0.81	2.2	3.36
225	0.69	0.2	3.36

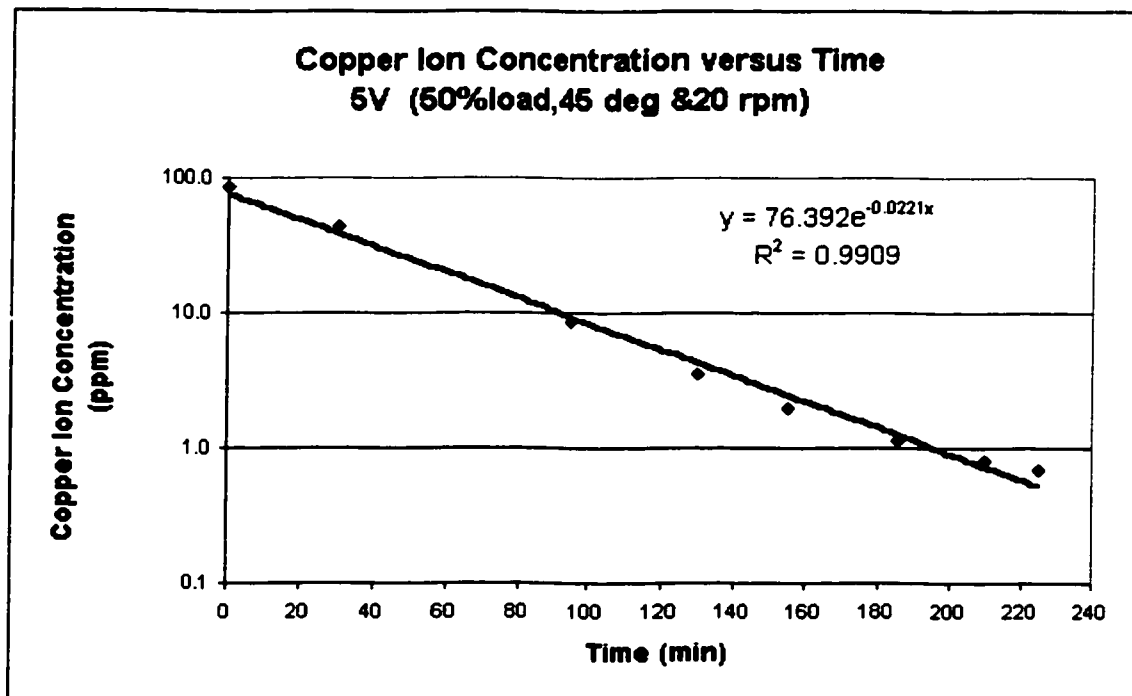


Figure. A-1. Copper ion concentration versus electrolysis time.

Table. A-3. Fixed operation parameters

Voltage (V)	7
Current (A)	2.11
Barrel load	50%
Barrel Immersion angle	45
Barrel Immersion percent	50%
Rotating speed (rpm)	20
Water Volume (lit.)	14
Na ₂ SO ₄ weight (g)	85.54
CuSO ₄ weight (g)	5.324
Temperature (C)	26

$$(\text{ppm})=0.677e^{0.0843 \cdot (\text{mV})}$$

$$\text{area (50\%)}=0.5905 \text{ m}^2$$

$$V/A=0.02371 \text{ m}$$

$$k=0.000569 \text{ m/min}$$

$$9.48E-06 \text{ m/s}$$

Table. A-4. Experimental measurements

Time (min)	ppm	mV	pH
0	81.99	56.9	4.25
30	32.71	46	3.58
60	17.53	38.6	3.33
120	3.91	20.8	3.31
150	1.50	9.4	3.3
180	1.05	5.2	3.32
200	0.69	0.3	3.31

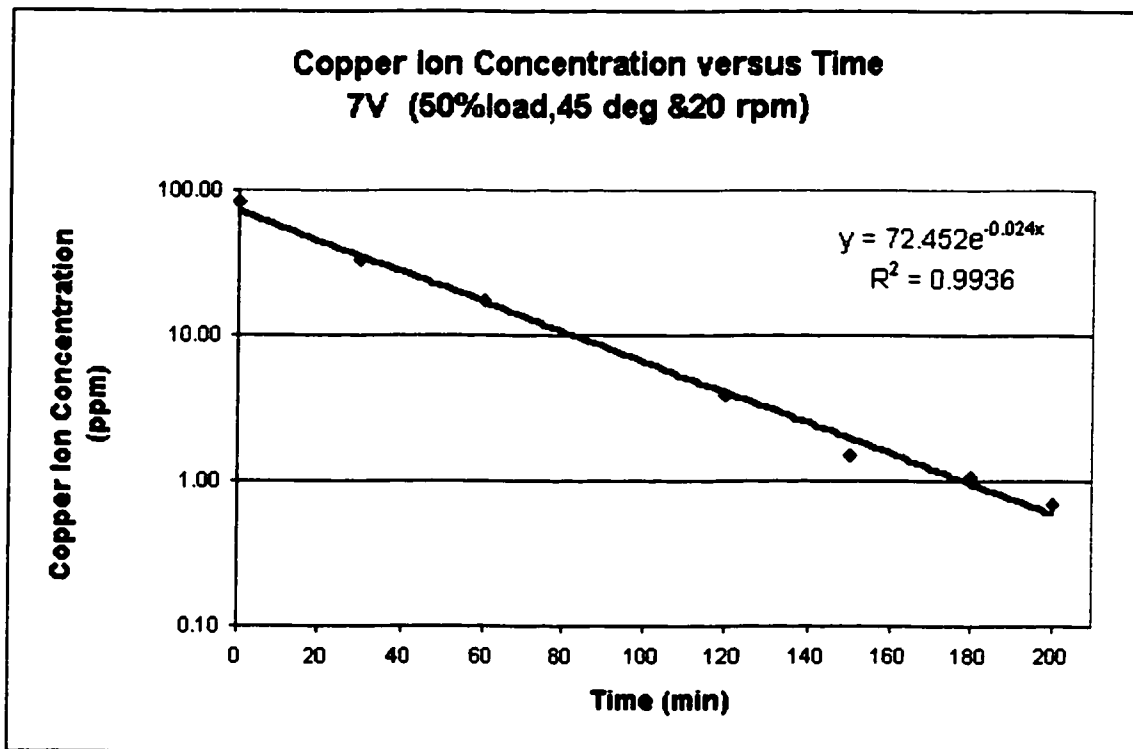


Figure. A-2. Copper ion concentration versus electrolysis time.

Table. A-5. Fixed operation parameters

Voltage (V)	3
Current (A)	0.5
Barrel load	50%
Barrel Immersion angle	45
Barrel Immersion percent	50%
Rotating speed (rpm)	20
Water Volume (lit.)	14
Na ₂ SO ₄ weight (g)	85.93
CuSO ₄ weight (g)	5.29

$$(\text{ppm})=0.4929e0.0844*(\text{mV})$$

$$\text{area (50\%)}=0.5905 \text{ m}^2$$

$$V/A=0.02371 \text{ m}$$

$$k= 0.000299 \text{ m/min}$$

$$4.98E-06 \text{ m/s}$$

Table. A-6. Experimental measurements

Time (min)	ppm	mV	pH
0	98.78	62.8	3.71
30	62.10	57.3	
60	39.37	51.9	3.85
120	27.15	47.5	3.79
150	22.18	45.1	3.7
180	16.64	41.7	3.63
210	10.12	35.8	3.56
240	5.51	28.6	3.49
270	3.83	24.3	3.44
300	2.02	16.7	3.43
330	1.37	12.1	3.41
360	1.02	8.6	3.45

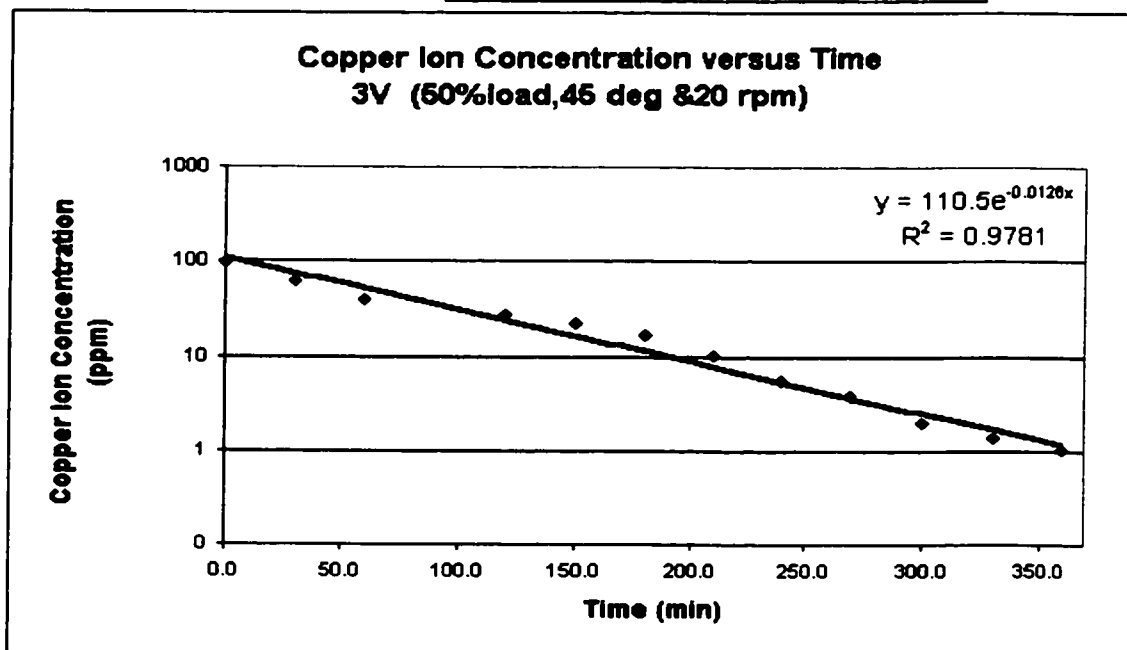


Figure. A-3. Copper ion concentration versus electrolysis time.

Table. A-7. Fixed operation parameters

Voltage (V)	7
Current (A)	3
Barrel load	50%
Barrel Immersion angle	45
Barrel Immersion percent	50%
Rotating speed (rpm)	20
Water Volume (lit.)	14
Na ₂ SO ₄ weight (g)	85.72
CuSO ₄ weight (g)	5.342
Temperature (C)	23.1

$$(\text{ppm}) = 0.4929e^{0.0844 \cdot (\text{mV})}$$

$$\text{area (50\%)} = 0.5905 \text{ m}^2$$

$$V/A = 0.02371 \text{ m}$$

$$k = 0.000638 \text{ m/min}$$

$$1.06E-05 \text{ m/s}$$

Table. A-8. Experimental measurements

Time (min)	ppm	mV	pH
0	108.39	63.9	5.61
15	57.07	56.3	4.1
30	29.80	48.6	3.66
60	18.57	43	3.41
90	6.63	30.8	3.31
120	2.62	19.8	3.27
150	1.58	13.8	3.29
180	0.80	5.8	3.29

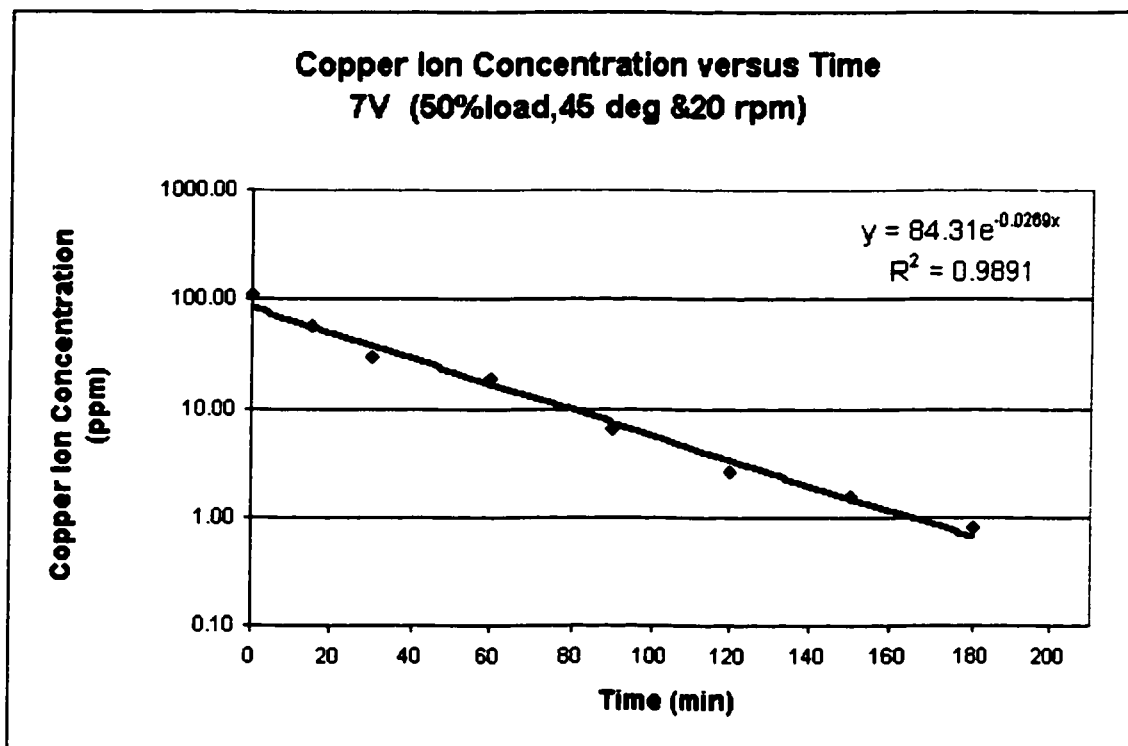


Figure. A-4. Copper ion concentration versus electrolysis time.

Table. A-9. Fixed operation parameters

Voltage (V)	5
Current (A)	2.1
Barrel load	50%
Barrel Immersion angle	45
Barrel Immersion percent	50%
Rotating speed (rpm)	20
water volume (lit.)	14
Na ₂ SO ₄ weight (g)	85.67
CuSO ₄ weight (g)	5.31
Temperature (C)	26.7

$$(\text{ppm})=0.4929e0.0844*(\text{mV})$$

$$\text{area (50\%)}=0.5905 \text{ m}^2$$

$$V/A=0.02371 \text{ m}$$

$$k= 0.000688 \text{ m/min}$$

$$1.15E-05 \text{ m/s}$$

Table. A-10. Experimental measurements

Time (min)	ppm	mV	pH	I (A)
0	113.06	64.4	5.5	2.1
30	37.42	51.3	3.54	
60	17.66	42.4	3.32	
90	6.52	30.6	3.18	
120	2.25	18	3.16	
150	1.15	10	3.16	1.8
180	0.68	3.8	3.16	1.7

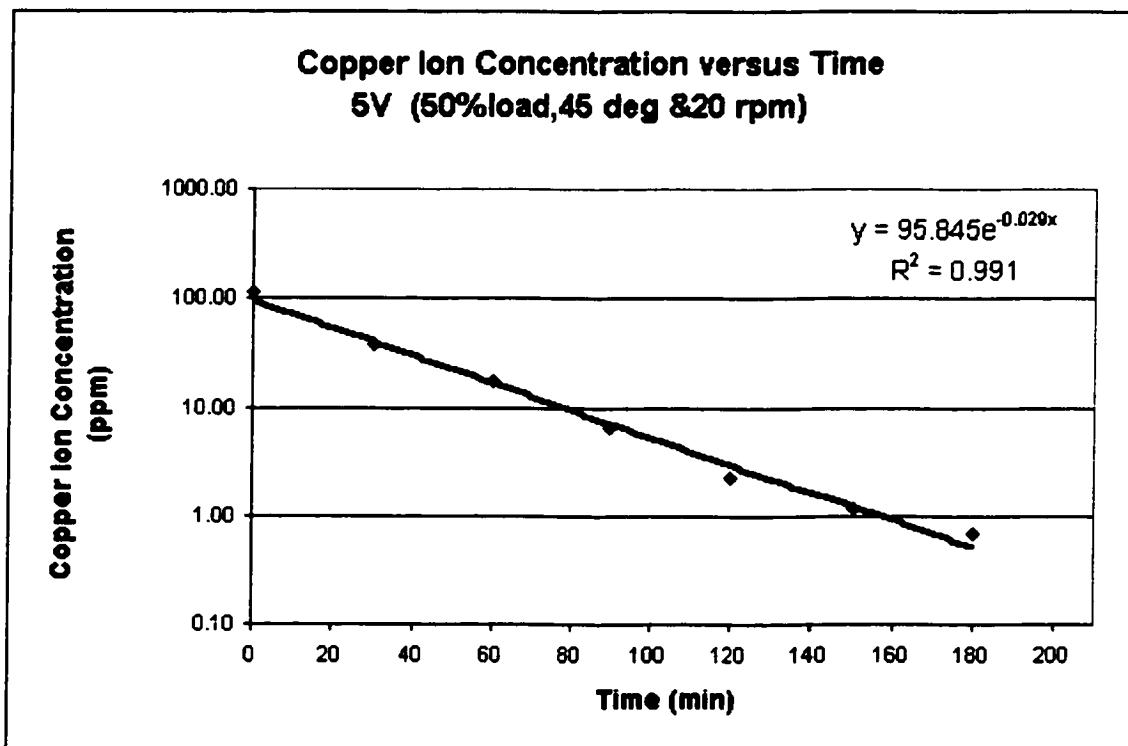


Figure. A-5. Copper ion concentration versus electrolysis time.

Table. A-11. Fixed operation parameters

Voltage (V)	3
Current (A)	1
Barrel load	50%
Barrel Immersion angle	45
Barrel Immersion percent	50%
Rotating speed (rpm)	20
water volume (lit.)	14
Na ₂ SO ₄ weight (g)	85.61
CuSO ₄ weight (g)	5.35
Temperature (C)	24.4

$$(\text{ppm})=0.4929e0.0844*(\text{mV})$$

$$\text{area (50\%)}=0.5905 \text{ m}^2$$

$$V/A=0.02371 \text{ m}$$

$$k= 0.000505 \text{ m/min}$$

$$8.42\text{E-}06 \text{ m/s}$$

Table. A-12. Experimental measurements

Time (min)	ppm	mV	pH	I (A)
0	97.12	62.6	5.33	1
30	47.00	54	3.78	
60	26.48	47.2	3.43	
90	13.59	39.3	3.22	
150	2.67	20	3.1	0.75
180	1.54	13.5	3.08	
210	1.09	9.4	3.06	
225	0.99	8.3	3.05	

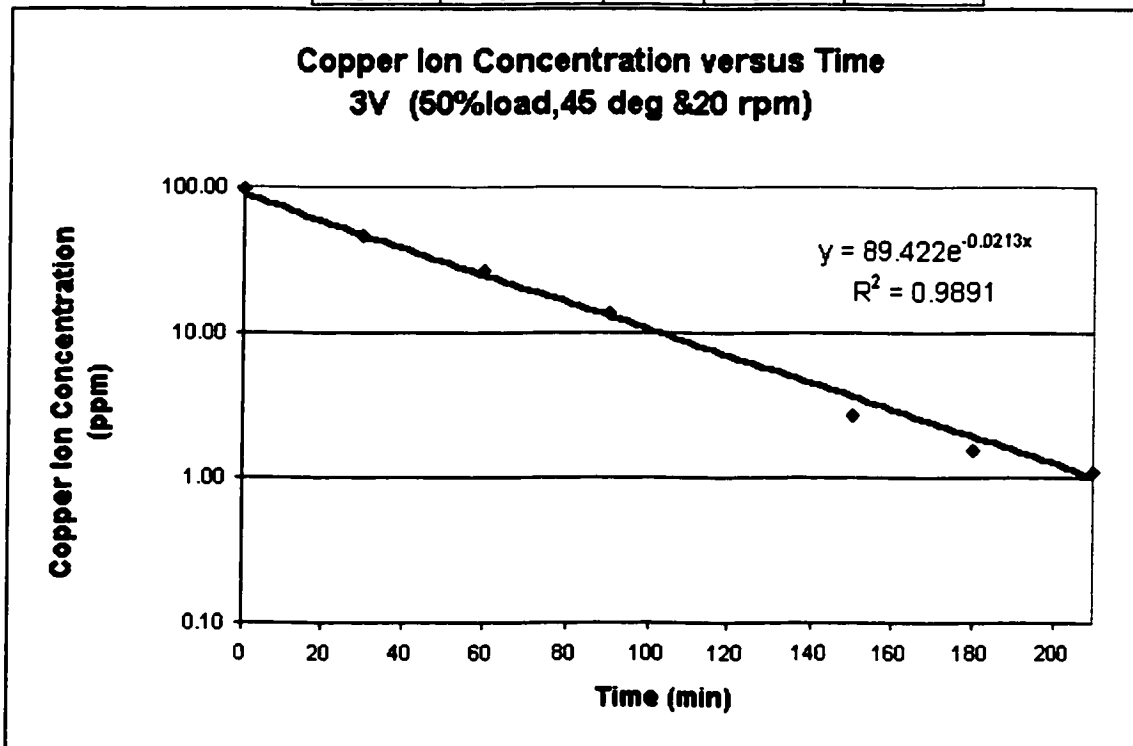


Figure. A-6. Copper ion concentration versus electrolysis time.

Table. A-13. Fixed operation parameters

Voltage (V)	4.05
Current (A)	1.45
Barrel load	50%
Barrel Immersion angle	45
Barrel Immersion percent	50%
Rotating speed (rpm)	20
water volume (lit.)	14
Na2SO4 weight (g)	85.51
CuSO4 weight (g)	5.415
Temperature (C)	24

$$(\text{ppm})=0.4929e^{0.0844*(\text{mV})}$$

$$\text{area (50\%)}=0.5905 \text{ m}^2$$

$$V/A=0.02371 \text{ m}$$

$$k= 0.000583 \text{ m/min}$$

$$9.72\text{E-}06 \text{ m/s}$$

Table. A-14. Experimental measurements

Time (min)	ppm	mV	pH
0	113.06	64.4	5.35
30	47.80	54.2	3.58
60	27.15	47.5	3.34
90	7.47	32.2	3.23
150	1.97	16.4	3.19
180	1.24	10.9	3.19
200	0.92	7.4	3.2

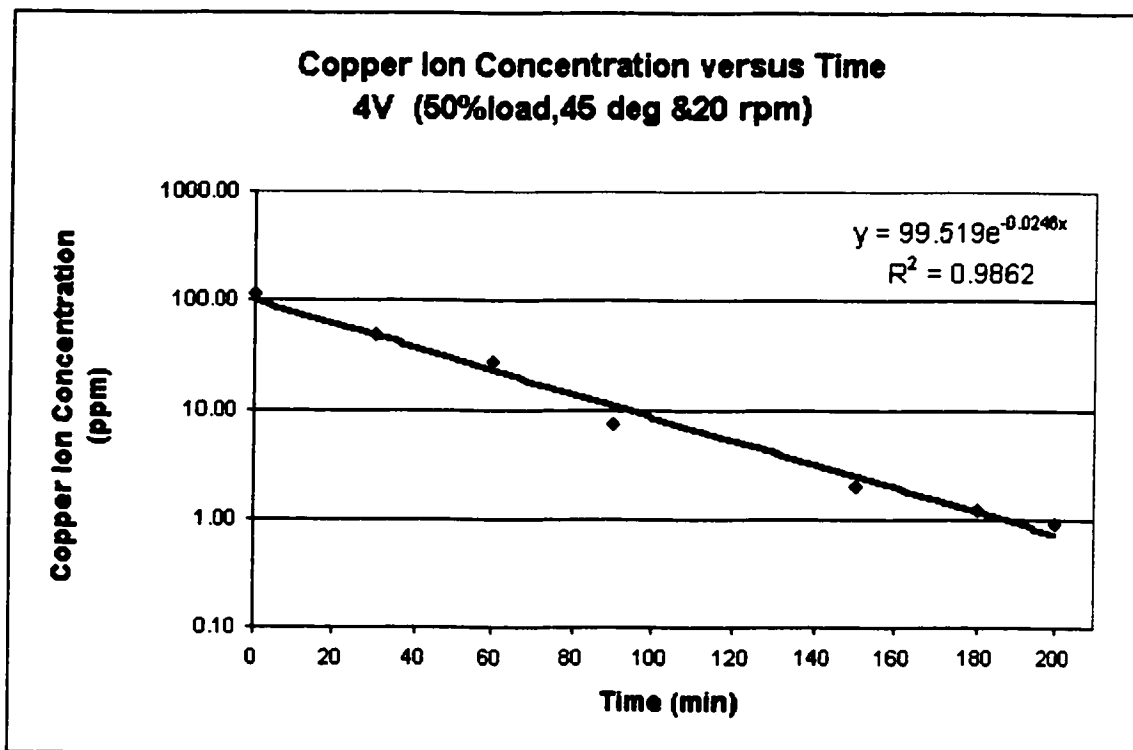


Figure. A-7. Copper ion concentration versus electrolysis time.

Table. A-15. Fixed operation parameters

Voltage (V)	6.02
Current (A)	2.5
Barrel load	50%
Barrel Immersion angle	45
Barrel Immersion percent	50%
Rotating speed (rpm)	20
water volume (lit.)	14
Na ₂ SO ₄ weight (g)	85.71
CuSO ₄ weight (g)	5.3
Temperature (C)	27.3

$$(\text{ppm}) = 0.4929e^{0.0844 * (\text{mV})}$$

$$\text{area (50\%)} = 0.5905 \text{ m}^2$$

$$V/A = 0.02371 \text{ m}$$

$$k = 0.000652 \text{ m/min}$$

$$1.09E-05 \text{ m/s}$$

Table. A-16. Experimental measurements

Time (min)	ppm	mV	pH
0	107.48	63.8	5.53
30	39.37	51.9	3.35
60	21.44	44.7	3.32
90	5.65	28.9	3.22
120	2.18	17.6	3.19
150	1.37	12.1	3.19
180	0.98	8.1	3.2

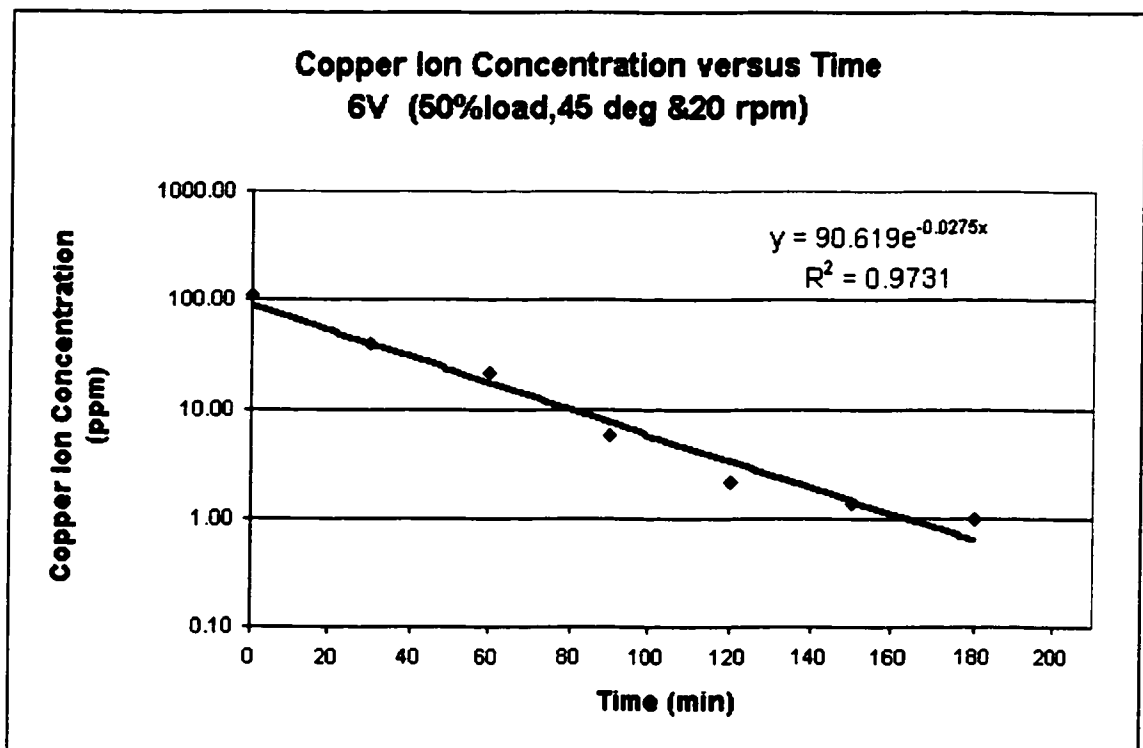


Figure. A-8. Copper ion concentration versus electrolysis time.

Table. A-17. Fixed operation parameters

Voltage (V)	2.51
Current (A)	0.73
Barrel load	50%
Barrel Immersion angle	45
Barrel Immersion percent	50%
Rotating speed (rpm)	20
water volume (lit.)	14
Na2SO4 weight (g)	85.74
CuSO4 weight (g)	5.32
Temperature (C)	22.5

$$(\text{ppm})=0.4929e0.0844*(\text{mV})$$

$$\text{area (50\%)}=0.5905 \text{ m}^2$$

$$V/A=0.02371 \text{ m}$$

$$k= 0.000332 \text{ m/min}$$

$$5.53E-06 \text{ m/s}$$

Table. A-18. Experimental measurements

Time (min)	ppm	mV	pH
0	95.50	62.4	3.75
30	71.07	58.9	3.52
120	18.89	43.2	3.09
150	11.10	36.9	3.02
180	6.10	29.8	3.01
215	3.93	24.6	2.99
250	2.90	21	2.99
275	2.62	19.8	2.99

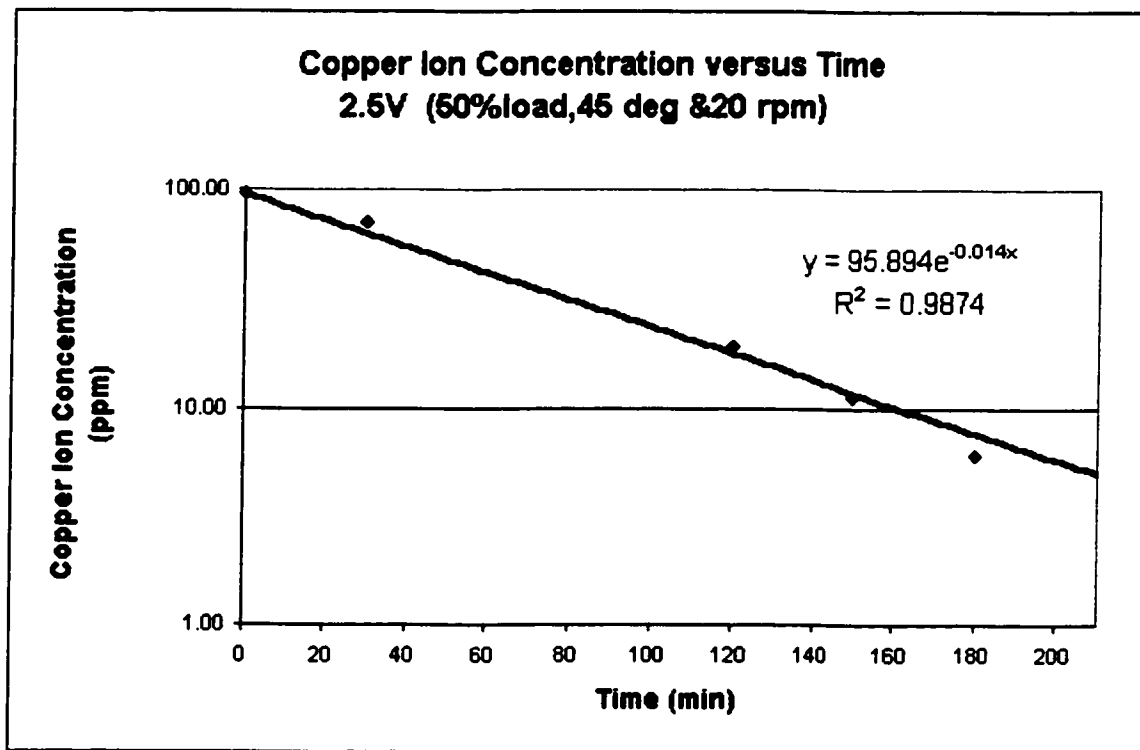


Figure. A-9. Copper ion concentration versus electrolysis time.

Barrel Load Effect

Table. A-19. Fixed operation parameters

Voltage (V)	4.01
Current (A)	1.3
Barrel load	25%
Barrel Immersion angle	45
Barrel Immersion percent	50%
Rotating speed (rpm)	20
water volume (lit.)	14
Na ₂ SO ₄ weight (g)	85.62
CuSO ₄ weight (g)	5.36
Temperature (C)	26.5

$$(\text{ppm})=0.4929e^{0.0844*(\text{mV})}$$

$$\text{area (25\%)}=0.295 \text{ m}^2$$

$$V/A=0.04746 \text{ m}$$

$$k= 0.000911 \text{ m/min}$$

$$1.52\text{E-}05 \text{ m/s}$$

Table. A-20. Experimental measurements

Time (min)	ppm	mV	pH
0	103.0	63.3	5.46
30	82.7	60.7	3.59
60	63.2	57.5	3.29
90	29.8	48.6	3.21
120	17.1	42	3.13
180	3.6	23.4	3.15
210	2.5	19.4	3.13

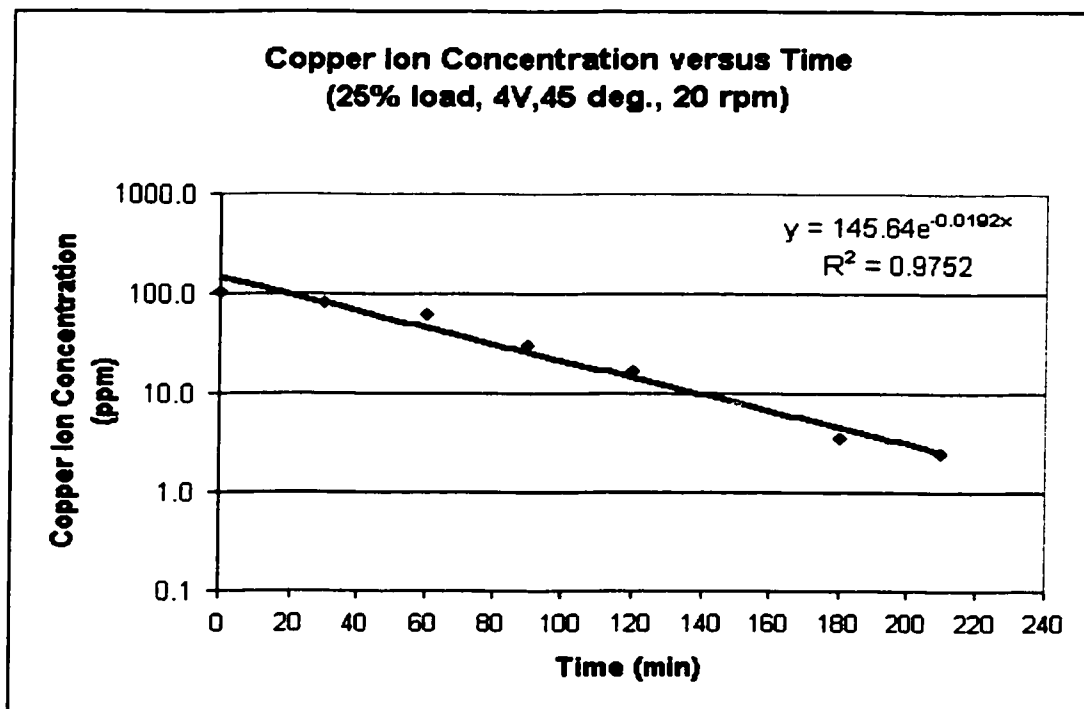


Figure. A-10. Copper ion concentration versus electrolysis time.

Table. A-21. Fixed operation parameters

Voltage (V)	3.22
Current (A)	0.92
Barrel load	25%
Barrel Immersion angle	45
Barrel Immersion percent	50%
Rotating speed (rpm)	20
water volume (lit.)	14
Na ₂ SO ₄ weight (g)	85.64
CuSO ₄ weight (g)	5.33
Temperature (C)	24.1

$$(\text{ppm}) = 0.4929e0.0844 * (\text{mV})$$

$$\text{area (25\%)} = 0.295 \text{ m}^2$$

$$V/A = 0.04746 \text{ m}$$

$$k = 0.000845 \text{ m/min}$$

$$1.41E-05 \text{ m/s}$$

Table. A-22. Experimental measurements

Time (min)	ppm	mV	pH	I (A)
0	124.06	65.5	5.43	0.92
30	70.48	58.8	3.67	
60	58.53	56.6	3.44	0.7
90	35.57	50.7	3.27	
120	23.13	45.6		
150	13.03	38.8	3.16	
180	6.31	30.2	3.15	
210	2.35	18.5	3.13	0.6

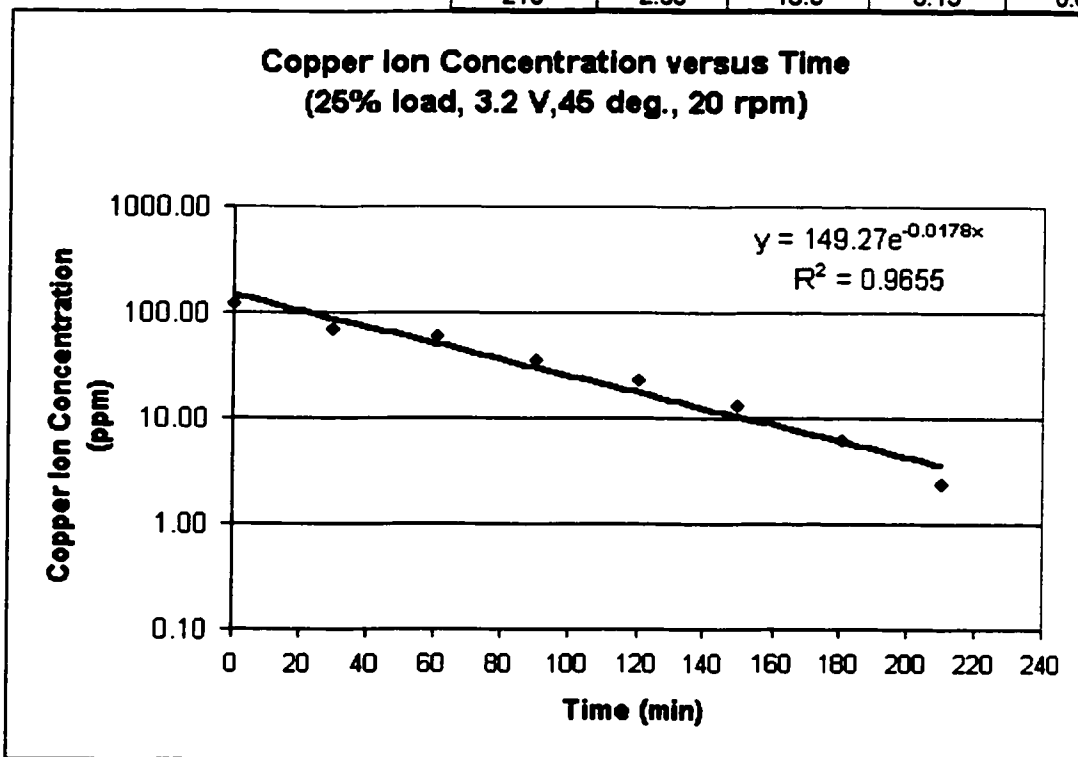


Figure. A-11. Copper ion concentration versus electrolysis time.

Table. A-23. Fixed operation parameters

Voltage (V)	6.04
Current (A)	1.95
Barrel load	25%
Barrel Immersion angle	45
Barrel Immersion percent	50%
Rotating speed (rpm)	20
water volume (lit.)	14
Na ₂ SO ₄ weight (g)	85.66
CuSO ₄ weight (g)	5.35
Temperature (C)	21.6

$$(\text{ppm})=0.4929e0.0844*(\text{mV})$$

$$\text{area (25\%)}=0.295 \text{ m}^2$$

$$V/A=0.04746 \text{ m}$$

$$k= 0.000921 \text{ m/min}$$

$$1.53E-05 \text{ m/s}$$

Table. A-24. Experimental measurements

Time (min)	ppm	mV	pH
0	129.4055	66	5.44
30	51.57263	55.1	3.6
60	28.80736	48.2	3.38
120	10.46285	36.2	3.2
180	3.292184	22.5	3.16
210	1.950861	16.3	3.16
240	0.976472	8.1	3.16

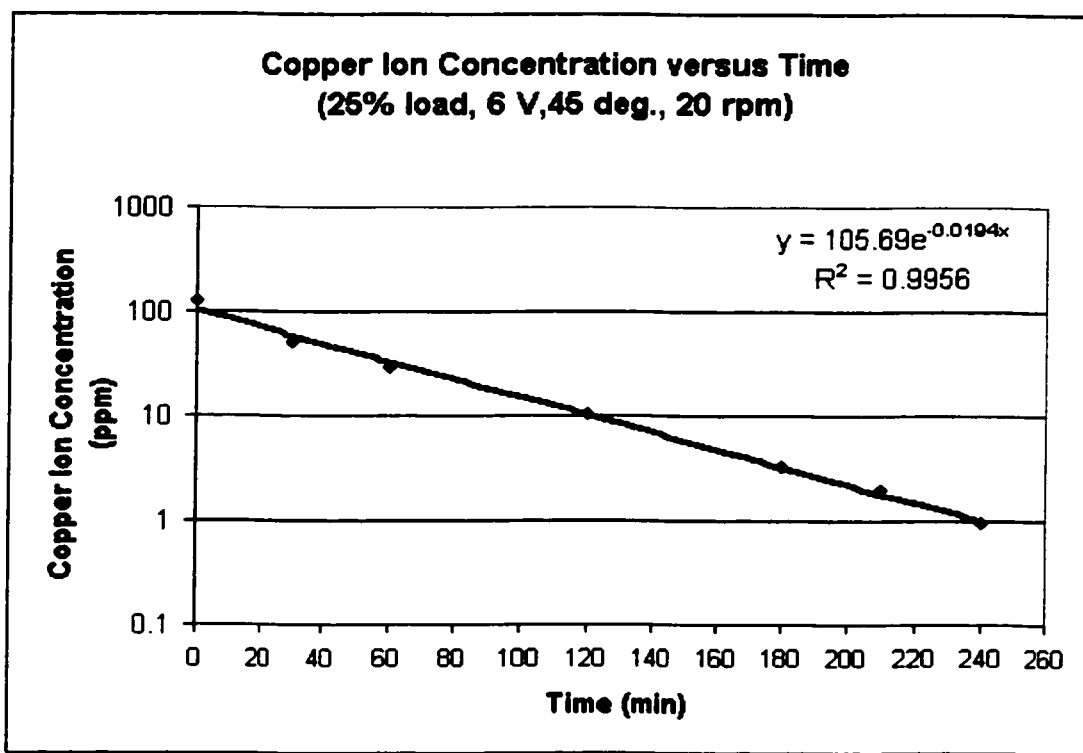


Figure. A-12. Copper ion concentration versus electrolysis time.

Table. A-25. Fixed operation parameters

Voltage (V)	5.01
Current (A)	1.6
Barrel load	25%
Barrel Immersion angle	45
Barrel Immersion percent	50%
Rotating speed (rpm)	20
water volume (lit.)	14
Na ₂ SO ₄ weight (g)	85.57
CuSO ₄ weight (g)	5.3123
Temperature (C)	21.6

$$(\text{ppm}) = 0.4929e0.0844 * (\text{mV})$$

$$\text{area (25\%)} = 0.295 \text{ m}^2$$

$$V/A = 0.04746 \text{ m}$$

$$k = 0.000978 \text{ m/min}$$

$$1.63E-05 \text{ m/s}$$

Table. A-26. Experimental measurements

Time (min)	ppm	mV	pH
0	170.9671	69.3	3.44
30	58.5330	56.6	3.34
60	26.2533	47.1	3.28
90	11.8749	37.7	3.25
120	8.3307	33.5	3.23
150	5.5090	28.6	3.22
180	3.8001	24.2	3.23

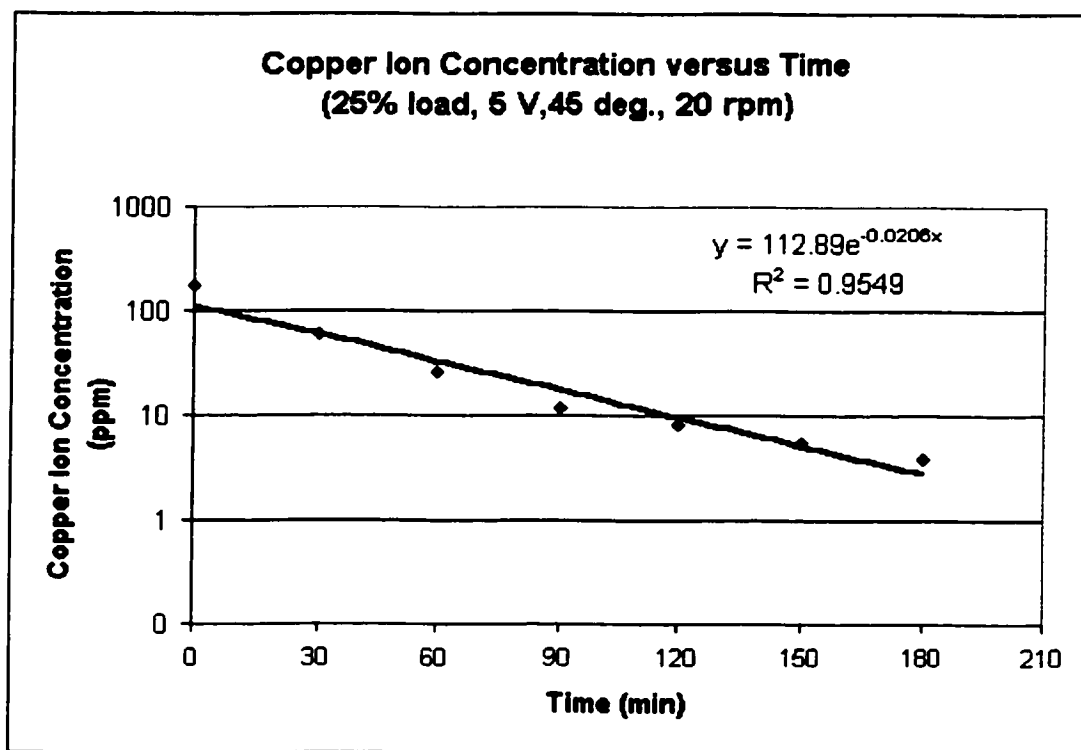


Figure. A-13. Copper ion concentration versus electrolysis time.

Table. A-27. Fixed operation parameters

Voltage (V)	7.01
Current (A)	2.56
Barrel load	25%
Barrel Immersion angle	45
Barrel Immersion percent	50%
Rotating speed (rpm)	20
water volume (lit.)	14
Na ₂ SO ₄ weight (g)	85.73
CuSO ₄ weight (g)	5.3
Temperature (C)	23

$$(\text{ppm})=0.4929e0.0844*(\text{mV})$$

$$\text{area (25\%)}=0.295 \text{ m}^2$$

$$V/A=0.04746 \text{ m}$$

$$k= 0.000797 \text{ m/min}$$

$$1.33E-05 \text{ m/s}$$

Table. A-28. Experimental measurements

Time (min)	ppm	mV	pH
0	116.9	64.8	5.62
30	51.57	55.1	3.81
80	18.73	43.1	3.35
140	10.82	36.6	3.23
170	12.70	38.5	3.23

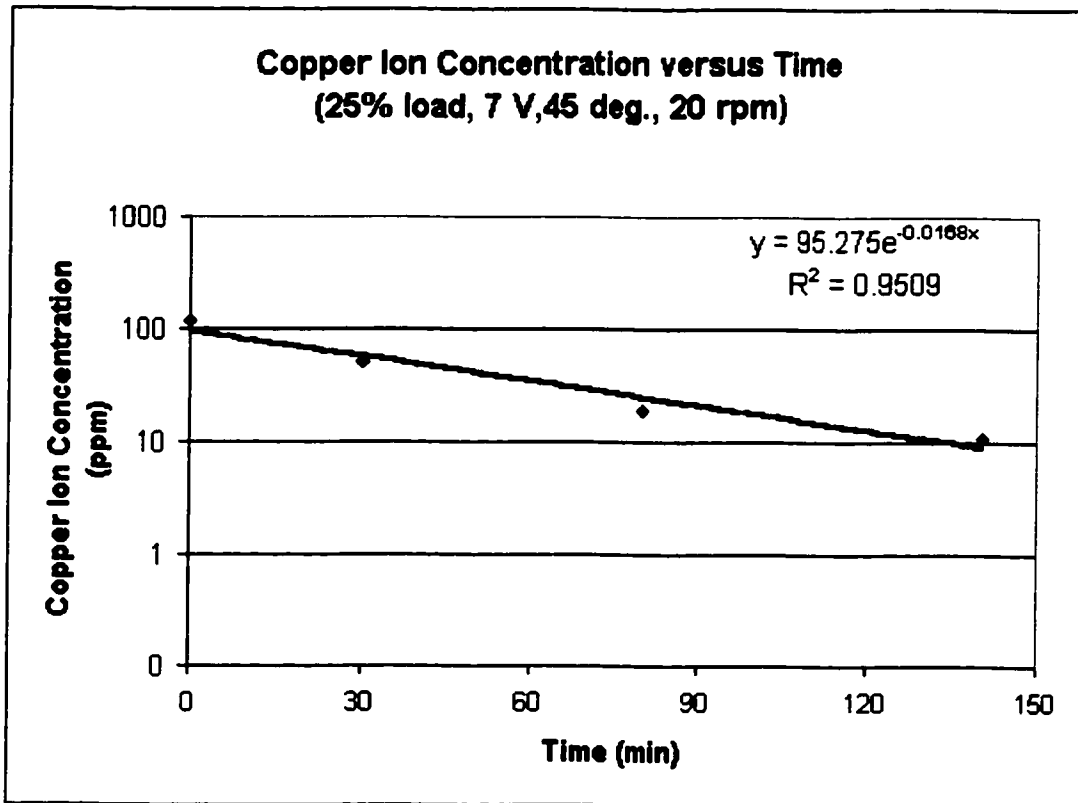


Figure. A-14. Copper ion concentration versus electrolysis time.

Table. A-29. Fixed operation parameters

Voltage (V)	3.04
Current (A)	1.1
Barrel load	70%
Barrel Immersion angle	45
Barrel Immersion percent	50%
Rotating speed (rpm)	20
water volume (lit.)	14
Na ₂ SO ₄ weight (g)	85.52
CuSO ₄ weight (g)	5.31
Temperature (C)	25.6

$$(\text{ppm})=0.3647e0.0852*(\text{mV})$$

$$\text{area (70\%)}=0.8383 \text{ m}^2$$

$$V/A=0.0167 \text{ m}$$

$$k= 0.000461 \text{ m/min}$$

$$7.68E-06 \text{ m/s}$$

Table. A-30. Experimental measurements

Time (min)	ppm	mV	pH
0	94.29	65.2	5.43
30	35.39	53.7	3.77
60	23.12	48.7	3.51
90	6.28	33.4	3.32
120	1.73	18.3	3.29
150	1.16	13.6	3.27
175	1.13	13.3	3.27

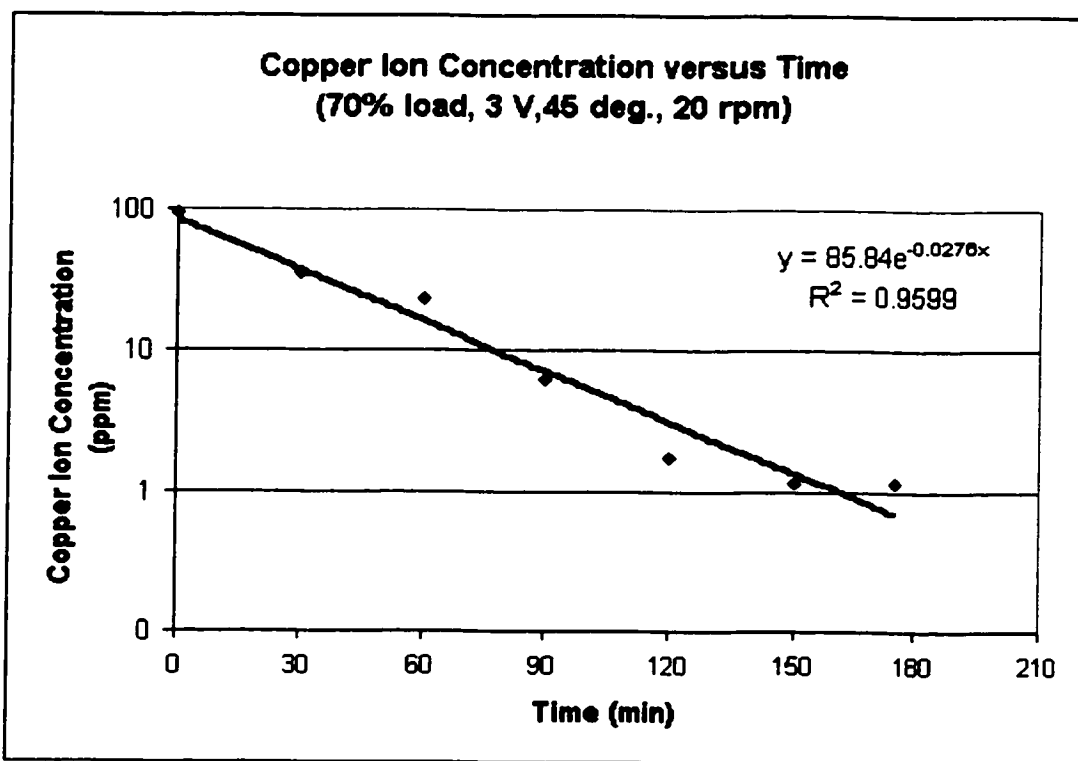


Figure. A-15. Copper ion concentration versus electrolysis time.

Table. A-31. Fixed operation parameters

Voltage (V)	4.02
Current (A)	1.26
Barrel load	70%
Barrel Immersion angle	45
Barrel Immersion percent	50%
Rotating speed (rpm)	20
water volume (lit.)	14
Na2SO4 weight (g)	85.5
CuSO4 weight (g)	5.3
Temperature (C)	23.4

$$(\text{ppm})=0.3647e^{0.0852*(\text{mV})}$$

$$\text{area (70\%)}=0.8383 \text{ m}^2$$

$$V/A=0.0167 \text{ m}$$

$$k= 0.000618 \text{ m/min}$$

$$1.03E-05 \text{ m/s}$$

Table. A-32. Experimental measurements

Time (min)	ppm	mV	pH
0	105.33	66.5	5.43
30	26.49	50.3	3.77
60	15.23	43.8	3.51
90	5.91	32.7	3.32
120	0.87	10.2	3.29

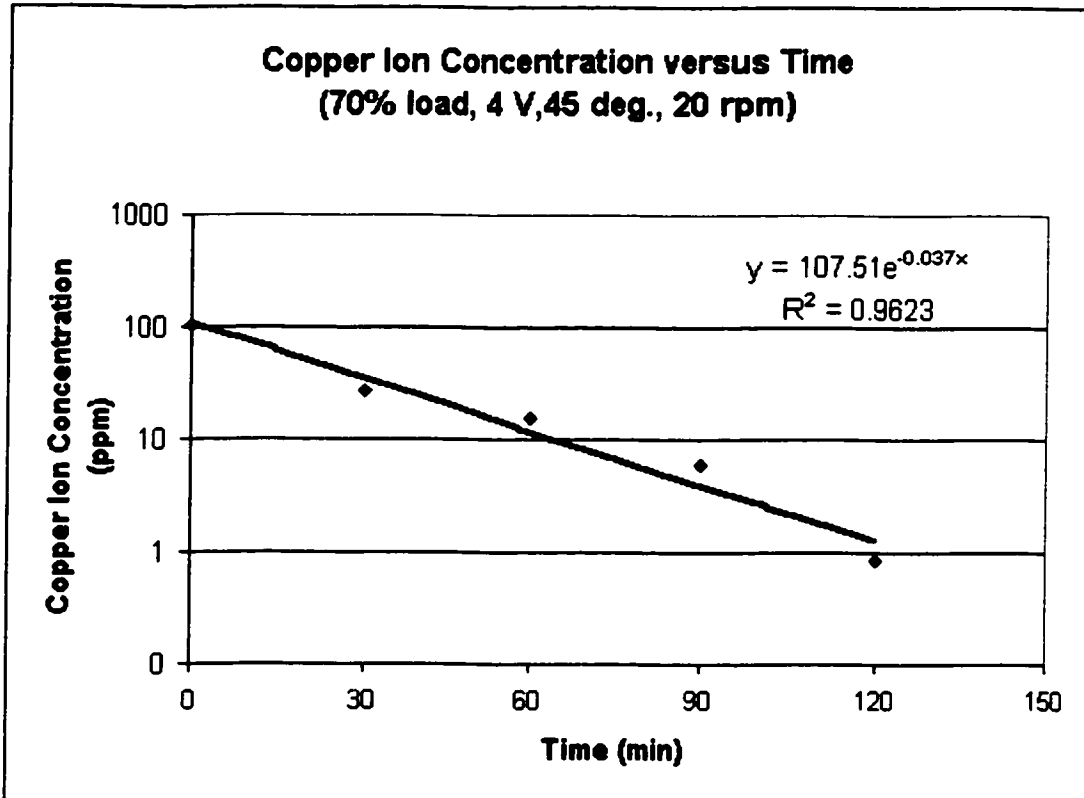


Figure. A-16. Copper ion concentration versus electrolysis time.

Table. A-33. Fixed operation parameters

Voltage (V)	5.03
Current (A)	1.65
Barrel load	70%
Barrel Immersion angle	45
Barrel Immersion percent	50%
Rotating speed (rpm)	20
water volume (lit.)	14
Na2SO4 weight (g)	85.64
CuSO4 weight (g)	5.34
Temperature (C)	22.9

$$(\text{ppm})=0.3647e^{0.0852*(\text{mV})}$$

$$\text{area (70\%)}=0.8383 \text{ m}^2$$

$$V/A=0.0167 \text{ m}$$

$$k= 0.000548 \text{ m/min}$$

$$9.13E-06 \text{ m/s}$$

Table. A-34. Experimental measurements

Time (min)	ppm	mV	pH
0	108.98	66.9	5.45
15	37.89	54.5	3.74
30	21.96	48.1	3.43
45	17.90	45.7	3.34
60	21.05	47.6	3.27
75	20.87	47.5	3.19
90	5.91	32.7	3.18
105	3.02	24.8	3.16
120	0.89	10.5	3.16

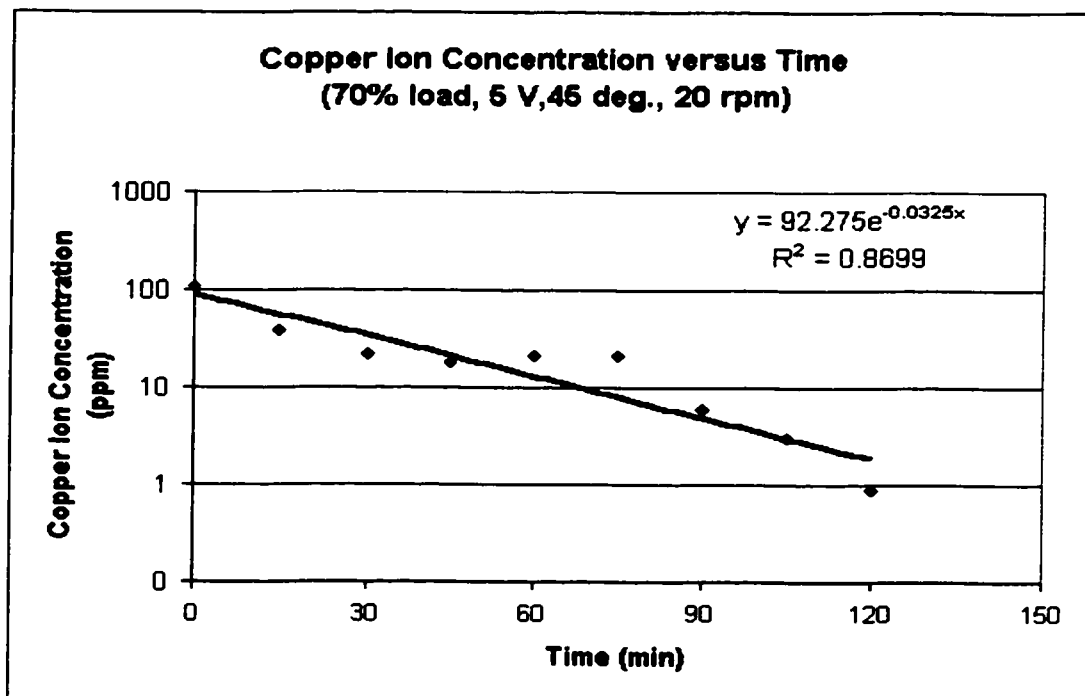


Figure. A-17. Copper ion concentration versus electrolysis time.

Table. A-35. Fixed operation parameters

Voltage (V)	6.03
Current (A)	2.2
Barrel load	70%
Barrel Immersion angle	45
Barrel Immersion percent	50%
Rotating speed (rpm)	20
water volume (lit.)	14
Na ₂ SO ₄ weight (g)	85.47
CuSO ₄ weight (g)	5.33
Temperature (C)	23.1

$$(\text{ppm})=0.3647e^{0.0852*(\text{mV})}$$

$$\text{area (70\%)}=0.8383 \text{ m}^2$$

$$V/A=0.0167 \text{ m}$$

$$k= 0.000666 \text{ m/min}$$

$$1.11\text{E-}05 \text{ m/s}$$

Table. A-36. Experimental measurements

Time (min)	ppm	mV	pH
0	117.6695	67.8	5.44
15	29.09597	51.4	3.76
30	26.49298	50.3	3.51
45	74.27689	62.4	3.33
60	31.41482	52.3	3.28
75	14.59209	43.3	3.19
90	3.428352	26.3	3.19
105	1.377734	15.6	3.18
120	0.608061	6	3.18

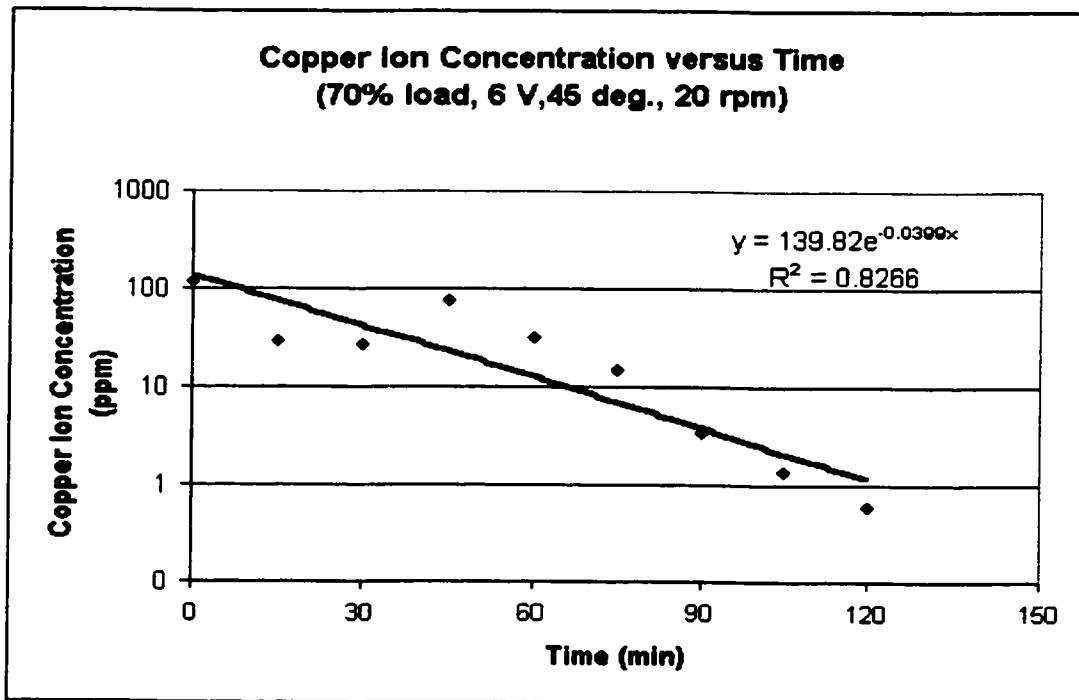


Figure. A-18. Copper ion concentration versus electrolysis time.

Table. A-37. Fixed operation parameters

Voltage (V)	2.5
Current (A)	0.8
Barrel load	70%
Barrel Immersion angle	45
Barrel Immersion percent	50%
Rotating speed (rpm)	20
water volume (lit.)	14
Na ₂ SO ₄ weight (g)	85.69
CuSO ₄ weight (g)	5.31
Temperature (C)	23.6

$$(\text{ppm}) = 0.3647e^{0.0852 \cdot (\text{mV})}$$

$$\text{area (70\%)} = 0.8383 \text{ m}^2$$

$$V/A = 0.0167 \text{ m}$$

$$k = 0.000247 \text{ m/min}$$

$$4.12E-06 \text{ m/s}$$

Table. A-38. Experimental measurements

Time (min)	ppm	mV	pH
0	102.67	66.2	5.5
15	40.56	55.3	3.84
30	36.31	54	3.69
45	32.78	52.8	3.56
75	21.96	48.1	3.42
115	16.87	45	3.2
135	11.20	40.2	3.15
155	9.06	37.7	3.12
175	4.50	29.5	3.11
195	3.49	26.5	3.1
210	2.77	23.8	3.1

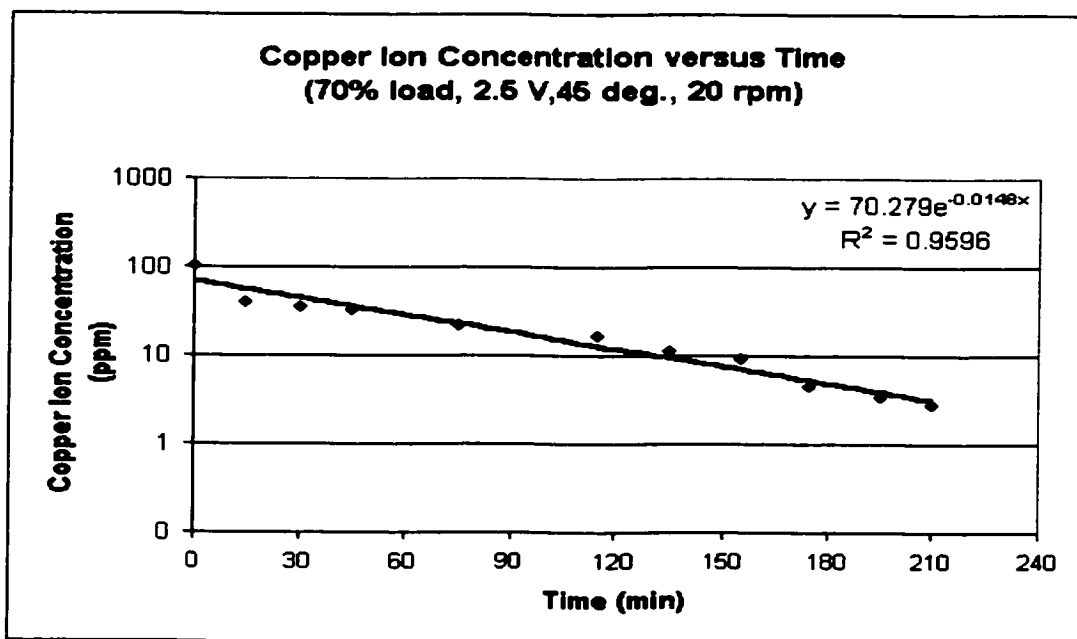


Figure. A-19. Copper ion concentration versus electrolysis time.

Table. A-39. Fixed operation parameters

Voltage (V)	5.3
Current (A)	2.02
Barrel load	70%
Barrel Immersion angle	45
Barrel Immersion percent	50%
Rotating speed (rpm)	20
water volume (lit.)	14
Na ₂ SO ₄ weight (g)	85.36
CuSO ₄ weight (g)	5.32
Temperature (C)	24.6

$$(\text{ppm})=0.3647e^{0.0852*(\text{mV})}$$

$$\text{area (70\%)}=0.8383 \text{ m}^2$$

$$V/A=0.0167 \text{ m}$$

$$k=0.000636 \text{ m/min}$$

$$1.06E-05 \text{ m/s}$$

Table. A-40. Experimental measurements

Time (min)	ppm	mV	pH
0	91.13	64.8	5.44
15	31.95	52.5	3.84
30	26.49	50.3	3.67
45	40.56	55.3	3.34
60	34.80	53.5	3.24
75	9.95	38.8	3.22
90	4.35	29.1	3.23
105	1.66	17.8	3.2
120	0.56	5	3.2

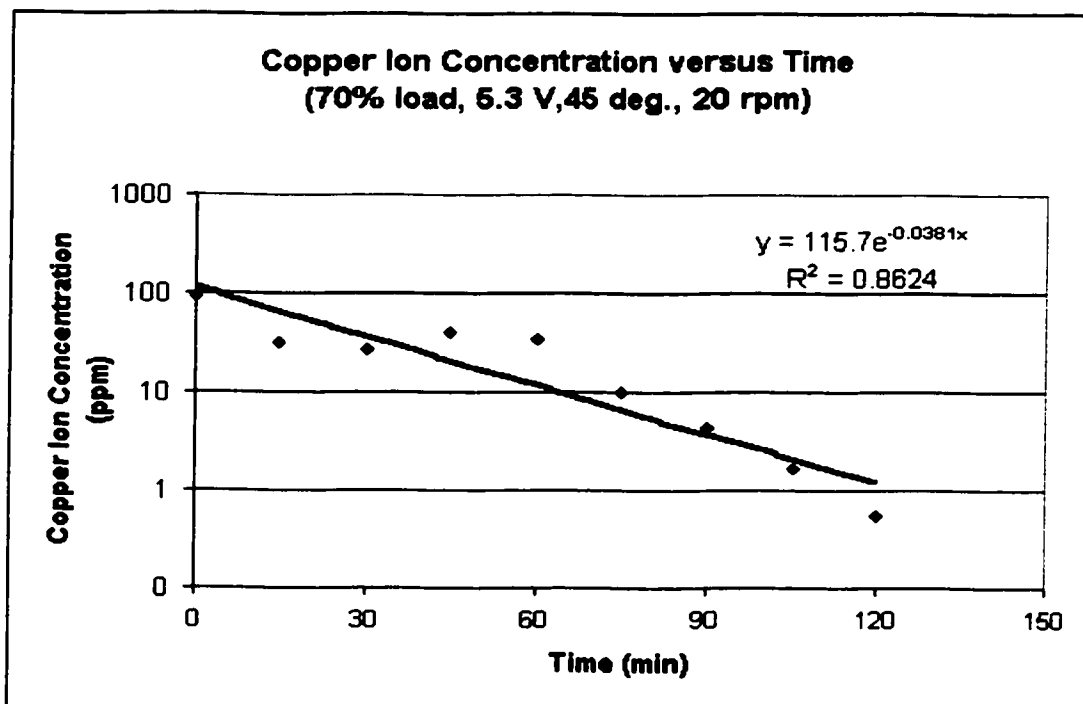


Figure. A-20. Copper ion concentration versus electrolysis time.

Table. A-41. Fixed operation parameters

Voltage (V)	7.02
Current (A)	2.85
Barrel load	70%
Barrel Immersion angle	45
Barrel Immersion percent	50%
Rotating speed (rpm)	20
water volume (lit.)	14
Na ₂ SO ₄ weight (g)	85.58
CuSO ₄ weight (g)	5.31
Temperature (C)	24.5

$$(\text{ppm})=0.3647e0.0852*(\text{mV})$$

$$\text{area (70\%)}=0.8383 \text{ m}^2$$

$$V/A=0.0167 \text{ m}$$

$$k= 0.000807 \text{ m/min}$$

$$1.34E-05 \text{ m/s}$$

Table. A-42. Experimental measurements

Time (min)	ppm	mV	pH
0	98.39	65.7	5.33
15	44.17	56.3	4.23
30	97.56	65.6	4.41
45	95.91	65.4	4.66
60	37.89	54.5	4.02
75	7.64	35.7	3.33
90	1.86	19.1	3.33
105	0.54	4.7	3.22

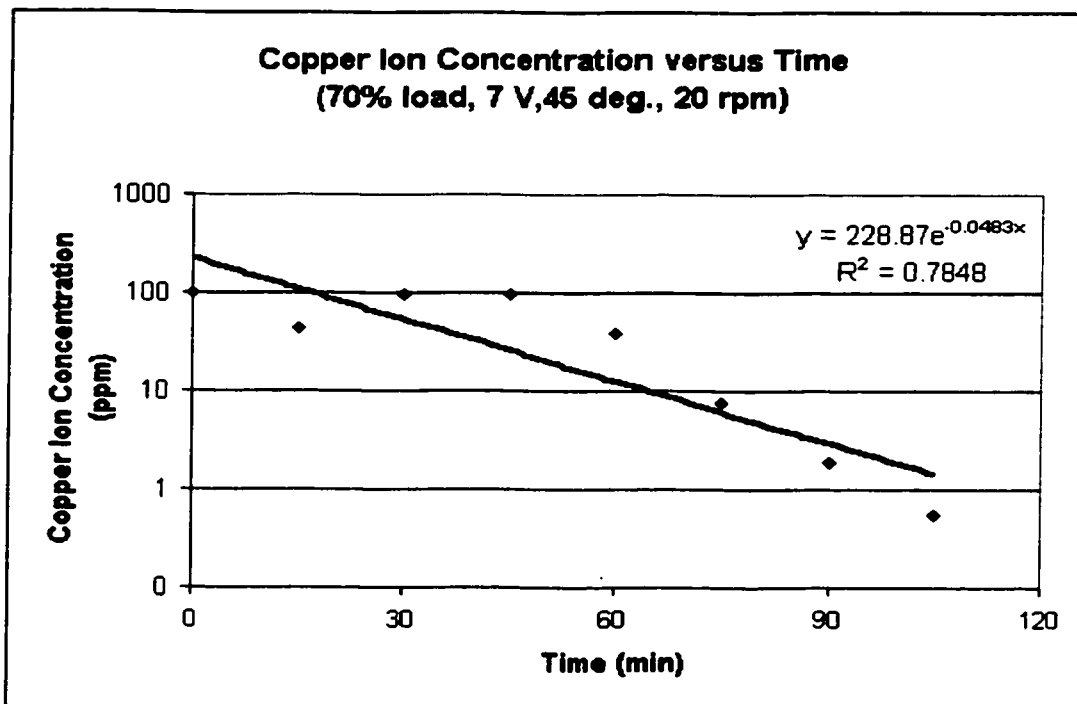


Figure. A-21. Copper ion concentration versus electrolysis time.

Table. A-43. Fixed operation parameters

Voltage (V)	4
Current (A)	1.1
Barrel load	15%
Barrel Immersion angle	45
Barrel Immersion percent	50%
Rotating speed (rpm)	20
water volume (lit.)	14
Na ₂ SO ₄ weight (g)	85.44
CuSO ₄ weight (g)	5.31
Temperature (C)	23.2

$$(\text{ppm})=0.3647e^{0.0852*(\text{mV})}$$

$$\text{area (15\%)}=0.1771 \text{ m}^2$$

$$V/A=0.079 \text{ m}$$

$$k= 0.00162 \text{ m/min}$$

$$2.7E-05 \text{ m/s}$$

Table. A-44. Experimental measurements

Time (min)	ppm	mV	pH
0	91.90908	64.9	5.42
15	39.8786	55.1	3.63
30	25.38808	49.8	3.41
45	29.84925	51.7	3.35
60	43.79676	56.2	3.26
75	38.54243	54.7	3.22
110	12.41121	41.4	3.14
140	5.431198	31.7	3.1
170	2.14573	20.8	3.08
190	1.500262	16.6	3.08
210	0.947015	11.2	3.08

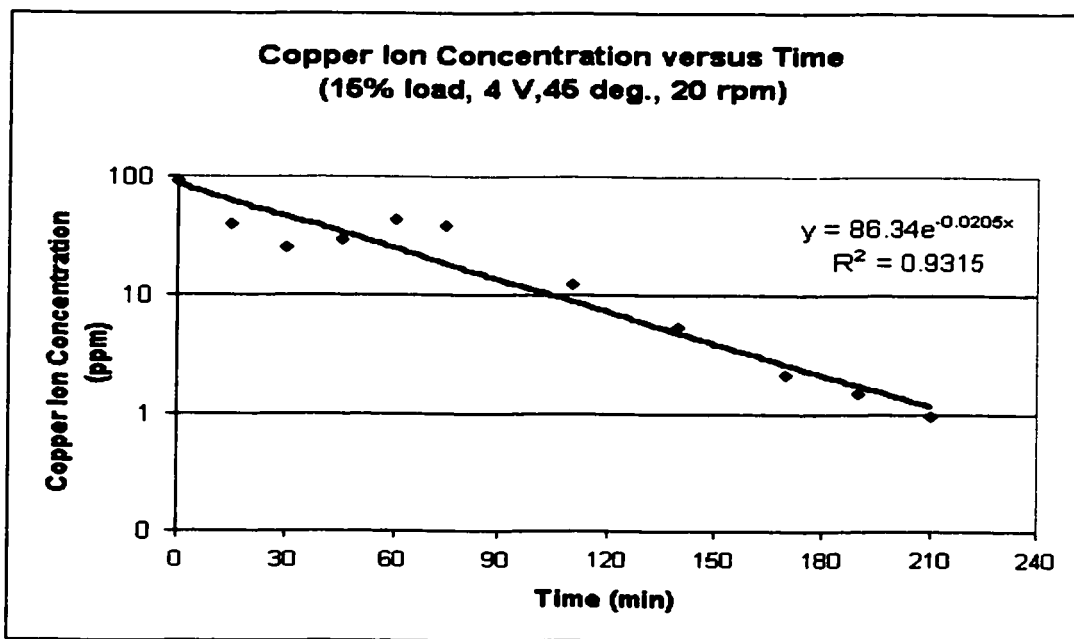


Figure. A-22. Copper ion concentration versus electrolysis time.

Table. A-45. Fixed operation parameters

Voltage (V)	6.04
Current (A)	1.75
Barrel load	15%
Barrel Immersion angle	45
Barrel Immersion percent	50%
Rotating speed (rpm)	20
water volume (lit.)	14
Na ₂ SO ₄ weight (g)	85.57
CuSO ₄ weight (g)	5.31
Temperature (C)	22.8

$$(\text{ppm}) = 0.3647e^{0.0852 \cdot (\text{mV})}$$

$$\text{area (15\%)} = 0.1771 \text{ m}^2$$

$$V/A = 0.079 \text{ m}$$

$$k = 0.001525 \text{ m/min}$$

$$2.54E-05 \text{ m/s}$$

Table. A-46. Experimental measurements

Time (min)	ppm	mV	pH
0	83.69	63.8	5.42
15	32.78	52.8	4.25
30	27.88	50.9	3.87
45	19.83	46.9	3.58
60	14.97	43.6	3.49
90	8.32	36.7	3.3
120	6.95	34.6	3.25

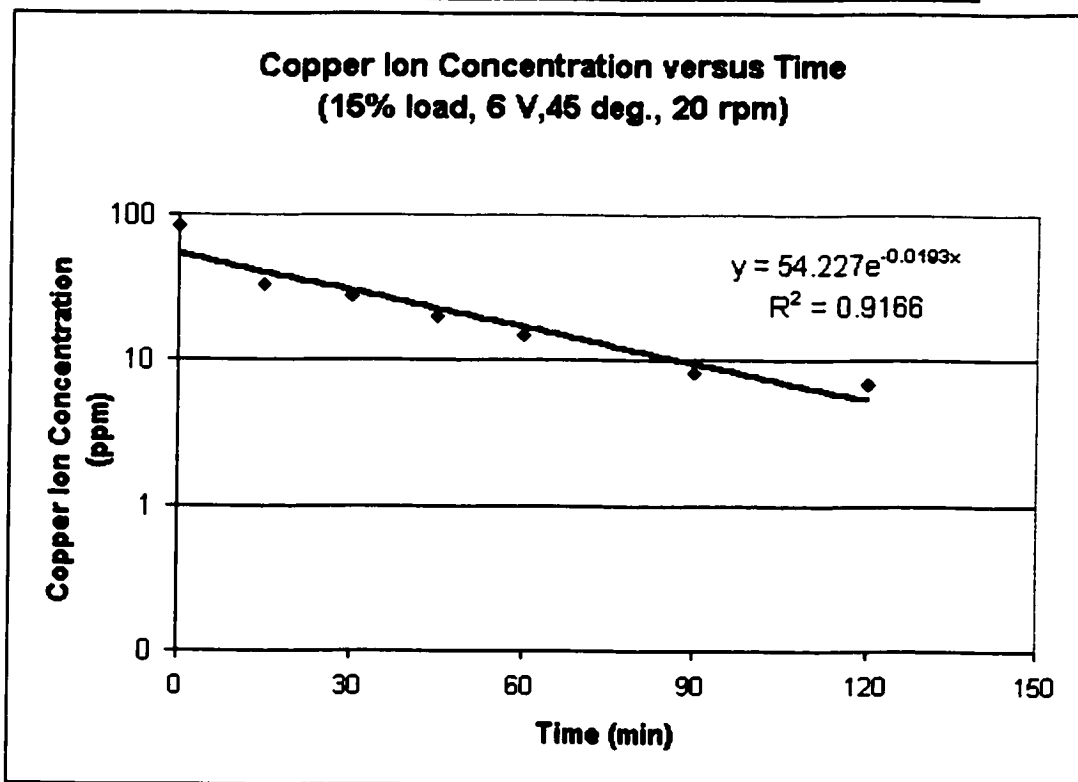


Figure. A-23. Copper ion concentration versus electrolysis time.

Table. A-49. Fixed operation parameters

Voltage (V)	3.02
Current (A)	0.78
Barrel load	15%
Barrel Immersion angle	45
Barrel Immersion percent	50%
Rotating speed (rpm)	20
water volume (lit.)	14
Na ₂ SO ₄ weight (g)	85.51
CuSO ₄ weight (g)	5.31
Temperature (C)	24.5

$$(\text{ppm}) = 0.383e^{0.0836 * (\text{mV})}$$

$$\text{area (15\%)} = 0.1771 \text{ m}^2$$

$$V/A = 0.079 \text{ m}$$

$$k = 0.000972 \text{ m/min}$$

$$1.62E-05 \text{ m/s}$$

Table. A-50. Experimental measurements

Time (min)	ppm	mV	pH
0	101.13	66.7	5.39
15	44.57	56.9	3.83
30	37.08	54.7	3.65
45	40.32	55.7	3.49
60	70.00	62.3	3.39
75	77.39	63.5	3.33
90	59.72	60.4	3.28
105	66.58	61.7	3.24
180	10.06	39.1	3.16
215	4.78	30.2	3.15
270	2.45	22.2	3.11
320	2.33	21.6	3.11

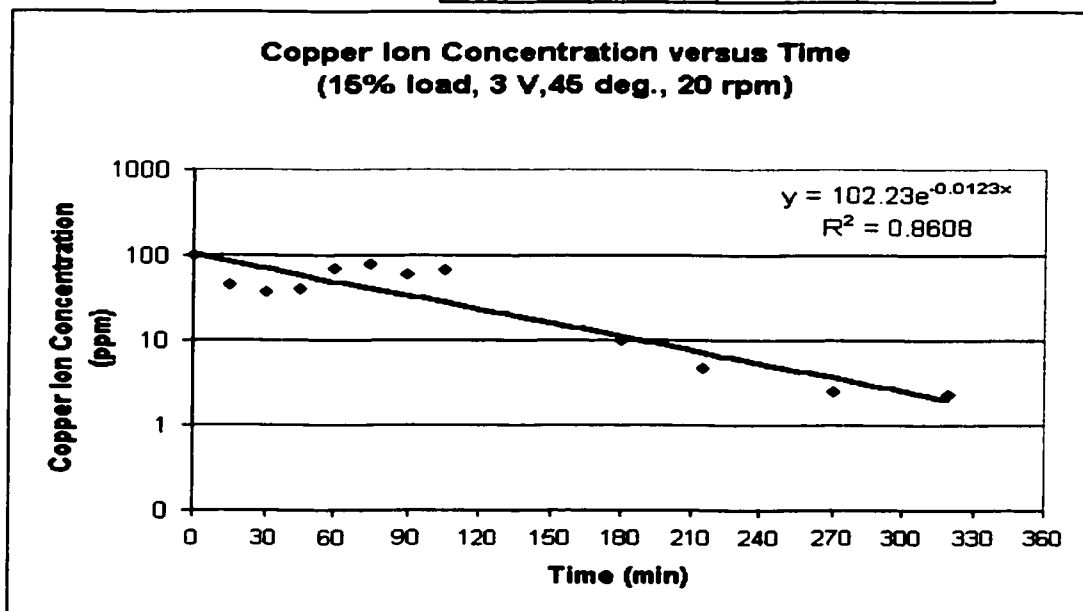


Figure. A-24. Copper ion concentration versus electrolysis time.

Table. A-51. Fixed operation parameters

Voltage (V)	2.54
Current (A)	0.58
Barrel load	15%
Barrel Immersion angle	45
Barrel Immersion percent	50%
Rotating speed (rpm)	20
water volume (lit.)	14
Na ₂ SO ₄ weight (g)	85.52
CuSO ₄ weight (g)	5.33
Temperature (C)	24

$$(\text{ppm})=0.383e^{0.0836*(\text{mV})}$$

$$\text{area (15\%)}=0.1771 \text{ m}^2$$

$$V/A=0.079 \text{ m}$$

$$k=0.00083 \text{ m/min}$$

$$1.38E-05 \text{ m/s}$$

Table. A-52. Experimental measurements

Time (min)	ppm	mV	pH
0	109.9471	67.7	5.43
15	56.32845	59.7	3.86
30	46.8654	57.5	3.69
45	38.99213	55.3	3.56
60	31.63802	52.8	3.45
75	34.11031	53.7	3.36
90	51.81086	58.7	3.3
105	39.64955	55.5	3.28
135	40.99785	55.9	3.22
205	13.94442	43	3.16
240	2.872089	24.1	3.14
256	3.913217	27.8	3.14
280	6.681882	34.2	3.14

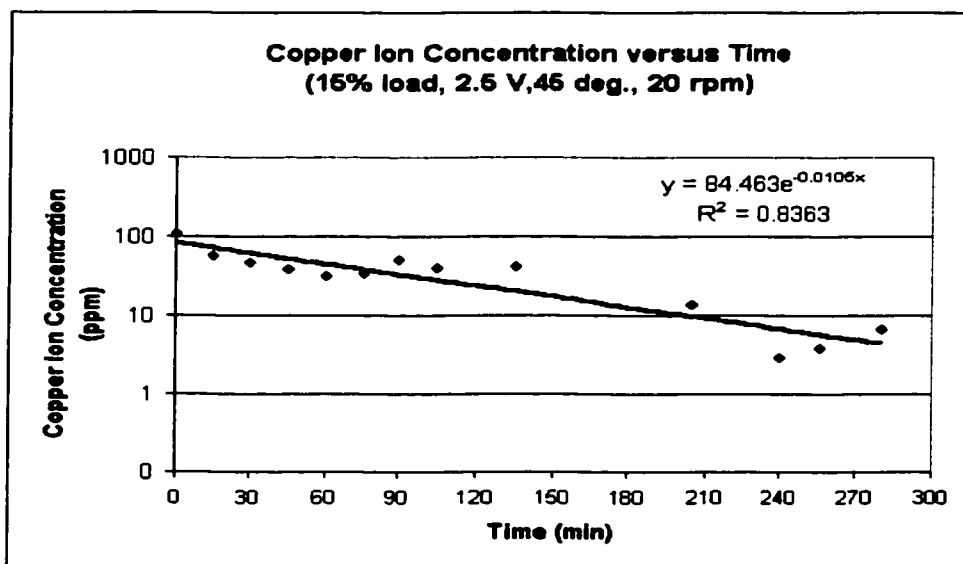


Figure. A-25. Copper ion concentration versus electrolysis time.

Table. A-53. Fixed operation parameters

Voltage (V)	5
Current (A)	1.25
Barrel load	15%
Barrel Immersion angle	45
Barrel Immersion percent	50%
Rotating speed (rpm)	20
water volume (lit.)	14
Na ₂ SO ₄ weight (g)	85.5
CuSO ₄ weight (g)	5.32
Temperature (C)	24.5

$$(\text{ppm})=0.383e0.0836*(\text{mV})$$

$$\text{area (15\%)}=0.1771 \text{ m}^2$$

$$V/A=0.079 \text{ m}$$

$$k= 0.000403 \text{ m/min}$$

$$6.72E-06 \text{ m/s}$$

Table. A-54. Experimental measurements

Time (min)	ppm	mV	pH
0	101.9783	66.8	5.33
15	56.32845	59.7	4.36
30	63.32244	61.1	4.06
60	105.4461	67.2	3.55
90	99.45246	66.5	3.45
155	28.61811	51.6	3.31

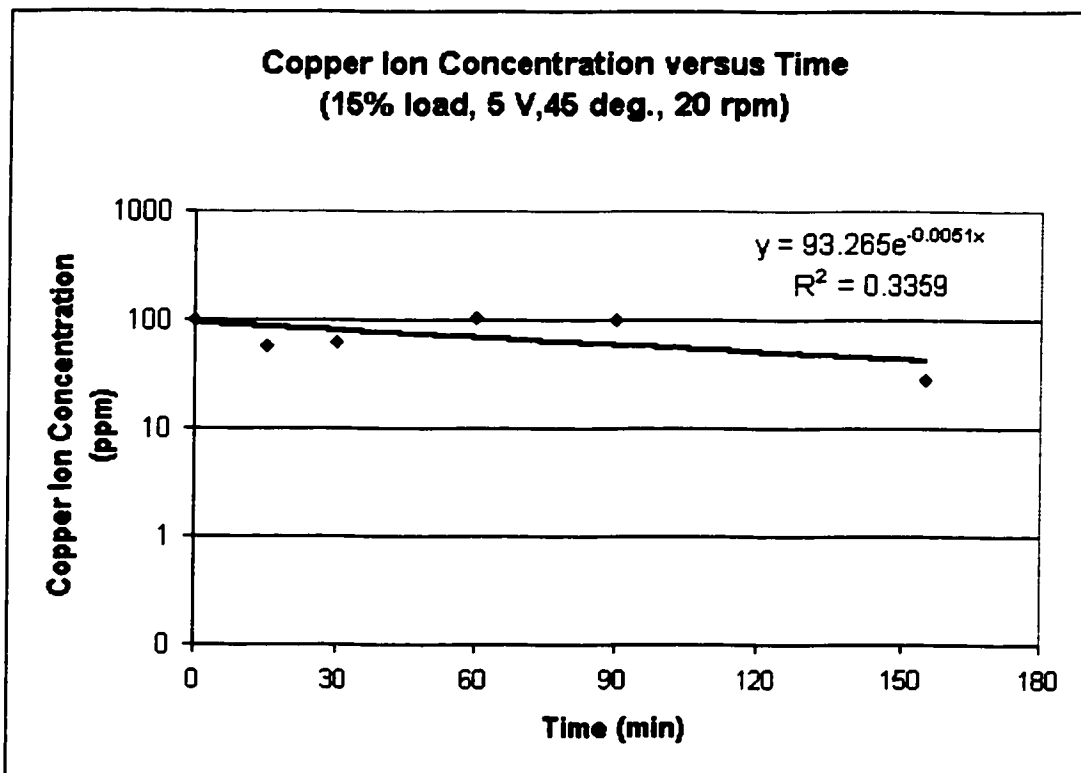


Figure. A-26. Copper ion concentration versus electrolysis time.

Table. A-55. Fixed operation parameters

Voltage (V)	4.51
Current (A)	1.25
Barrel load	15%
Barrel Immersion angle	45
Barrel Immersion percent	50%
Rotating speed (rpm)	20
water volume (lit.)	14
Na ₂ SO ₄ weight (g)	85.56
CuSO ₄ weight (g)	5.33
Temperature (C)	23.5

$$(\text{ppm})=0.383e0.0836*(\text{mV})$$

$$\text{area (15\%)}=0.1771 \text{ m}^2$$

$$V/A=0.079 \text{ m}$$

$$k= 0.000909 \text{ m/min}$$

$$1.51E-05 \text{ m/s}$$

Table. A-56. Experimental measurements

Time (min)	ppm	mV	pH
0	100.29	66.6	5.38
15	41.34	56	3.81
30	30.34	52.3	3.58
75	13.71	42.8	3.26
95	10.85	40	3.2
115	9.73	38.7	3.16
150	7.77	36	3.11
230	5.65	32.2	3.07

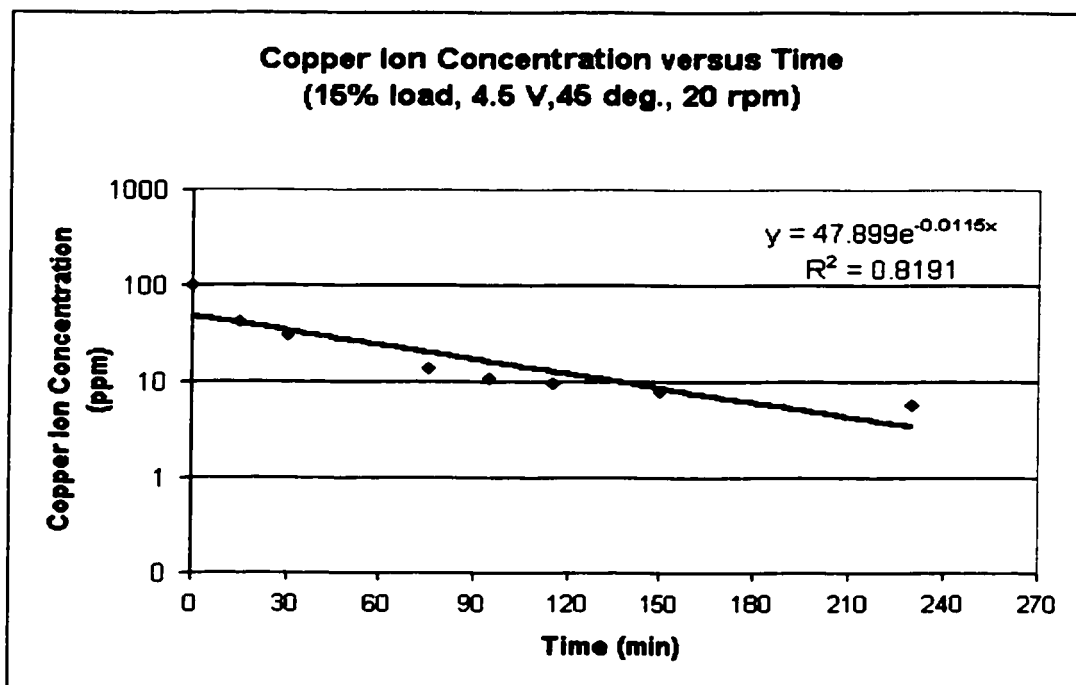


Figure. A-27. Copper ion concentration versus electrolysis time.

Barrel Rotation Speed Effect

Table. A-57. Fixed operation parameters

Voltage (V)	4.51
Current (A)	1.42
Barrel load	50%
Barrel Immersion angle	45
Barrel Immersion percent	50%
Rotating speed (rpm)	16
water volume (lit.)	14
Na ₂ SO ₄ weight (g)	85.5
CuSO ₄ weight (g)	5.32
Temperature (C)	22.5

$$(\text{ppm})=0.383e0.0836*(\text{mV})$$

$$\text{area (50\%)}=0.5905 \text{ m}^2$$

$$V/A=0.02371 \text{ m}$$

$$k= 0.000692 \text{ m/min}$$

$$1.15E-05 \text{ m/s}$$

Table. A-58. Experimental measurements

Time (min)	ppm	mV	pH
0	100.29	66.6	5.2
15	43.83	56.7	3.75
38	23.61	49.3	3.52
53	15.29	44.1	3.34
73	9.26	38.1	3.24
115	2.82	23.9	3.15
170	0.56	4.6	3.13

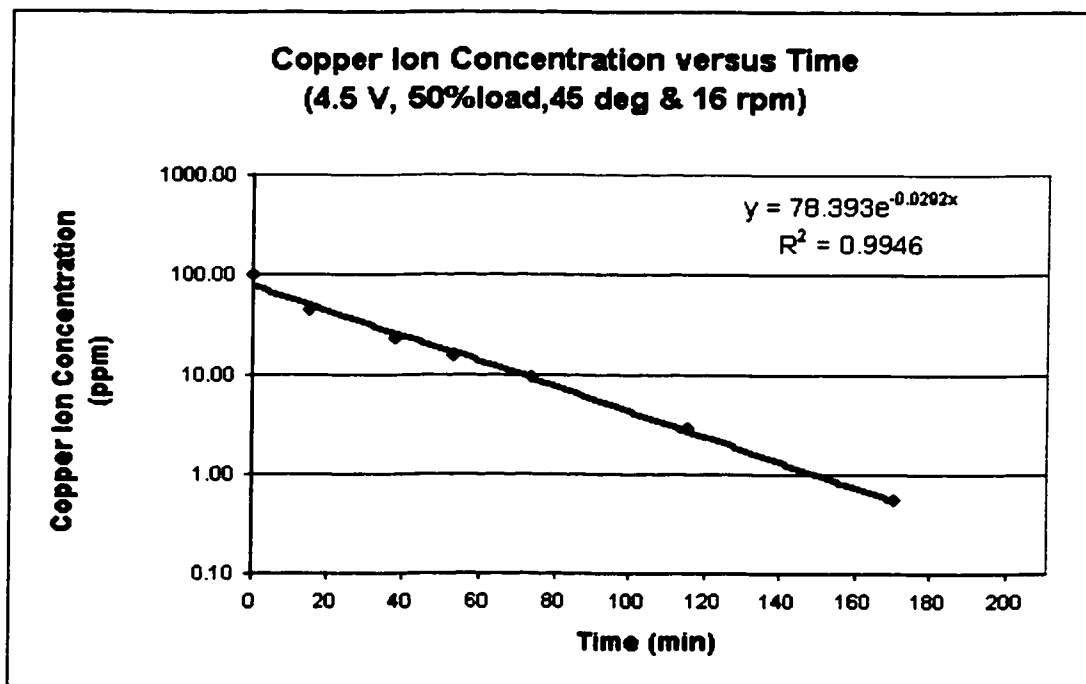


Figure. A-28. Copper ion concentration versus electrolysis time.

Table. A-59. Fixed operation parameters

Voltage (V)	4.51
Current (A)	1.28
Barrel load	50%
Barrel Immersion angle	45
Barrel Immersion percent	50%
Rotating speed (rpm)	12
water volume (lit.)	14
Na2SO4 weight (g)	85.58
CuSO4 weight (g)	5.31
Temperature (C)	21.5

$$(\text{ppm})=0.383e0.0836*(\text{mV})$$

$$\text{area (50\%)}=0.5905 \text{ m}^2$$

$$V/A=0.02371 \text{ m}$$

$$k= 0.000595 \text{ m/min}$$

$$9.92E-06 \text{ m/s}$$

Table. A-60. Experimental measurements

Time (min)	ppm	mV	pH
0	114.64	68.2	5.42
15	52.25	58.8	3.78
30	34.40	53.8	3.53
60	19.32	46.9	3.31
90	10.41	39.5	3.22
140	2.55	22.7	3.18
165	1.50	16.3	3.16
175	1.04	12	3.16

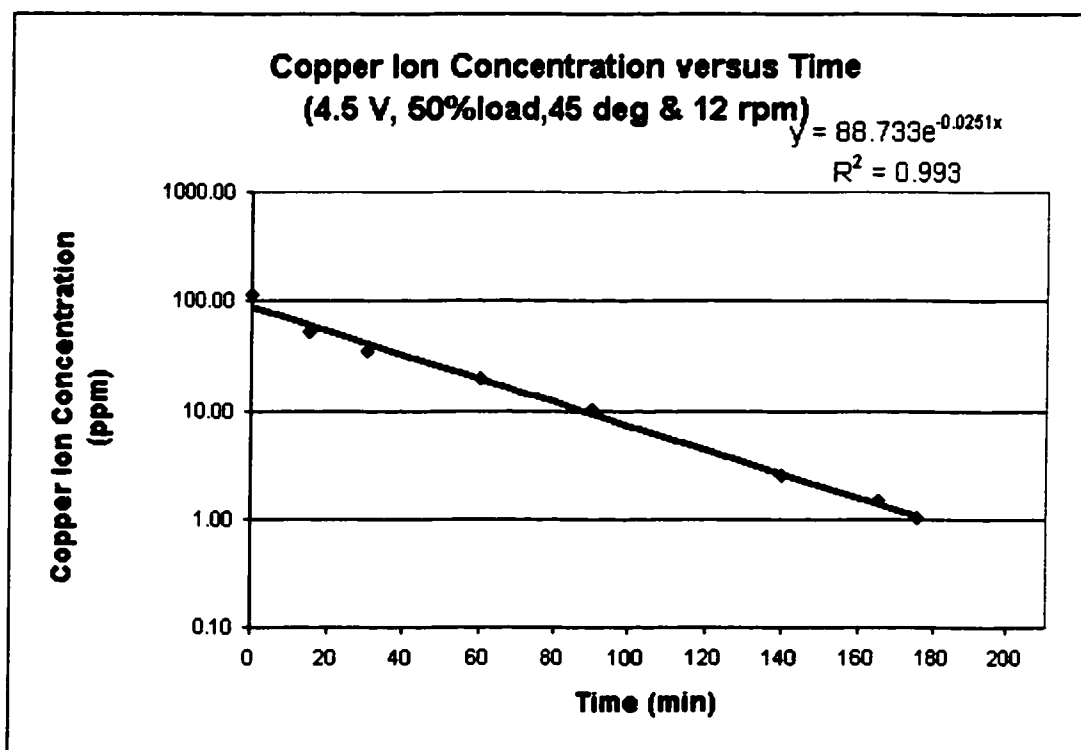


Figure. A-29. Copper ion concentration versus electrolysis time.

Table. A-61. Fixed operation parameters

Voltage (V)	4.52
Current (A)	1.23
Barrel load	50%
Barrel Immersion angle	45
Barrel Immersion percent	50%
Rotating speed (rpm)	8
water volume (lit.)	14
Na ₂ SO ₄ weight (g)	85.5
CuSO ₄ weight (g)	5.32
Temperature (C)	21.7

$$(\text{ppm})=0.383e0.0836*(\text{mV})$$

$$\text{area (50\%)}=0.5905 \text{ m}^2$$

$$V/A=0.02371 \text{ m}$$

$$k= 0.000538 \text{ m/min}$$

$$8.97\text{E-}06 \text{ m/s}$$

Table. A-62. Experimental measurements

Time (min)	ppm	mV	pH
0	126.74	69.4	5.39
15	62.27	60.9	3.94
30	40.66	55.8	3.68
60	22.27	48.6	3.47
120	6.30	33.5	3.25
140	3.57	26.7	3.23
160	2.39	21.9	3.26
180	1.91	19.2	3.3

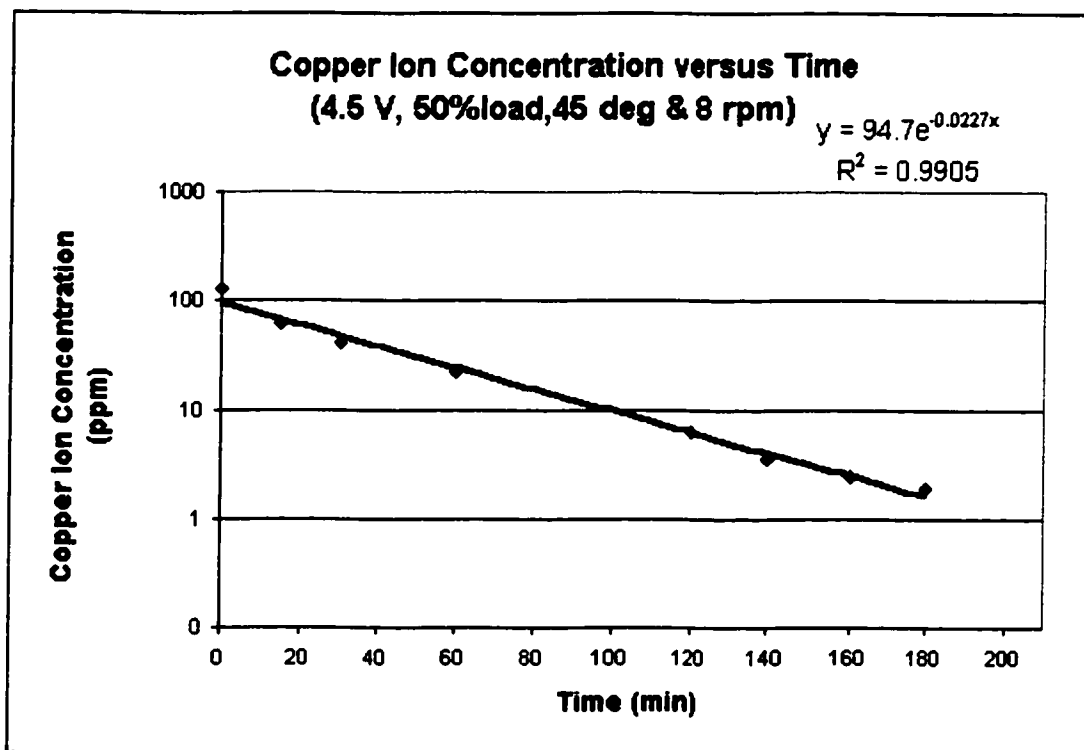


Figure. A-30. Copper ion concentration versus electrolysis time.

Table. A-63. Fixed operation parameters

Voltage (V)	4.51
Current (A)	1.4
Barrel load	50%
Barrel Immersion angle	45
Barrel Immersion percent	50%
Rotating speed (rpm)	20
water volume (lit.)	14
Na2SO4 weight (g)	85.55
CuSO4 weight (g)	5.31
Temperature (C)	22.4

$$(\text{ppm})=0.383e0.0836*(\text{mV})$$

$$\text{area (50\%)}=0.5905 \text{ m}^2$$

$$V/A=0.02371 \text{ m}$$

$$k= 0.000676 \text{ m/min}$$

$$1.13E-05 \text{ m/s}$$

Table. A-64. Experimental measurements

Time (min)	ppm	mV	pH
0	105.45	67.2	5.32
15	43.83	56.7	3.73
30	27.68	51.2	3.51
60	10.58	39.7	3.24
90	4.63	29.8	3.17
130	1.59	17	3.14
145	1.33	14.9	3.13
155	1.05	12.1	3.15

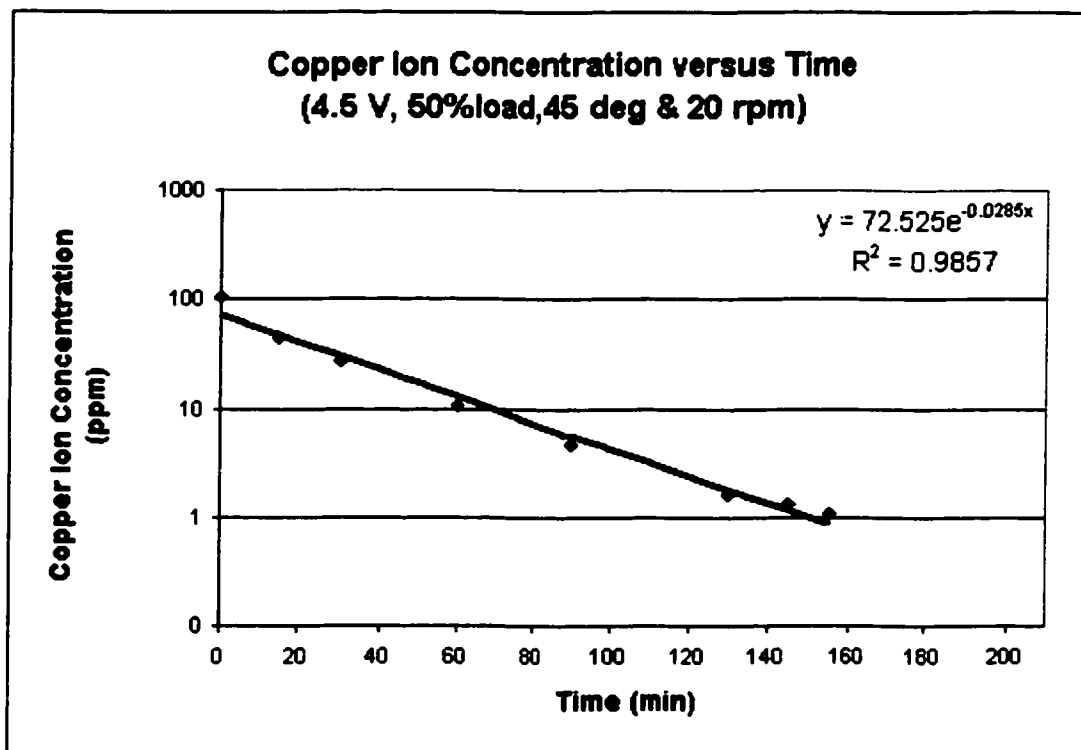


Figure. A-31. Copper ion concentration versus electrolysis time.

Table. A-65. Fixed operation parameters

Voltage (V)	4.52
Current (A)	1.2
Barrel load	50%
Barrel Immersion angle	45
Barrel Immersion percent	50%
Rotating speed (rpm)	4
water volume (lit.)	14
Na ₂ SO ₄ weight (g)	85.45
CuSO ₄ weight (g)	5.33
Temperature (C)	21.4

$$(\text{ppm})=0.383e0.0836*(\text{mV})$$

$$\text{area (50\%)}=0.5905 \text{ m}^2$$

$$V/A=0.02371 \text{ m}$$

$$k= 0.000424 \text{ m/min}$$

$$7.07\text{E-}06 \text{ m/s}$$

Table. A-66. Experimental measurements

Time (min)	ppm	mV	pH
0	126.74	69.4	5.29
15	53.13	59	3.89
30	55.86	59.6	3.78
45	98.62	66.4	3.65
70	47.66	57.7	3.49
120	11.22	40.4	3.31
150	7.45	35.5	3.23

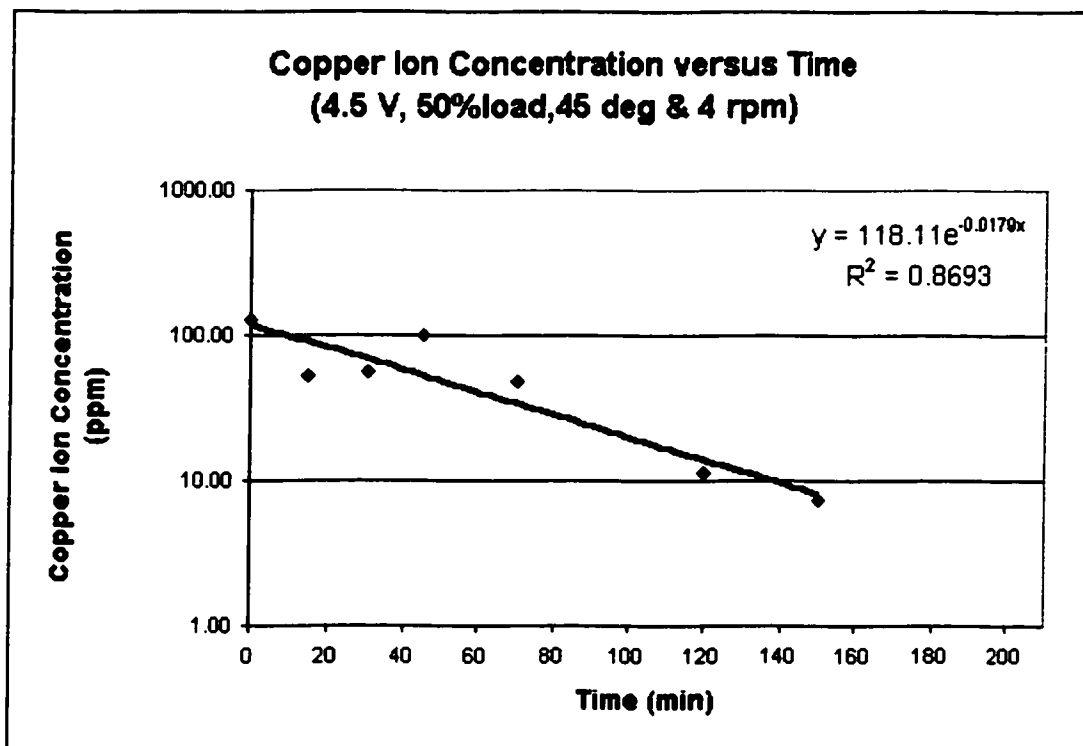


Figure. A-32. Copper ion concentration versus electrolysis time.

Table. A-67. Fixed operation parameters

Voltage (V)	3.51
Current (A)	0.95
Barrel load	50%
Barrel Immersion angle	45
Barrel Immersion percent	50%
Rotating speed (rpm)	16
water volume (lit.)	14
Na ₂ SO ₄ weight (g)	85.4
CuSO ₄ weight (g)	5.33
Temperature (C)	22.3

$$(\text{ppm})=0.383e^{0.0836*(\text{mV})}$$

$$\text{area (50\%)}=0.5905 \text{ m}^2$$

$$V/A=0.02371 \text{ m}$$

$$k=0.00056 \text{ m/min}$$

$$9.33E-06 \text{ m/s}$$

Table. A-68. Experimental measurements

Time (min)	ppm	mV	pH	I (A)
0	109.03	67.6	5.44	0.95
15	57.28	59.9	3.76	
30	38.99	55.3	3.51	
60	45.70	57.2	3.24	
120	4.82	30.3	3.08	0.82
140	5.29	31.4	3.18	
160	2.80	23.8	3.04	
180	1.26	14.2	3.04	
190	0.98	11.2	3.05	0.8

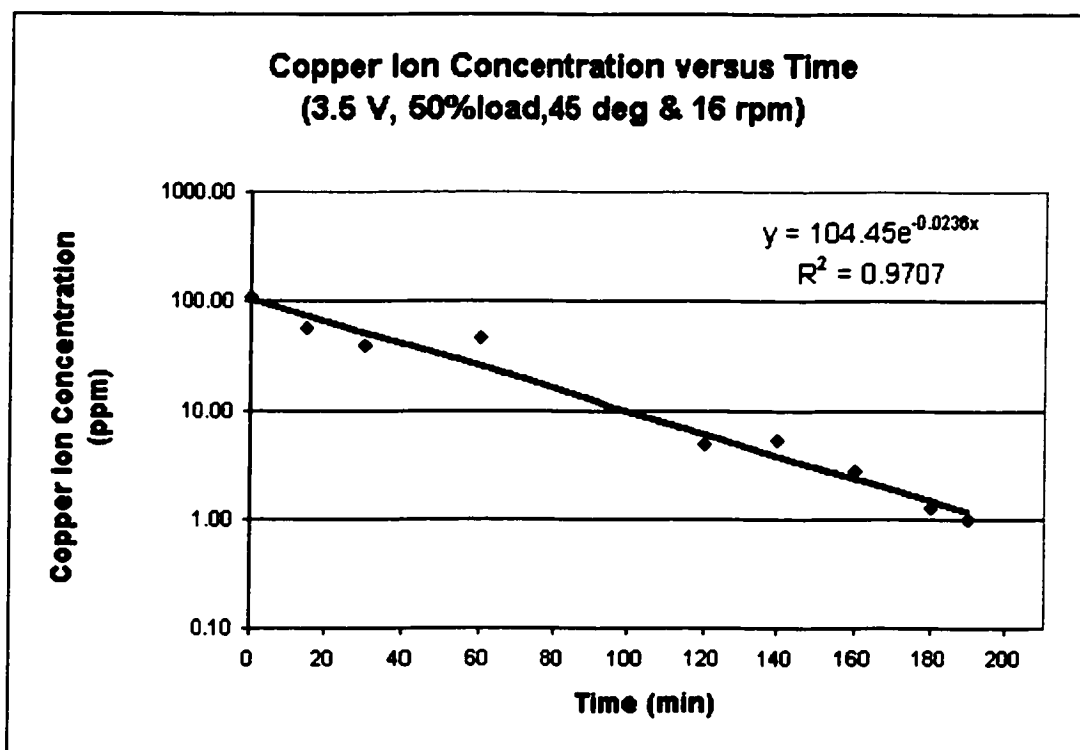


Figure. A-33. Copper ion concentration versus electrolysis time.

Table. A-69. Fixed operation parameters

Voltage (V)	4.52
Current (A)	1.55
Barrel load	50%
Barrel Immersion angle	45
Barrel Immersion percent	50%
Rotating speed (rpm)	18
water volume (lit.)	14
Na2SO4 weight (g)	85.46
CuSO4 weight (g)	5.32
Temperature (C)	28.3

$$(\text{ppm})=0.383e^{0.0836*(\text{mV})}$$

$$\text{area (50\%)}=0.5905 \text{ m}^2$$

$$V/A=0.02371 \text{ m}$$

$$k= 0.000825 \text{ m/min}$$

$$1.38E-05 \text{ m/s}$$

Table. A-70. Experimental measurements

Time (min)	ppm	mV	pH	I (A)
0	117.55	68.5	5.25	1.55
15	42.75	56.4	3.83	
30	23.61	49.3	3.57	
45	21.54	48.2	3.38	
65	17.19	45.5	3.28	
95	4.40	29.2	3.19	1.42
110	2.00	19.8	3.17	
125	1.12	12.8	3.17	
140	0.64	6.2	3.16	1.4

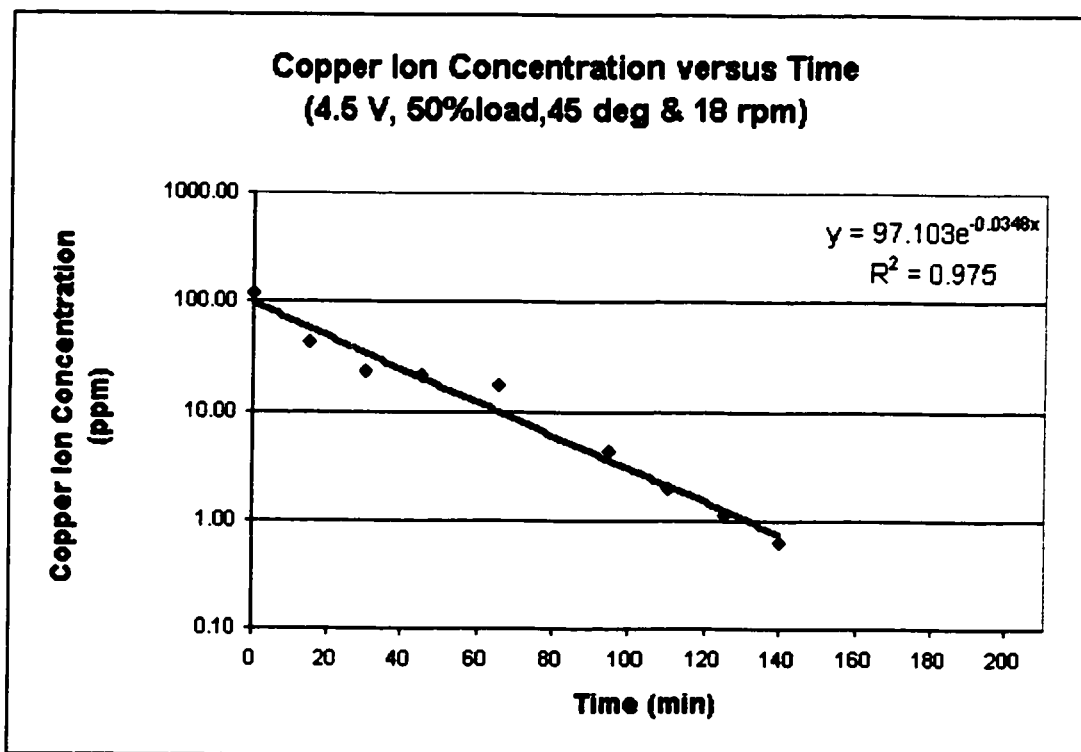


Figure. A-34. Copper ion concentration versus electrolysis time.

Table. A-71. Fixed operation parameters

Voltage (V)	3.51
Current (A)	1.1
Barrel load	50%
Barrel Immersion angle	45
Barrel Immersion percent	50%
Rotating speed (rpm)	18
water volume (lit.)	14
Na2SO4 weight (g)	85.5
CuSO4 weight (g)	5.32
Temperature (C)	23.2

$$(\text{ppm})=0.383e0.0836*(\text{mV})$$

$$\text{area (50\%)}=0.5905 \text{ m}^2$$

$$V/A=0.02371 \text{ m}$$

$$k= 0.000723 \text{ m/min}$$

$$1.21\text{E-}05 \text{ m/s}$$

Table. A-72. Experimental measurements

Time (min)	ppm	mV	pH	I (A)
0	109.03	67.6	5.3	1.1
15	43.11	56.5	3.73	
30	38.35	55.1	3.5	
45	22.46	48.7	3.38	
75	11.90	41.1	3.19	
97	4.66	29.9	3.08	
110	3.18	25.3	3.11	
125	1.59	17	3.11	
140	1.33	14.9	3.11	
157	0.81	9	3.15	0.84

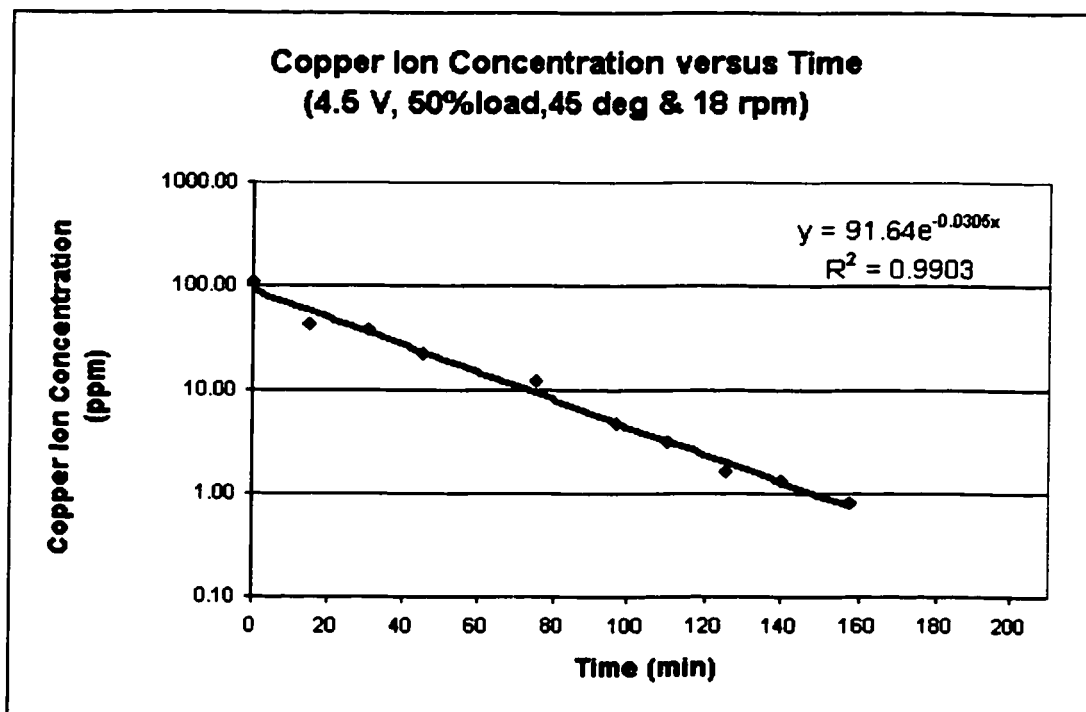


Figure. A-35. Copper ion concentration versus electrolysis time.

Table. A-73. Fixed operation parameters

Voltage (V)	3.5
Current (A)	0.95
Barrel load	50%
Barrel Immersion angle	45
Barrel Immersion percent	50%
Rotating speed (rpm)	12
water volume (lit.)	14
Na2SO4 weight (g)	85.66
CuSO4 weight (g)	5.31
Temperature (C)	24.6

$$(\text{ppm})=0.383e0.0836*(\text{mV})$$

$$\text{area (50\%)}=0.5905 \text{ m}^2$$

$$V/A=0.02371 \text{ m}$$

$$k= 0.000536 \text{ m/min}$$

$$8.93E-06 \text{ m/s}$$

Table. A-74. Experimental measurements

Time (min)	ppm	mV	pH	I (A)
0	124.64	69.2	5.31	0.95
15	53.13	59	3.83	
35	38.03	55	3.59	
60	20.14	47.4	3.38	0.88
85	17.04	45.4	3.26	
105	12.72	41.9	3.22	
140	4.59	29.7	3.18	0.8
160	2.69	23.3	3.17	
180	1.64	17.4	3.17	
195	0.98	11.2	3.16	0.78

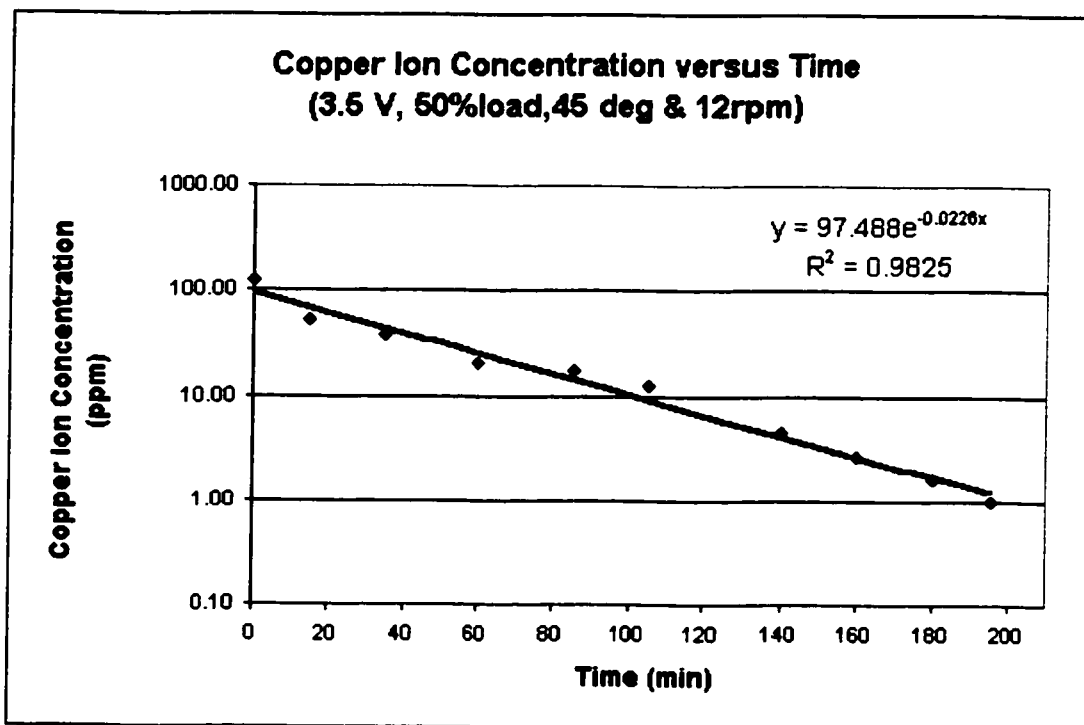


Figure. A-36. Copper ion concentration versus electrolysis time.

Table. A-75. Fixed operation parameters

Voltage (V)	3.51
Current (A)	1.1
Barrel load	50%
Barrel Immersion angle	45
Barrel Immersion percent	50%
Rotating speed (rpm)	20
water volume (lit.)	14
Na ₂ SO ₄ weight (g)	85.49
CuSO ₄ weight (g)	5.32
Temperature (C)	22.4

$$(\text{ppm})=0.383e^{0.0836*(\text{mV})}$$

$$\text{area (50\%)}=0.5905 \text{ m}^2$$

$$V/A=0.02371 \text{ m}$$

$$k= 0.000666 \text{ m/min}$$

$$1.11E-05 \text{ m/s}$$

Table. A-76. Experimental measurements

Time (min)	ppm	mV	pH	I(A)
0	110.87	67.8	5.31	
16	52.25	58.8	3.73	
30	59.72	60.4	3.53	
49	38.35	55.1		
70	21.54	48.2	3.23	
90	10.94	40.1	3.15	
110	8.03	36.4	3.13	
125	3.20	25.4	3.11	
140	2.35	21.7	3.12	0.85
158	1.40	15.5	3.1	
175	0.74	7.8	3.1	

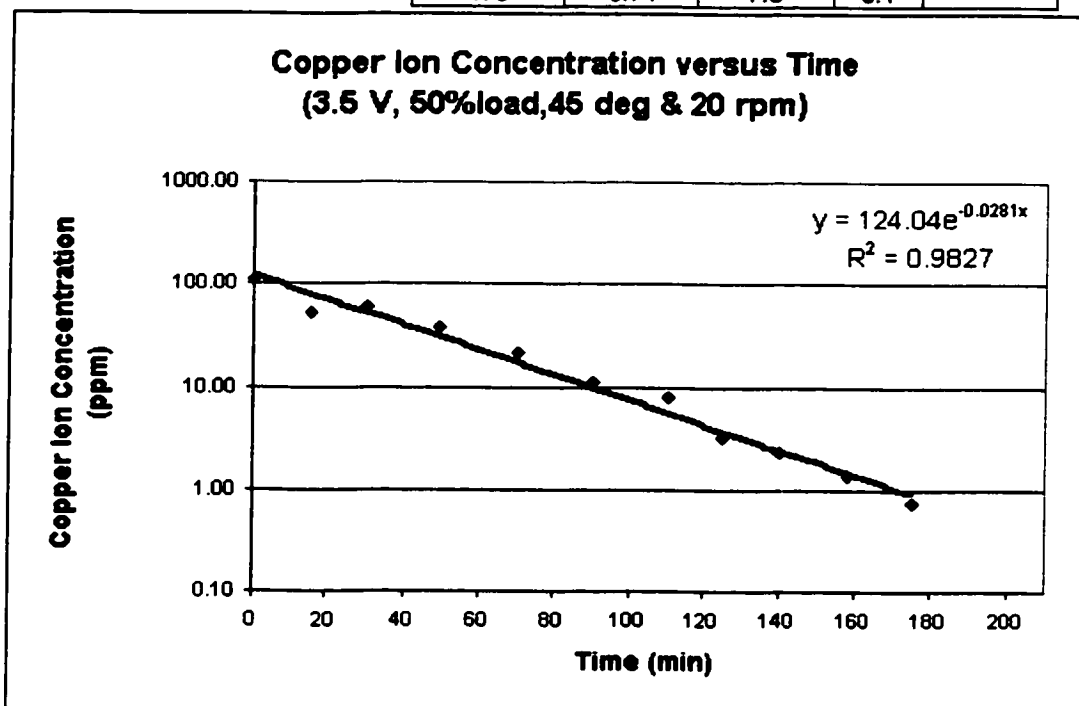


Figure. A-37. Copper ion concentration versus electrolysis time.

Table. A-77. Fixed operation parameters

Voltage (V)	3.5
Current (A)	1.42
Barrel load	50%
Barrel Immersion angle	45
Barrel Immersion percent	50%
Rotating speed (rpm)	8
water volume (lit.)	14
Na2SO4 weight (g)	85.5
CuSO4 weight (g)	5.32
Temperature (C)	20.8

$$(\text{ppm})=0.383e0.0836*(\text{mV})$$

$$\text{area (50\%)}=0.5905 \text{ m}^2$$

$$V/A=0.02371 \text{ m}$$

$$k= 0.000474 \text{ m/min}$$

$$7.9E-06 \text{ m/s}$$

Table. A-78. Experimental measurements

Time (min)	ppm	mV	I (A)
0	93.79952	65.8	0.86
20	29.34493	51.9	
40	23.61211	49.3	
60	23.81033	49.4	0.77
85	11.31444	40.5	
102	7.702306	35.9	
130	4.664216	29.9	
150	2.896201	24.2	0.78
170	2.125654	20.5	
190	1.496247	16.3	
205	1.098164	12.6	
212	0.952676	10.9	0.8

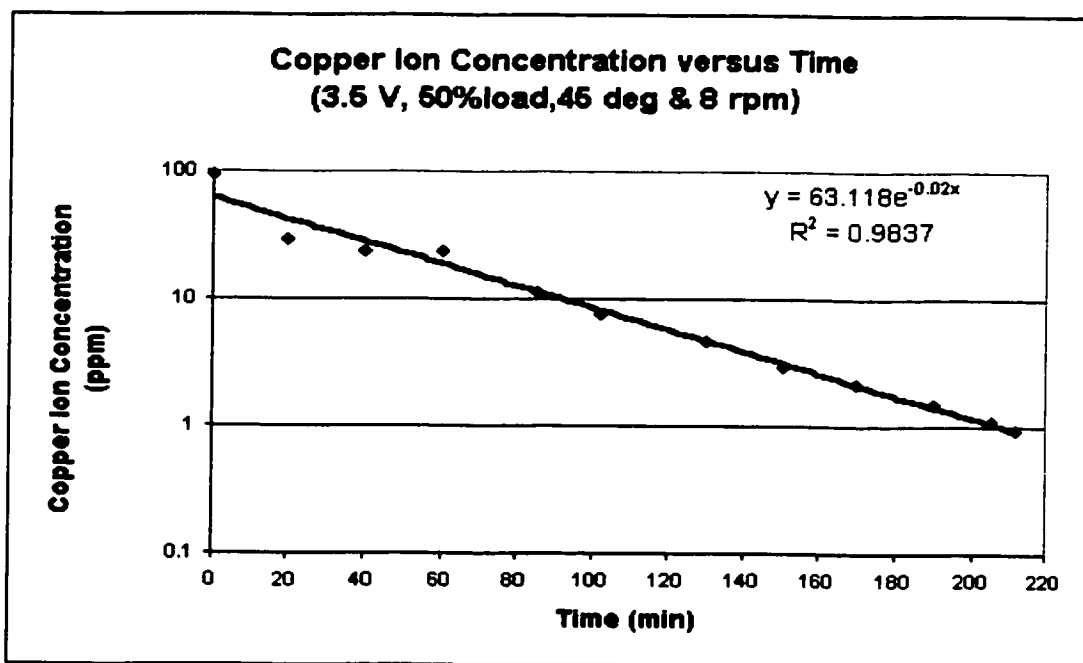


Figure. A-38. Copper ion concentration versus electrolysis time.

Table. A-79. Fixed operation parameters

Voltage (V)	3.5
Current (A)	0.83
Barrel load	50%
Barrel Immersion angle	45
Barrel Immersion percent	50%
Rotating speed (rpm)	4
water volume (lit.)	14
Na2SO4 weight (g)	85.55
CuSO4 weight (g)	5.33
Temperature (C)	23.4

$$(\text{ppm})=0.383e0.0836*(\text{mV})$$

$$\text{area (50\%)}=0.5905 \text{ m}^2$$

$$V/A=0.02371 \text{ m}$$

$$k=0.00033 \text{ m/min}$$

$$5.49E-06 \text{ m/s}$$

Table. A-80. Experimental measurements

Time (min)	ppm	mV	I (A)
0	96.18	66.1	0.83
20	43.11	56.5	
40	39.32	55.4	
55	27.68	51.2	0.82
65	24.01	49.5	
110	15.55	44.3	0.79
135	8.37	36.9	
155	7.57	35.7	
170	6.09	33.1	
190	4.86	30.4	0.8
210	3.72	27.2	
230	2.78	23.7	
255	2.22	21	

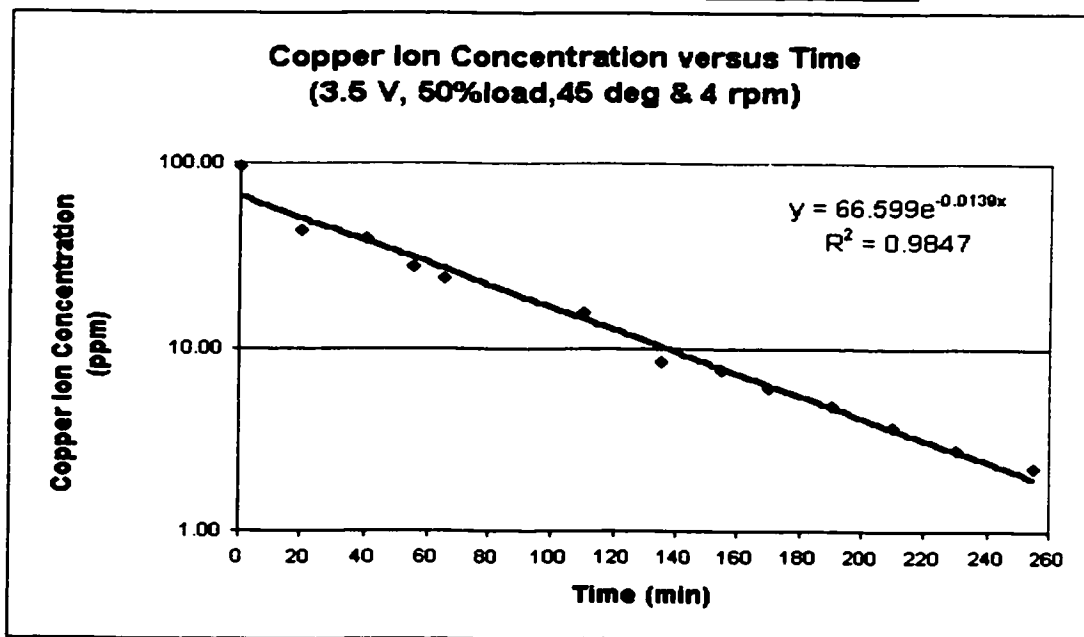


Figure. A-39. Copper ion concentration versus electrolysis time.

Table. A-81. Fixed operation parameters

Voltage (V)	4.51
Current (A)	1.57
Barrel load	50%
Barrel Immersion angle	45
Barrel Immersion percent	50%
Rotating speed (rpm)	18
water volume (lit.)	14
Na2SO4 weight (g)	85.42
CuSO4 weight (g)	5.33
Temperature (C)	23.4

$$(\text{ppm})=0.9616e0.0847*(\text{mV})$$

$$\text{area (50\%)}=0.5905 \text{ m}^2$$

$$V/A=0.02371 \text{ m}$$

$$k= 0.000811 \text{ m/min}$$

$$1.35E-05 \text{ m/s}$$

Table. A-82. Experimental measurements

Time (min)	ppm	mV	I (A)
0	104.0377	55.3	1.57
15	57.50393	48.3	
30	38.94823	43.7	
45	28.46978	40	
70	8.407829	25.6	1.39
85	5.599086	20.8	
105	2.568606	11.6	
120	1.846022	7.7	1.41
140	0.921727	-0.5	1.36

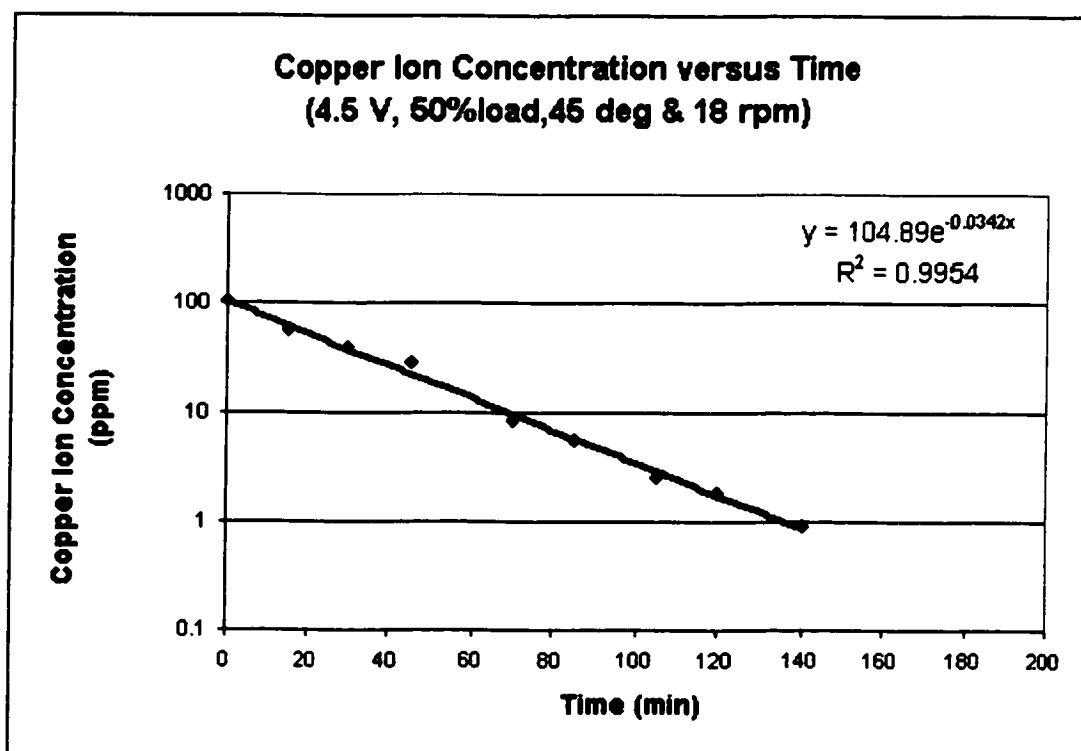


Figure. A-40. Copper ion concentration versus electrolysis time.

Table. A-83. Fixed operation parameters

Voltage (V)	4.5
Current (A)	1.57
Barrel load	50%
Barrel Immersion angle	45
Barrel Immersion percent	50%
Rotating speed (rpm)	20
water volume (lit.)	14
Na ₂ SO ₄ weight (g)	85.47
CuSO ₄ weight (g)	5.33
Temperature (C)	23.3

$$(\text{ppm})=0.9616e^{0.0847*(\text{mV})}$$

$$\text{area (50\%)}=0.5905 \text{ m}^2$$

$$V/A=0.02371 \text{ m}$$

$$k= 0.000707 \text{ m/min}$$

$$1.18E-05 \text{ m/s}$$

Table. A-84. Experimental measurements

Time (min)	ppm	mV	I (A)
0	94.78	54.2	1.57
15	28.23	39.9	
30	17.87	34.5	
45	9.55	27.1	
60	7.73	24.6	1.48
80	5.84	21.3	
100	2.75	12.4	
115	1.77	7.2	1.4
140	0.91	-0.6	

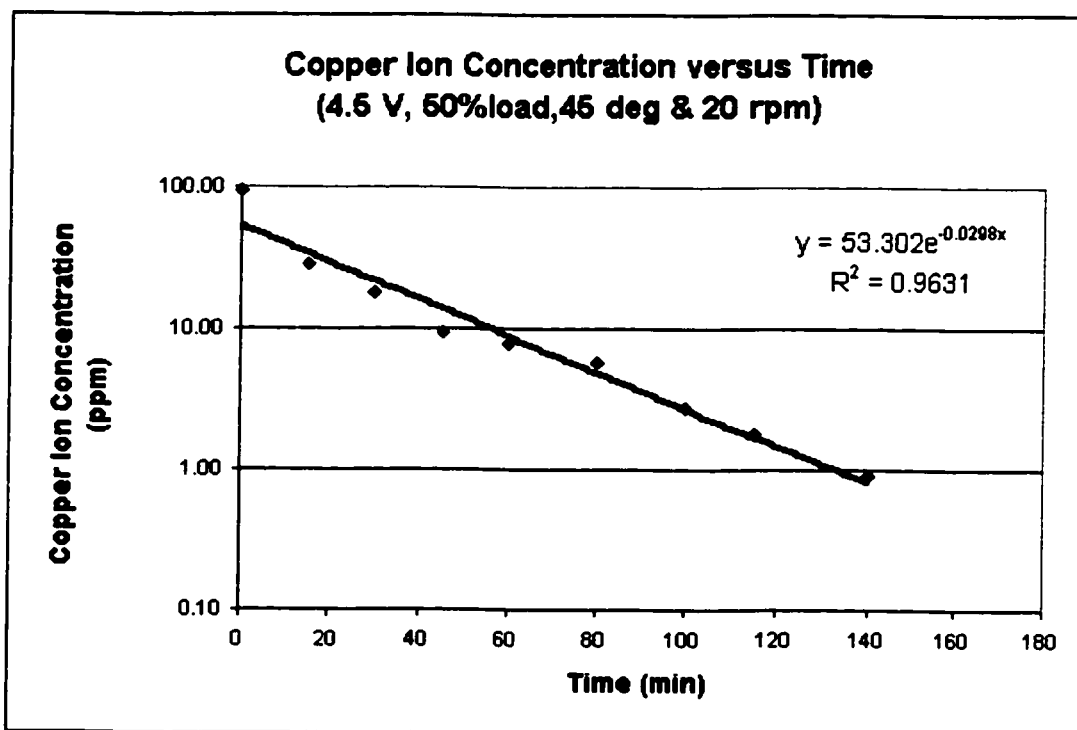


Figure. A-41. Copper ion concentration versus electrolysis time.

Table. A-85. Fixed operation parameters

Voltage (V)	3.5
Current (A)	1.1
Barrel load	50%
Barrel Immersion angle	45
Barrel Immersion percent	50%
Rotating speed (rpm)	20
water volume (lit.)	14
Na2SO4 weight (g)	85.65
CuSO4 weight (g)	5.33
Temperature (C)	22.7

$$(\text{ppm})=0.9619e0.0847*(\text{mV})$$

$$\text{area (50\%)}=0.5905 \text{ m}^2$$

$$V/A=0.02371 \text{ m}$$

$$k= 0.000695 \text{ m/min}$$

$$1.16\text{E-}05 \text{ m/s}$$

Table. A-86. Experimental measurements

Time (min)	ppm	mV	I (A)
0	118.13	56.8	1.1
15	49.79	46.6	
30	42.03	44.6	
45	30.21	40.7	1
60	23.43	37.7	
80	11.12	28.9	
100	6.75	23	
120	2.89	13	0.9
140	1.70	6.7	
160	0.92	-0.5	0.92

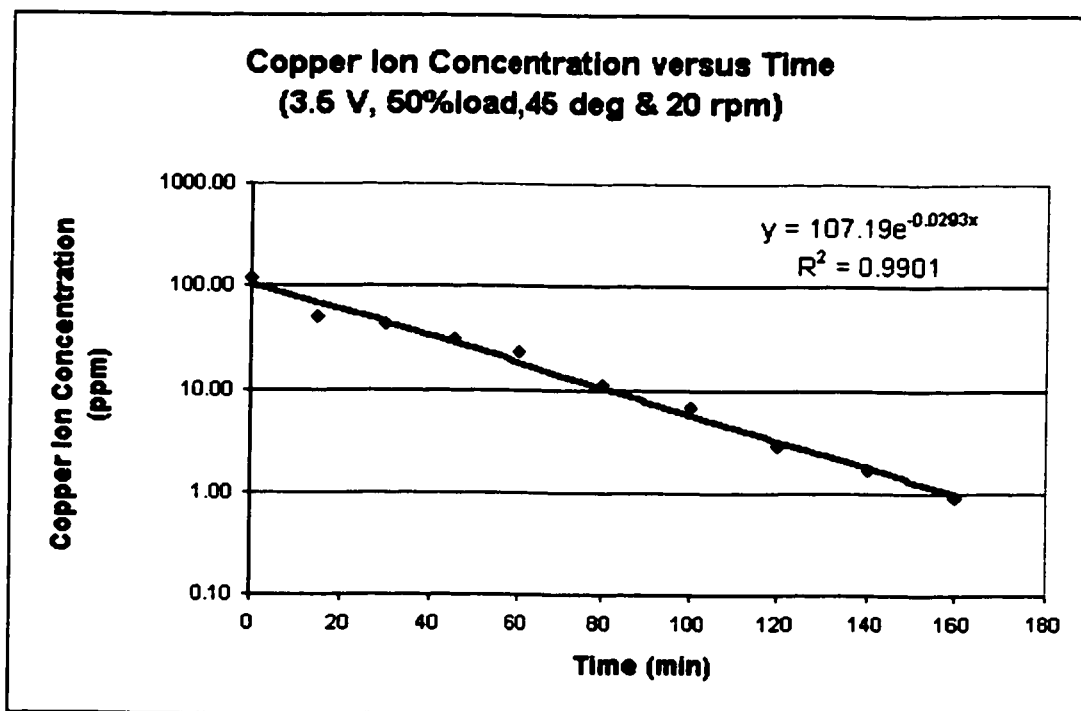


Figure. A-42. Copper ion concentration versus electrolysis time.

Table. A-87. Fixed operation parameters

Voltage (V)	3.5
Current (A)	1
Barrel load	50%
Barrel Immersion angle	45
Barrel Immersion percent	50%
Rotating speed (rpm)	4
water volume (lit.)	14
Na ₂ SO ₄ weight (g)	85.46
CuSO ₄ weight (g)	5.34
Temperature (C)	22

$$(\text{ppm}) = 0.9619e^{0.0847 \cdot (\text{mV})}$$

$$\text{area (50\%)} = 0.5905 \text{ m}^2$$

$$V/A = 0.02371 \text{ m}$$

$$k = 0.000709 \text{ m/min}$$

$$1.18E-05 \text{ m/s}$$

Table. A-88. Experimental measurements

Time (min)	ppm	mV	I (A)
0	136.43	58.5	1
15	48.54	46.3	
30	46.14	45.7	
45	40.98	44.3	
60	30.72	40.9	
80	19.78	35.7	0.85
100	5.79	21.2	
115	3.34	14.7	
132	2.10	9.2	
150	1.05	1	0.81
170	0.98	0.2	

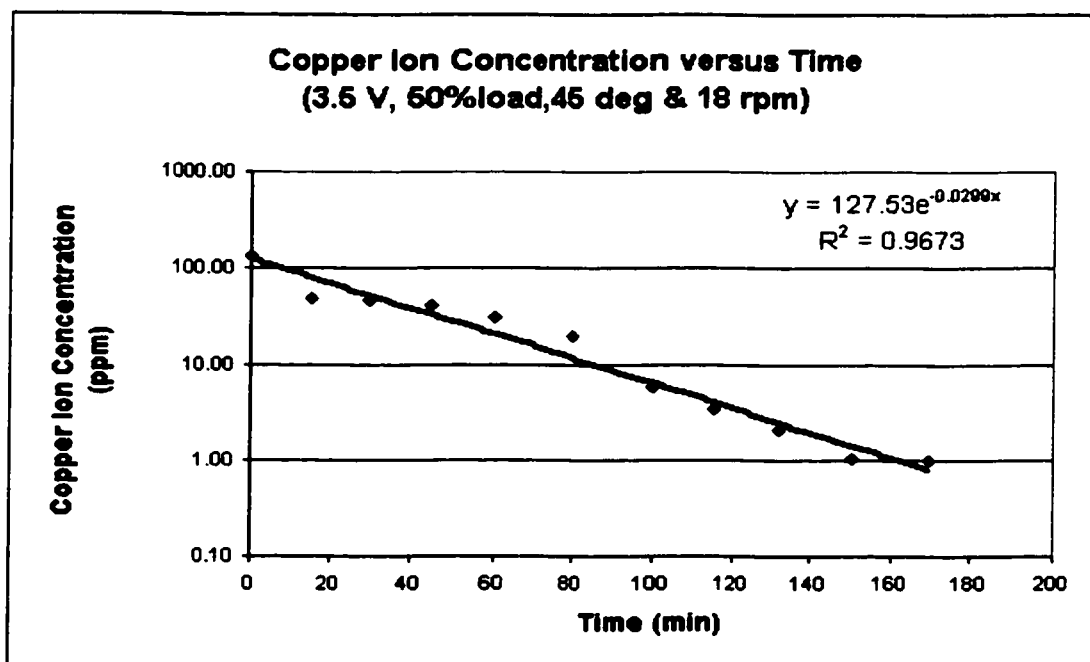


Figure. A-43. Copper ion concentration versus electrolysis time.

Barrel Tilt Angle Effect

Table. A-89. Fixed operation parameters

Voltage (V)	4.51
Current (A)	1.51
Barrel load	50%
Barrel Immersion angle	30
Barrel Immersion percent	50%
Rotating speed (rpm)	18
water volume (lit.)	14
Na ₂ SO ₄ weight (g)	85.43
CuSO ₄ weight (g)	5.32
Temperature (C)	23.6

$$(\text{ppm})=0.6465e^{0.0853*(\text{mV})}$$

$$\text{area (50\%)}=0.5905 \text{ m}^2$$

$$V/A=0.02371 \text{ m}$$

$$k= 0.000851 \text{ m/min}$$

$$1.42E-05 \text{ m/s}$$

Table. A-90. Experimental measurements

Time (min)	ppm	mV	I (A)
0	108.89	60.1	1.51
15	73.55	55.5	
30	58.42	52.8	
60	49.68	50.9	
80	15.84	37.5	1.43
95	5.18	24.4	
110	2.93	17.7	
125	1.70	11.3	1.4
140	0.73	1.5	

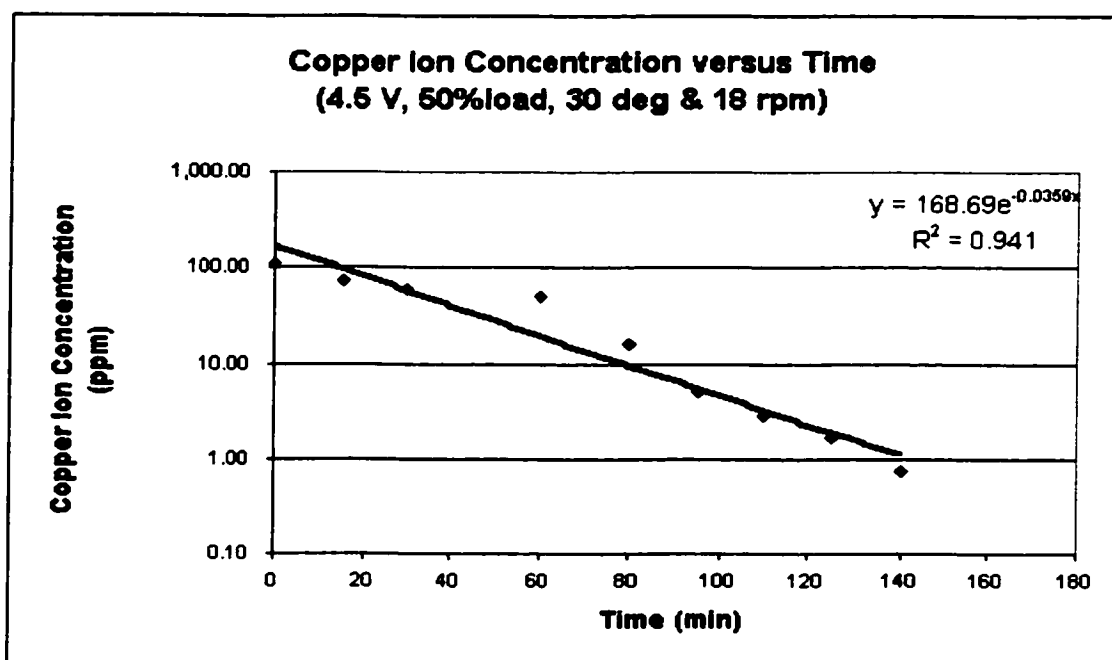


Figure. A-44. Copper ion concentration versus electrolysis time.

Table. A-91. Fixed operation parameters

Voltage (V)	4.51
Current (A)	1.25
Barrel load	50%
Barrel Immersion angle	60
Barrel Immersion percent	50%
Rotating speed (rpm)	18
water volume (lit.)	14
Na ₂ SO ₄ weight (g)	85.5
CuSO ₄ weight (g)	5.33
Temperature (C)	23.5

$$(\text{ppm}) = 0.6465e0.0853 * (\text{mV})$$

$$\text{area (50\%)} = 0.5905 \text{ m}^2$$

$$V/A = 0.02371 \text{ m}$$

$$k = 0.000657 \text{ m/min}$$

$$1.09E-05 \text{ m/s}$$

Table. A-92. Experimental measurements

Time (min)	ppm	mV	I (A)
0	96.63	58.7	1.25
15	37.17	47.5	
30	47.61	50.4	
50	28.78	44.5	
65	16.82	38.2	1.25
85	8.14	29.7	
105	5.14	24.3	
125	2.43	15.5	
140	1.70	11.3	
155	1.26	7.8	1.28
170	0.85	3.2	

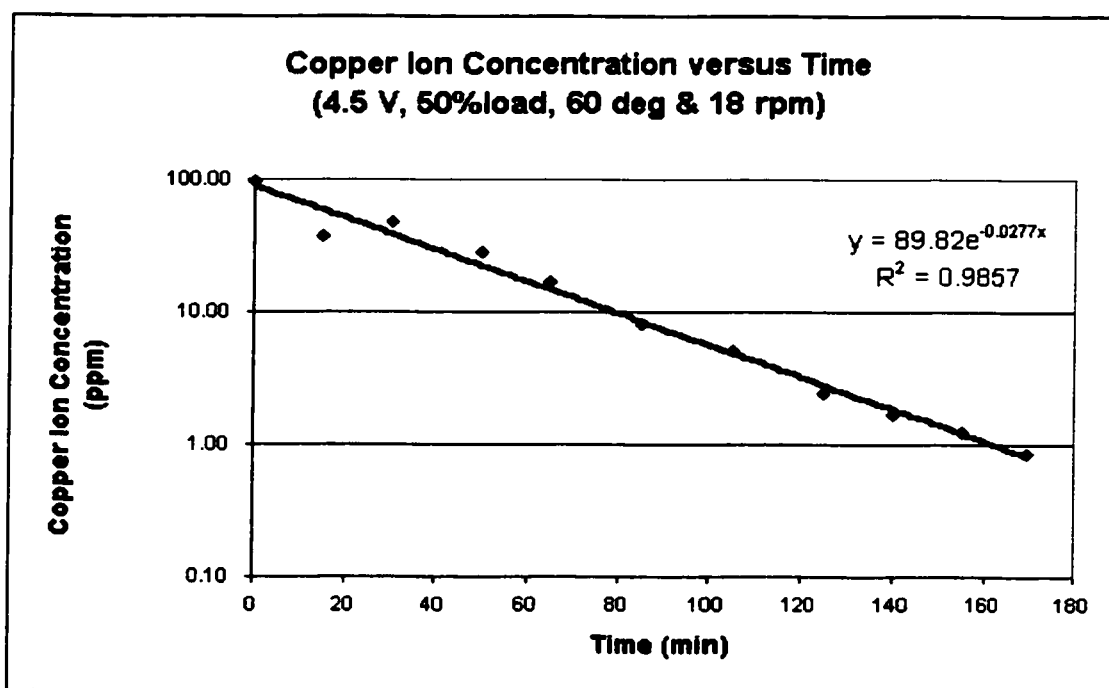


Figure. A-45. Copper ion concentration versus electrolysis time.

Table. A-93. Fixed operation parameters

Voltage (V)	4.51
Current (A)	1.35
Barrel load	50%
Barrel Immersion angle	75
Barrel Immersion percent	50%
Rotating speed (rpm)	18
water volume (lit.)	14
Na ₂ SO ₄ weight (g)	85.6
CuSO ₄ weight (g)	5.32
Temperature (C)	23.3

$$(\text{ppm}) = 0.6465e0.0853 * (\text{mV})$$

$$\text{area (50\%)} = 0.5905 \text{ m}^2$$

$$V/A = 0.02371 \text{ m}$$

$$k = 0.00074 \text{ m/min}$$

$$1.23E-05 \text{ m/s}$$

Table. A-94. Experimental measurements

Time (min)	ppm	mV	I (A)
0	86.49	57.4	1.25
15	33.84	46.4	
30	29.03	44.6	
45	27.81	44.1	
62	17.55	38.7	1.2
85	4.92	23.8	
100	3.30	19.1	1.21
115	2.25	14.6	
130	1.25	7.7	
145	0.89	3.8	1.2

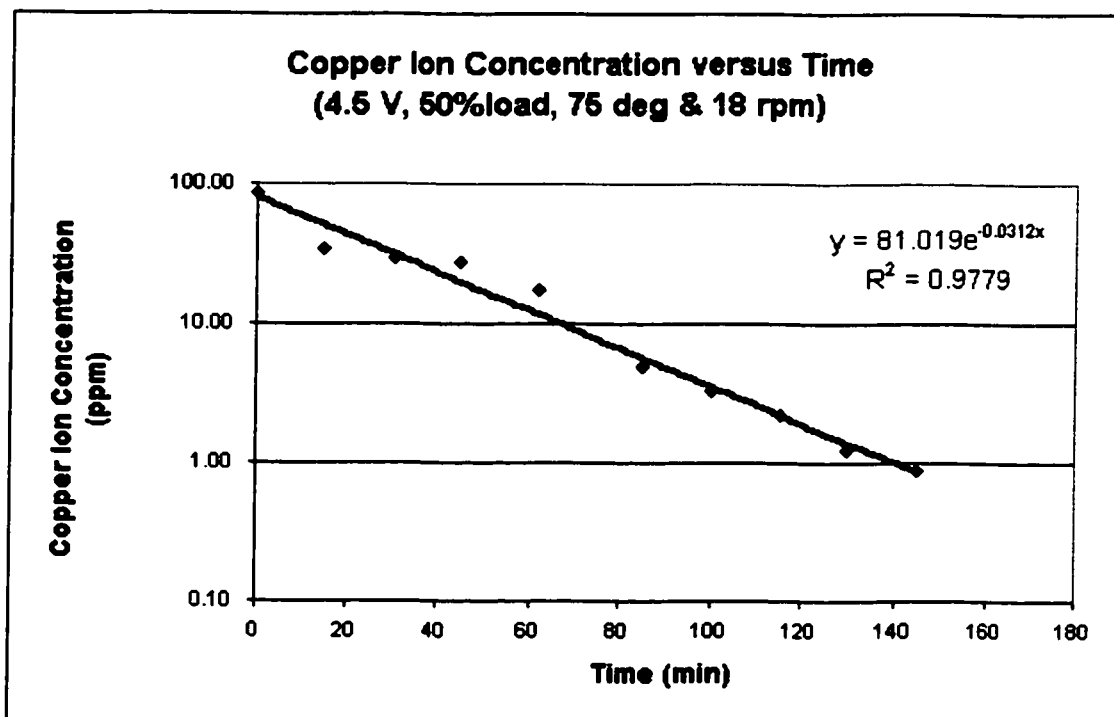


Figure. A-46. Copper ion concentration versus electrolysis time.

Table. A-95. Fixed operation parameters

Voltage (V)	4.51
Current (A)	1.5
Barrel load	50%
Barrel Immersion angle	15
Barrel Immersion percent	50%
Rotating speed (rpm)	18
water volume (lit.)	14
Na ₂ SO ₄ weight (g)	85.59
CuSO ₄ weight (g)	5.32
Temperature (C)	24.9

$$(\text{ppm}) = 0.6465e0.0853 * (\text{mV})$$

$$\text{area (50\%)} = 0.5905 \text{ m}^2$$

$$V/A = 0.02371 \text{ m}$$

$$k = 0.001057 \text{ m/min}$$

$$1.76E-05 \text{ m/s}$$

Table. A-96. Experimental measurements

Time (min)	ppm	mV	I (A)
0	95.81	58.6	1.5
15	65.83	54.2	
30	79.42	56.4	
45	39.12	48.1	1.33
60	19.77	40.1	
80	3.91	21.1	
106	1.37	8.8	
125	0.52	-2.6	1.22

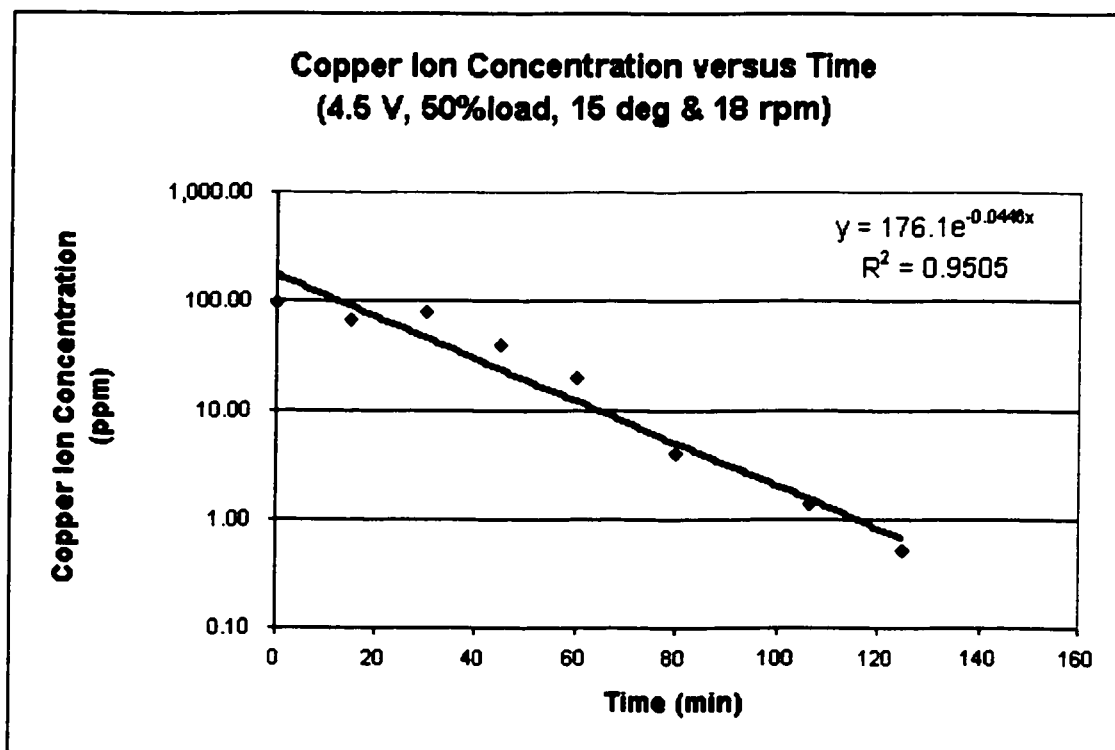


Figure. A-47. Copper ion concentration versus electrolysis time.

Table. A-97. Fixed operation parameters

Voltage (V)	4.51
Current (A)	1.21
Barrel load	50%
Barrel Immersion angle	90
Barrel Immersion percent	50%
Rotating speed (rpm)	18
water volume (lit.)	14
Na ₂ SO ₄ weight (g)	85.5
CuSO ₄ weight (g)	5.32
Temperature (C)	24.7

$$(\text{ppm}) = 0.6465e^{0.0853 \cdot (\text{mV})}$$

$$\text{area (50\%)} = 0.5905 \text{ m}^2$$

$$V/A = 0.02371 \text{ m}$$

$$k = 0.000595 \text{ m/min}$$

$$9.92E-06 \text{ m/s}$$

Table. A-98. Experimental measurements

Time (min)	ppm	mV	I (A)
0	95.81	58.6	1.21
15	32.99	46.1	
30	37.81	47.7	
45	28.78	44.5	
60	12.91	35.1	
70	11.95	34.2	1.2
90	6.81	27.6	
108	3.98	21.3	
128	2.43	15.5	1.12
145	1.78	11.9	
160	1.31	8.3	
180	0.97	4.8	0.97

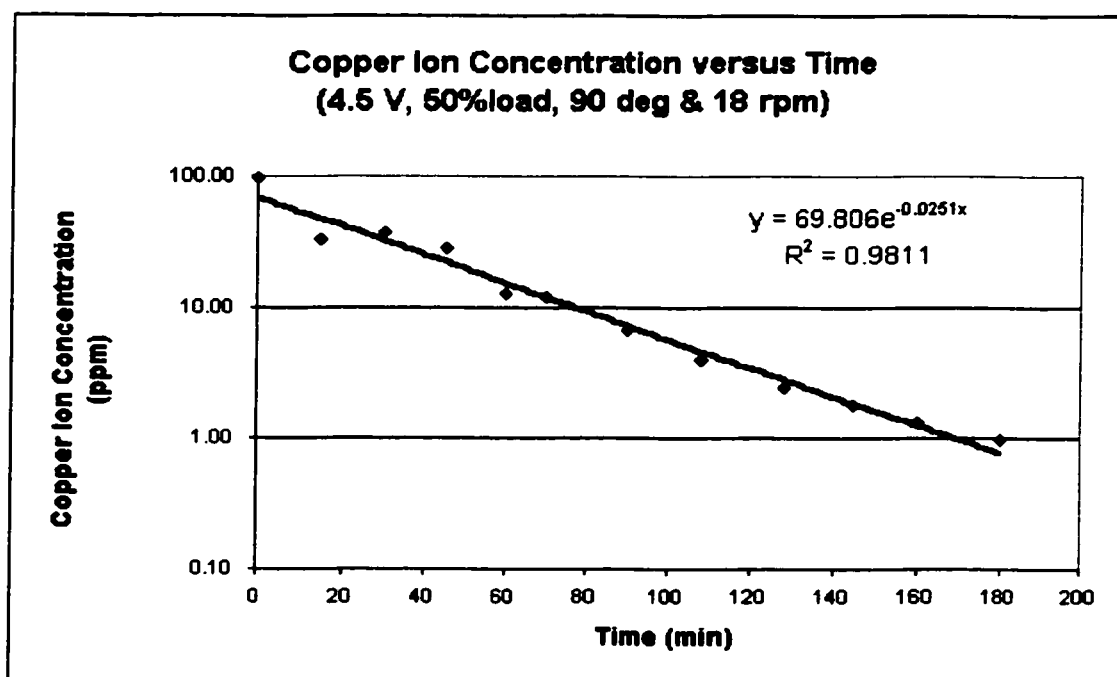


Figure. A-48. Copper ion concentration versus electrolysis time.

Table. A-99. Fixed operation parameters

Voltage (V)	4.52
Current (A)	1.31
Barrel load	50%
Barrel Immersion angle	60
Barrel Immersion percent	50%
Rotating speed (rpm)	18
water volume (lit.)	14
Na ₂ SO ₄ weight (g)	85.53
CuSO ₄ weight (g)	5.34
Temperature (C)	24.9

$$(\text{ppm}) = 0.6465e0.0853 * (\text{mV})$$

$$\text{area (50\%)} = 0.5905 \text{ m}^2$$

$$V/A = 0.02371 \text{ m}$$

$$k = 0.000647 \text{ m/min}$$

$$1.08E-05 \text{ m/s}$$

Table. A-100. Experimental measurements

Time (min)	ppm	mV	I (A)
0	112.67	60.5	1.31
20	63.08	53.7	
35	43.34	49.3	
50	23.65	42.2	
65	17.10	38.4	
85	10.17	32.3	
105	8.07	29.6	1.35
125	4.72	23.3	
158	1.47	9.6	
170	0.84	3.1	

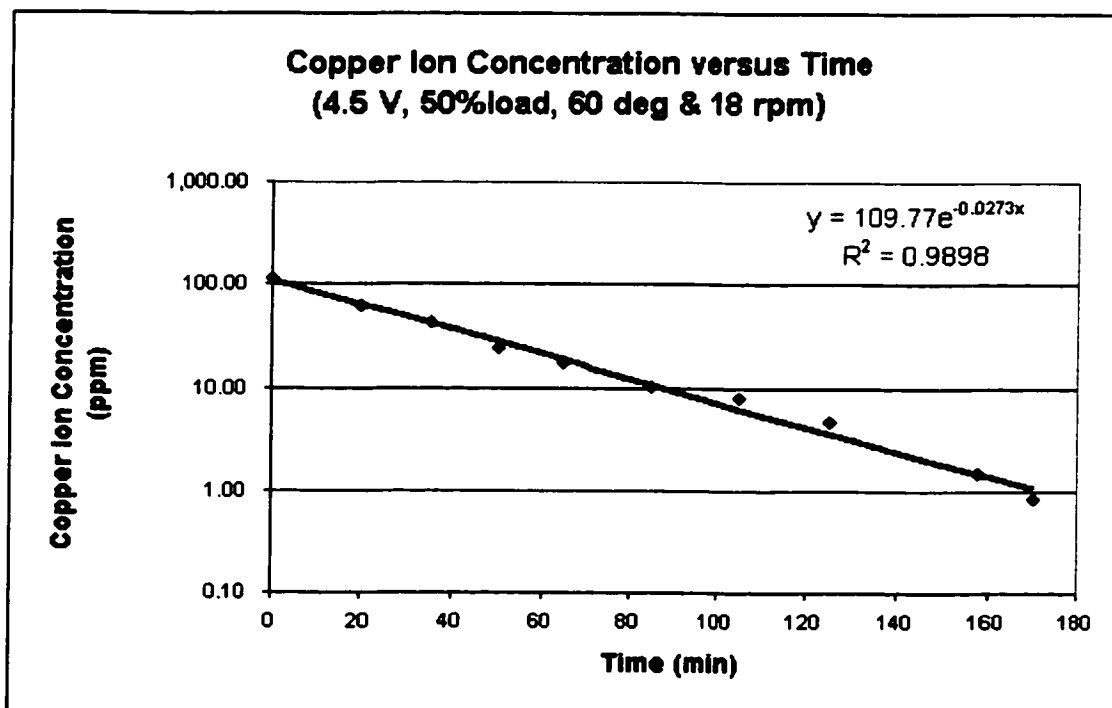


Figure. A-49. Copper ion concentration versus electrolysis time.

Table. A-101. Fixed operation parameters

Voltage (V)	4.51
Current (A)	1.23
Barrel load	50%
Barrel Immersion angle	75
Barrel Immersion percent	50%
Rotating speed (rpm)	18
water volume (lit.)	14
Na ₂ SO ₄ weight (g)	85.43
CuSO ₄ weight (g)	5.32
Temperature (C)	23.6

$$(\text{ppm}) = 5.646e0.0871 \cdot (\text{mV})$$

$$\text{area (50\%)} = 0.5905 \text{ m}^2$$

$$V/A = 0.02371 \text{ m}$$

$$k = 0.000657 \text{ m/min}$$

$$1.09E-05 \text{ m/s}$$

Table. A-102. Experimental measurements

Time (min)	ppm	mV	I (A)
0	95.74	32.5	1.23
16	31.13	19.6	
30	27.79	18.3	
45	25.92	17.5	
60	15.92	11.9	1.21
80	6.38	1.4	
95	4.05	-3.8	
110	2.58	-9	1.05
132	1.74	-13.5	
145	1.46	-15.5	
160	0.97	-20.2	1.13

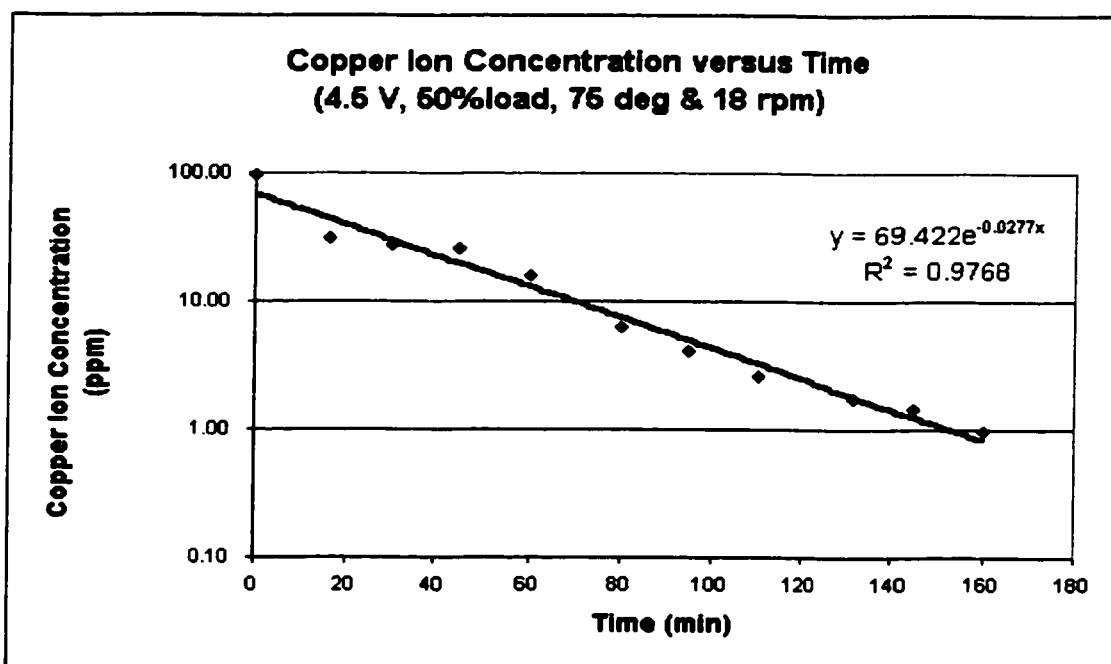


Figure. A-50. Copper ion concentration versus electrolysis time.

Percent Barrel Immersion Effect

Table. A-103. Fixed operation parameters

Voltage (V)	4.52
Current (A)	1.77
Barrel load	50%
Barrel Immersion angle	30
Barrel Immersion percent	75%
Rotating speed (rpm)	18
water volume (lit.)	14
Na2SO4 weight (g)	85.53
CuSO4 weight (g)	5.33
Temperature (C)	23.8

(ppm)=5.646e0.0871*(mV)

area (50%)=0.5905 m²

V/A=0.02371 m

k= 0.000989m/min
1.65E-05m/s

Table. A-104. Experimental measurements

Time (min)	ppm	mV
0	124.33	35.5
16	79.74	30.4
31	59.82	27.1
55	42.96	23.3
75	11.14	7.8
95	4.24	-3.3
105	1.82	-13
120	1.03	-19.5
130	0.74	-23.4

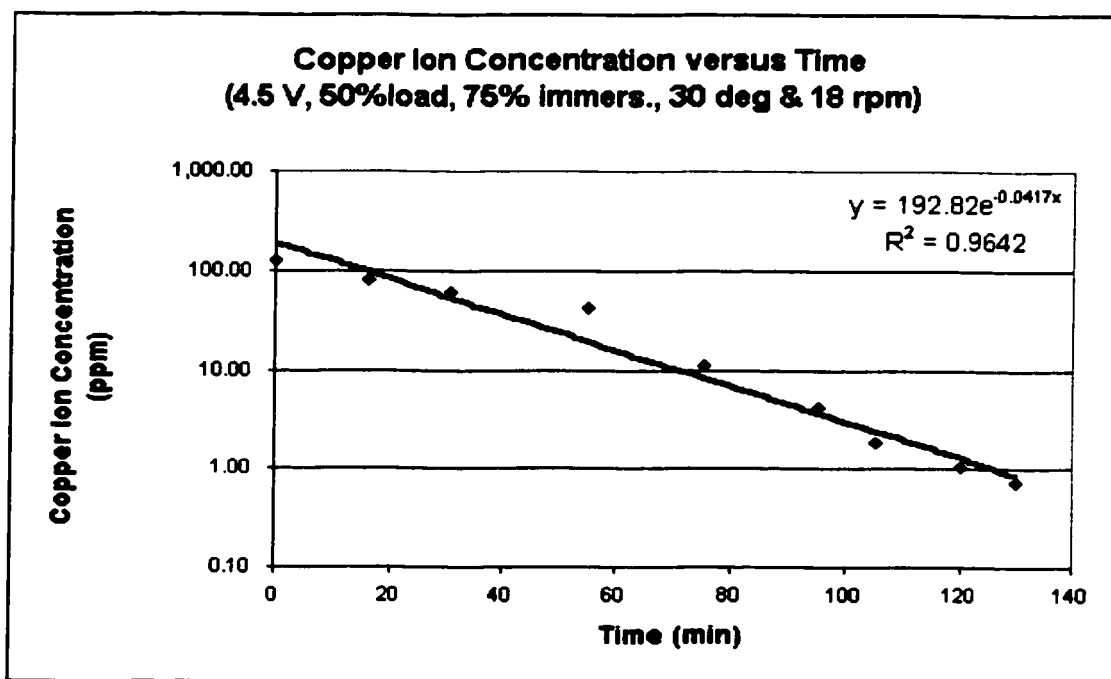


Figure. A-51. Copper ion concentration versus electrolysis time.

Table. A-105. Fixed operation parameters

Voltage (V)	4.52
Current (A)	1.2
Barrel load	50%
Barrel Immersion angle	30
Barrel Immersion percent	25%
Rotating speed (rpm)	18
water volume (lit.)	14
Na ₂ SO ₄ weight (g)	85.55
CuSO ₄ weight (g)	5.33
Temperature (C)	23.9

$$(\text{ppm}) = 5.646e0.0871 * (\text{mV})$$

$$\text{area (50\%)} = 0.5905 \text{ m}^2$$

$$V/A = 0.02371 \text{ m}$$

$$k = 0.000154 \text{ m/min}$$

$$2.57E-06 \text{ m/s}$$

Table. A-106. Experimental measurements

Time (min)	ppm	mV	I (A)
0	124.33	35.5	1.2
15	38.03	21.9	
30	29.03	18.8	
50	30.86	19.5	
70	33.37	20.4	
100	34.56	20.8	
120	31.13	19.6	1.13

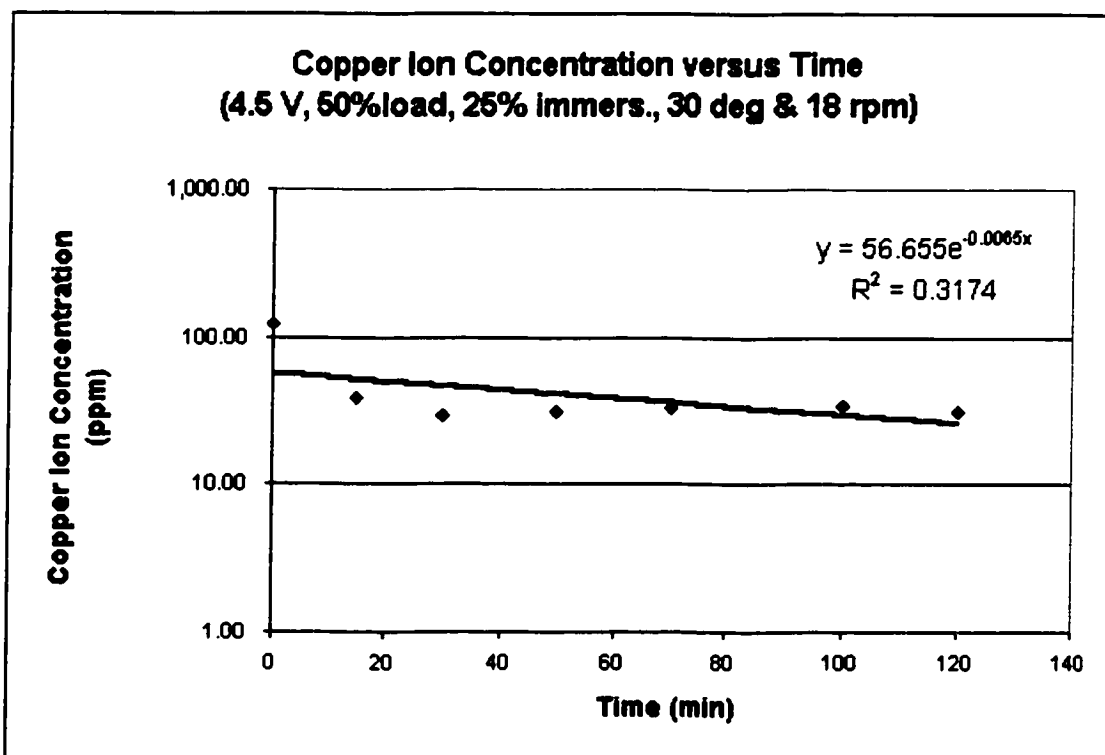


Figure. A-52. Copper ion concentration versus electrolysis time.

Table. A-107. Fixed operation parameters

Voltage (V)	4.52
Current (A)	1.85
Barrel load	50%
Barrel Immersion angle	30
Barrel Immersion percent	100%
Rotating speed (rpm)	18
water volume (lit.)	18
Na ₂ SO ₄ weight (g)	110.08
CuSO ₄ weight (g)	6.8
Temperature (C)	25.7

$$(\text{ppm})=4.887e0.0868^*(\text{mV})$$

$$\text{area (50\%)}=0.5905 \text{ m}^2$$

$$V/A=0.03026 \text{ m}$$

$$k= 0.000983 \text{ m/min}$$

$$1.64E-05 \text{ m/s}$$

Table. A-108. Experimental measurements

Time (min)	ppm	mV	I (A)
0	117.15	36.6	1.85
15	43.93	25.3	
30	25.43	19	
45	25.65	19.1	
60	17.81	14.9	1.65
95	4.64	-0.6	
110	2.53	-7.6	1.51
125	1.53	-13.4	
140	0.92	-19.3	1.45

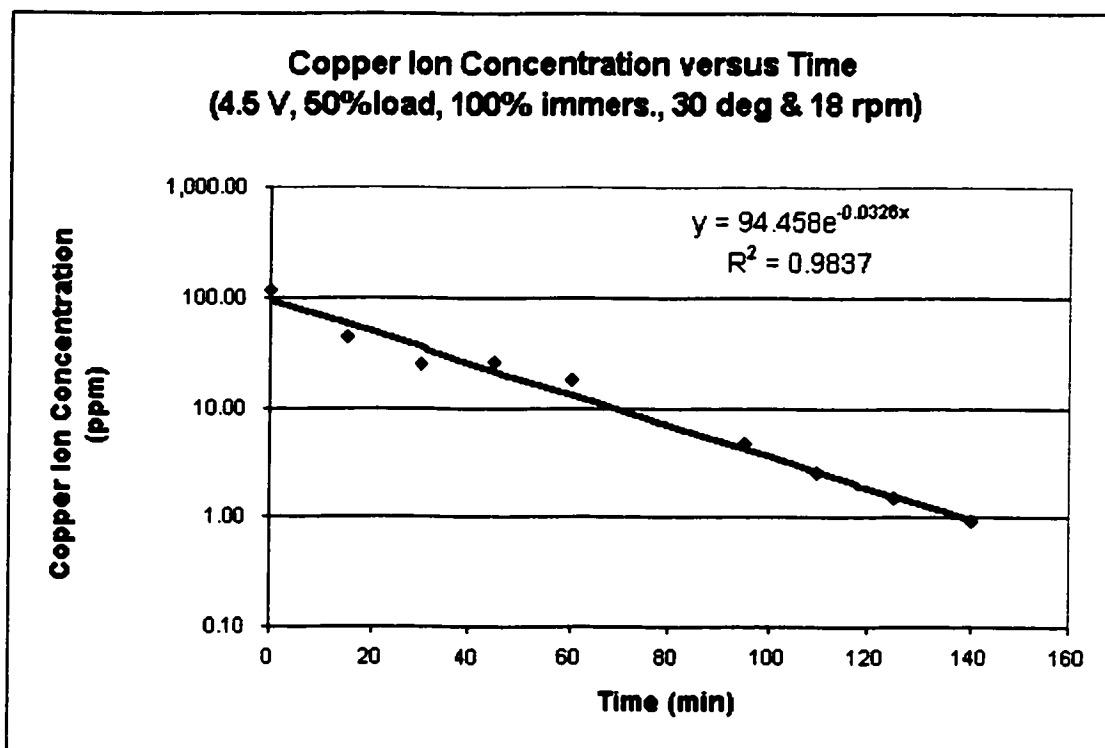


Figure. A-53. Copper ion concentration versus electrolysis time.

Table. A-109. Fixed operation parameters

Voltage (V)	4.52
Current (A)	1.9
Barrel load	70%
Barrel Immersion angle	30
Barrel Immersion percent	100%
Rotating speed (rpm)	18
water volume (lit.)	18
Na2SO4 weight (g)	110.12
CuSO4 weight (g)	6.81
Temperature (C)	25.7

(ppm)=4.887e0.0868*(mV)

area (70%)=0.8383 m²

V/A=0.02147 m

k= 0.00082m/min

1.37E-05m/s

Table. A-110. Experimental measurements

Time (min)	ppm	mV	I (A)
0	127.77	37.6	1.9
20	79.96	32.2	
40	82.79	32.6	
60	36.29	23.1	1.75
80	18.12	15.1	
100	4.29	-1.5	
115	2.05	-10	1.79
135	0.96	-18.8	

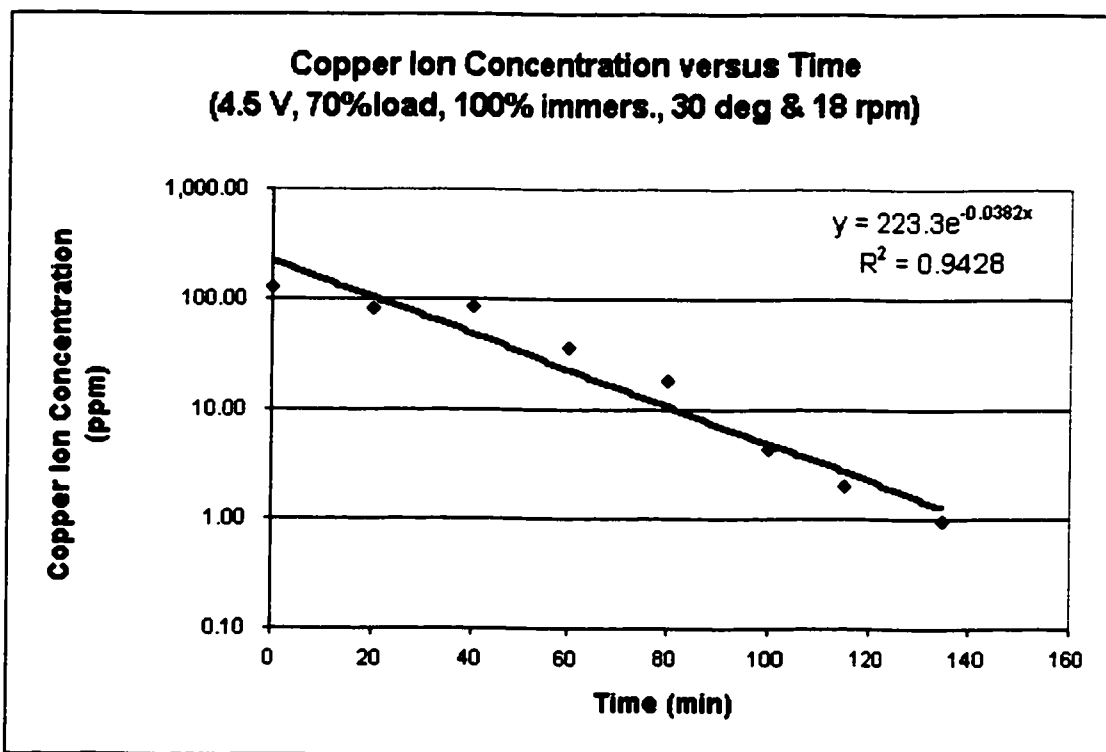


Figure. A-54. Copper ion concentration versus electrolysis time.

Table. A-111. Fixed operation parameters

Voltage (V)	4.52
Current (A)	1.85
Barrel load	70%
Barrel Immersion angle	30
Barrel Immersion percent	75%
Rotating speed (rpm)	18
water volume (lit.)	14
Na ₂ SO ₄ weight (g)	85.53
CuSO ₄ weight (g)	5.33
Temperature (C)	24.9

$$(\text{ppm})=4.887\text{e}0.0868^*(\text{mV})$$

$$\text{area (70\%)}=0.8383 \text{ m}^2$$

$$V/A=0.0167 \text{ m}$$

$$k= 0.000733 \text{ m/min}$$

$$1.22\text{E-}05 \text{ m/s}$$

Table. A-112. Experimental measurements

Time (min)	ppm	mV	I (A)
0	131.14	37.9	1.85
15	45.48	25.7	
30	31.32	21.4	
50	21.19	16.9	
71	6.29	2.9	
90	2.36	-8.4	1.6
105	1.02	-18	
115	0.76	-21.4	

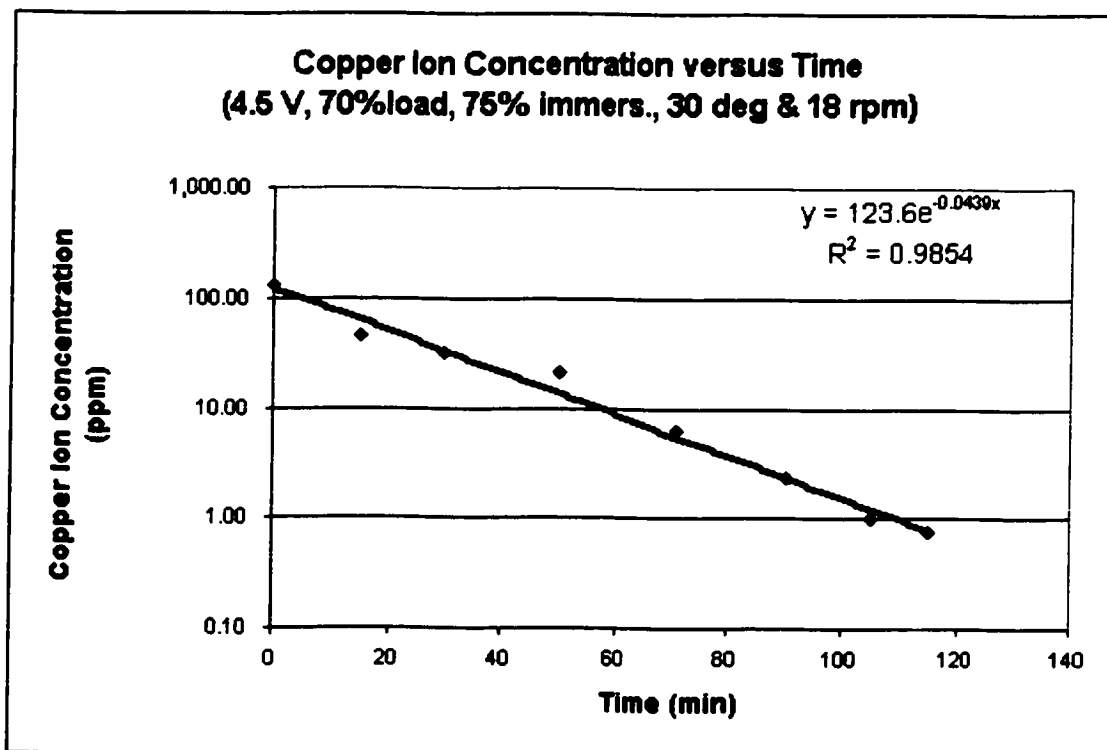


Figure. A-55. Copper ion concentration versus electrolysis time.

Table. A-113. Fixed operation parameters

Voltage (V)	4.52
Current (A)	1.66
Barrel load	70%
Barrel Immersion angle	30
Barrel Immersion percent	50%
Rotating speed (rpm)	18
water volume (lit.)	14
Na ₂ SO ₄ weight (g)	85.52
CuSO ₄ weight (g)	5.33
Temperature (C)	24.8

$$(\text{ppm}) = 4.526e0.0853 \cdot (\text{mV})$$

$$\text{area (70\%)} = 0.8383 \text{ m}^2$$

$$V/A = 0.0167 \text{ m}$$

$$k = \begin{matrix} 0.000558 \text{ m/min} \\ 9.3E-06 \text{ m/s} \end{matrix}$$

Table. A-114. Experimental measurements

Time (min)	ppm	mV	I (A)
0	109.95	37.4	1.66
15	55.57	29.4	
30	33.59	23.5	
45	22.88	19	1.57
60	13.60	12.9	
80	5.90	3.1	
100	2.21	-8.4	1.5
120	1.76	-11.1	
130	1.34	-14.3	
145	0.96	-18.2	1.4

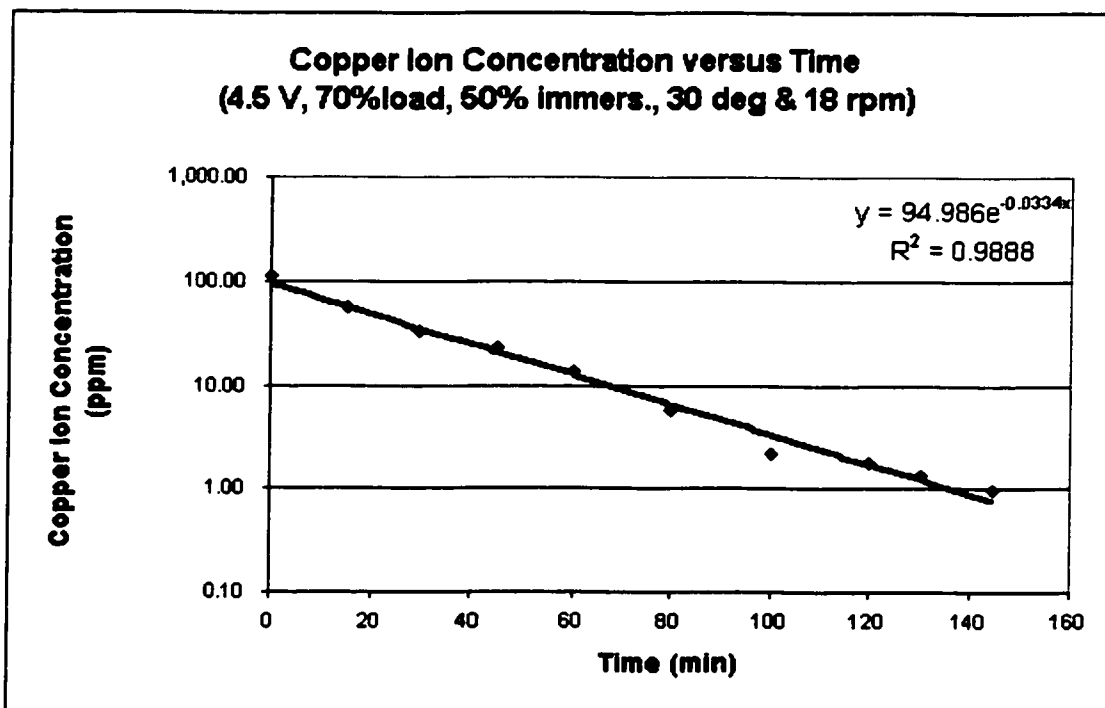


Figure. A-56. Copper ion concentration versus electrolysis time.

Table. A-115. Fixed operation parameters

Voltage (V)	4.52
Current (A)	1.4
Barrel load	70%
Barrel Immersion angle	30
Barrel Immersion percent	25%
Rotating speed (rpm)	18
water volume (lit.)	14
Na2SO4 weight (g)	85.5
CuSO4 weight (g)	5.32
Temperature (C)	24.9

$$(\text{ppm})=4.526e0.0853*(\text{mV})$$

$$\text{area (70\%)}=0.8383 \text{ m}^2$$

$$V/A=0.0167 \text{ m}$$

$$k= 5.51E-05 \text{ m/min}$$

$$9.19E-07 \text{ m/s}$$

Table. A-116. Experimental measurements

Time (min)	ppm	mV	I (A)
0	111.84	37.6	1.4
15	56.04	29.5	
30	35.97	24.3	
45	32.47	23.1	1.21
60	27.37	21.1	
80	40.87	25.8	
100	24.71	19.9	1.2
125	51.90	28.6	
135	49.31	28	1.14

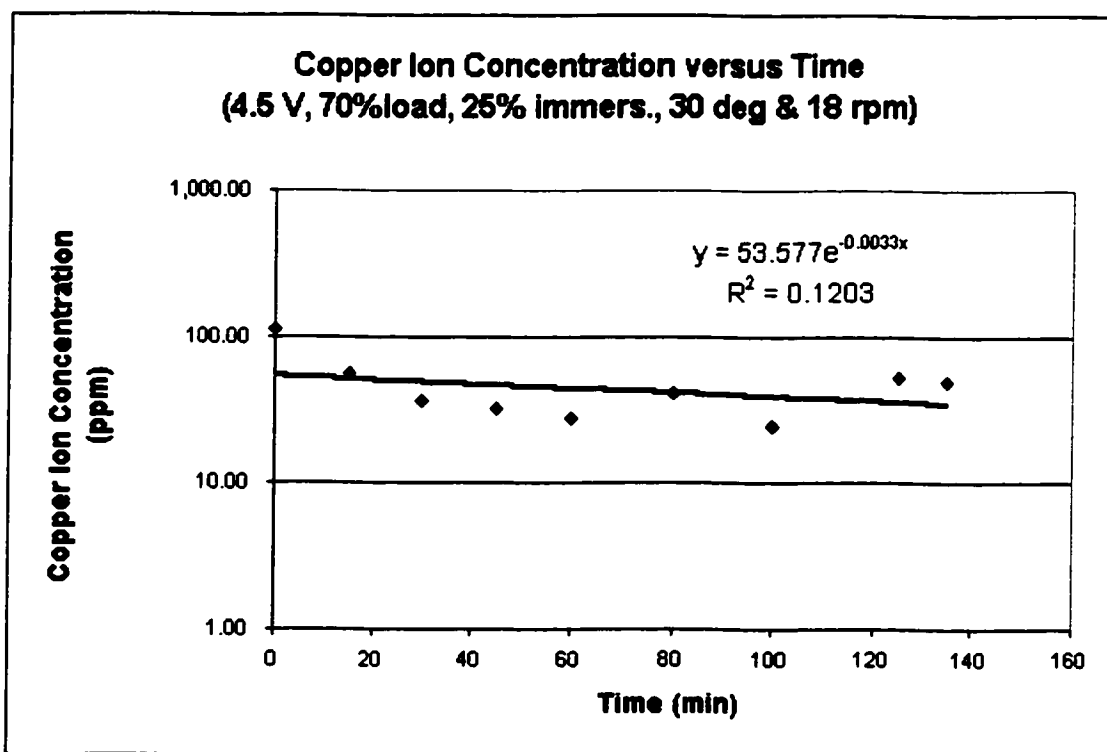


Figure. A-57. Copper ion concentration versus electrolysis time.

Table. A-117. Fixed operation parameters

Voltage (V)	4.52
Current (A)	1.85
Barrel load	25%
Barrel Immersion angle	30
Barrel Immersion percent	50%
Rotating speed (rpm)	18
water volume (lit.)	14
Na2SO4 weight (g)	85.53
CuSO4 weight (g)	5.33
Temperature (C)	24.9

$$(\text{ppm})=4.526e0.0853*(\text{mV})$$

$$\text{area (25\%)}=0.2953 \text{ m}^2$$

$$V/A=0.04742 \text{ m}$$

$$k= 0.001385 \text{ m/min}$$

$$2.31E-05 \text{ m/s}$$

Table. A-118. Experimental measurements

Time (min)	ppm	mV	I (A)
0	109.95	37.4	1.85
18	40.18	25.6	
30	26.46	20.7	
45	23.28	19.2	
60	16.69	15.3	1.2
80	8.58	7.5	
100	4.76	0.6	1.14
120	2.41	-7.4	
140	1.44	-13.4	
160	0.76	-20.9	

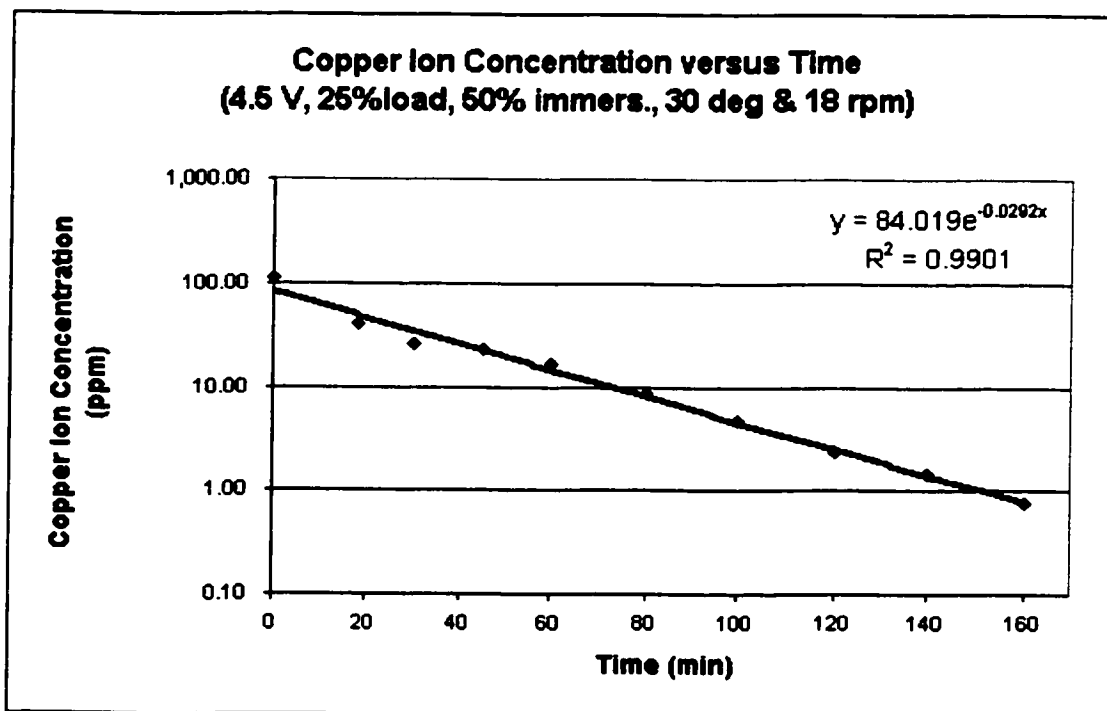


Figure. A-58. Copper ion concentration versus electrolysis time.

Table. A-119. Fixed operation parameters

Voltage (V)	4.5
Current (A)	1.45
Barrel load	25%
Barrel Immersion angle	30
Barrel Immersion percent	75%
Rotating speed (rpm)	18
water volume (lit.)	14
Na ₂ SO ₄ weight (g)	85.54
CuSO ₄ weight (g)	5.33

$$(\text{ppm}) = 4.526e0.0853 * (\text{mV})$$

$$\text{area (25\%)} = 0.2953 \text{ m}^2$$

$$V/A = 0.04742 \text{ m}$$

$$k = 0.001835 \text{ m/min}$$

$$3.06E-05 \text{ m/s}$$

Table. A-120. Experimental measurements

Time (min)	ppm	mV	I (A)
0	109.01	37.3	1.45
15	62.08	30.7	
30	46.85	27.4	
45	33.88	23.6	1.22
70	14.32	13.5	1.21
90	6.70	4.6	
110	3.42	-3.3	1.15
130	2.00	-9.6	
150	1.23	-15.3	
160	0.99	-17.8	1.16

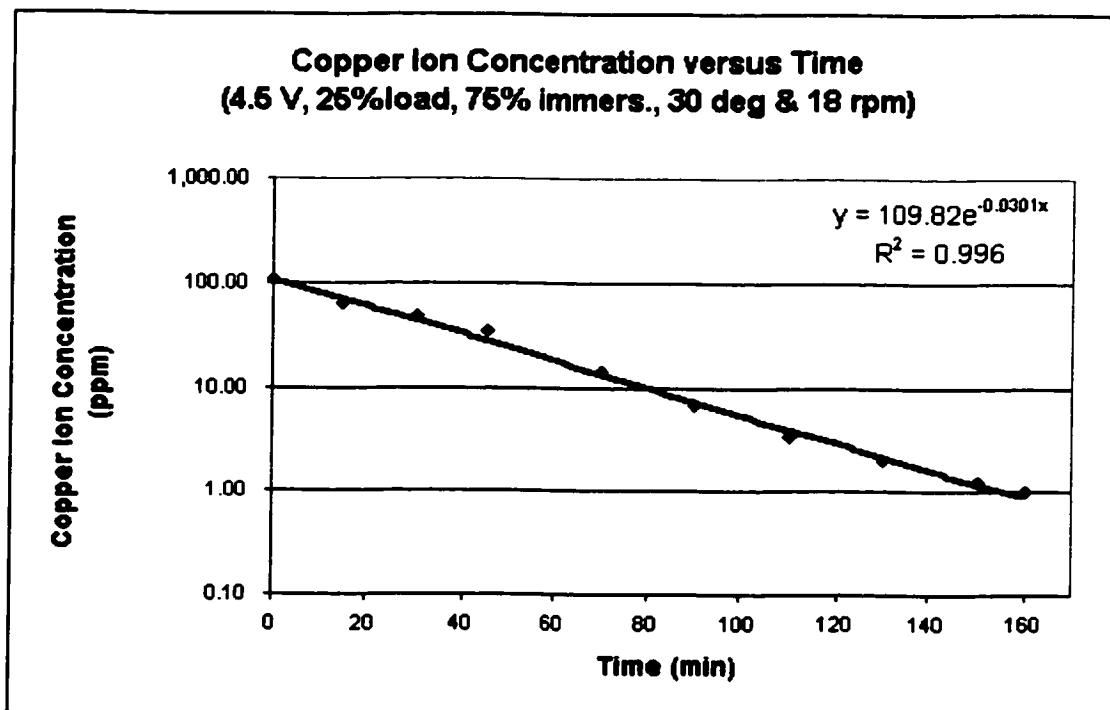


Figure. A-59. Copper ion concentration versus electrolysis time.

Table. A-121. Fixed operation parameters

Voltage (V)	4.5
Current (A)	1.57
Barrel load	25%
Barrel Immersion angle	30
Barrel Immersion percent	100%
Rotating speed (rpm)	18
water volume (lit.)	18
Na2SO4 weight (g)	110.05
CuSO4 weight (g)	6.81

$$(\text{ppm})=4.526e0.0853*(\text{mV})$$

$$\text{area (25\%)}=0.2953 \text{ m}^2$$

$$V/A=0.06096 \text{ m}$$

$$k= 0.001341 \text{ m/min}$$

$$2.24E-05 \text{ m/s}$$

Table. A-122. Experimental measurements

Time (min)	ppm	mV	I (A)
0	101.82	36.5	1.57
15	57.99	29.9	
30	40.87	25.8	
45	33.59	23.5	1.45
60	26.23	20.6	
80	15.99	14.8	1.35
100	8.88	7.9	
120	5.51	2.3	
140	3.56	-2.8	1.28
160	2.39	-7.5	
180	1.74	-11.2	
200	1.16	-16	1.24
210	0.93	-18.5	

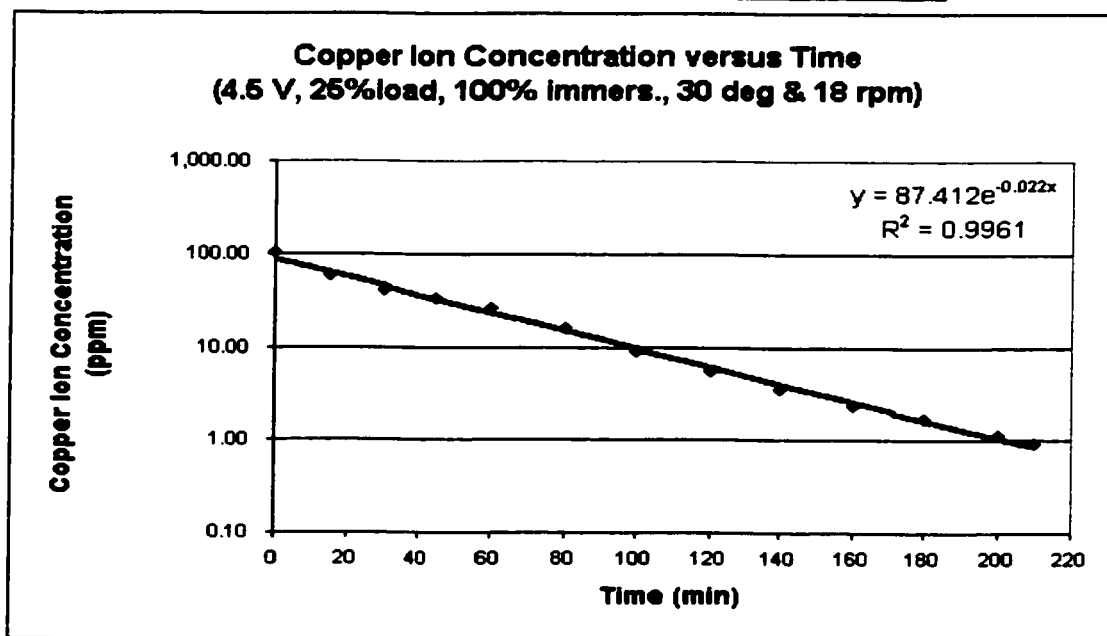


Figure. A-60. Copper ion concentration versus electrolysis time.

Table. A-123. Fixed operation parameters

Voltage (V)	4.52
Current (A)	0.95
Barrel load	25%
Barrel Immersion angle	30
Barrel Immersion percent	25%
Rotating speed (rpm)	18
water volume (lit.)	14
Na ₂ SO ₄ weight (g)	85.55
CuSO ₄ weight (g)	5.33

$$(\text{ppm})=4.526e0.0853*(\text{mV})$$

$$\text{area (25\%)}=0.2953 \text{ m}^2$$

$$V/A=0.04742 \text{ m}$$

$$k= 0.000986 \text{ m/min}$$

$$1.64E-05 \text{ m/s}$$

Table. A-124. Experimental measurements

Time (min)	ppm	mV	I (A)
0	109.95	37.4	0.95
15	71.77	32.4	
30	54.16	29.1	
60	25.14	20.1	0.92
80	13.49	12.8	
100	9.59	8.8	
120	6.59	4.4	0.83
155	5.51	2.3	0.8

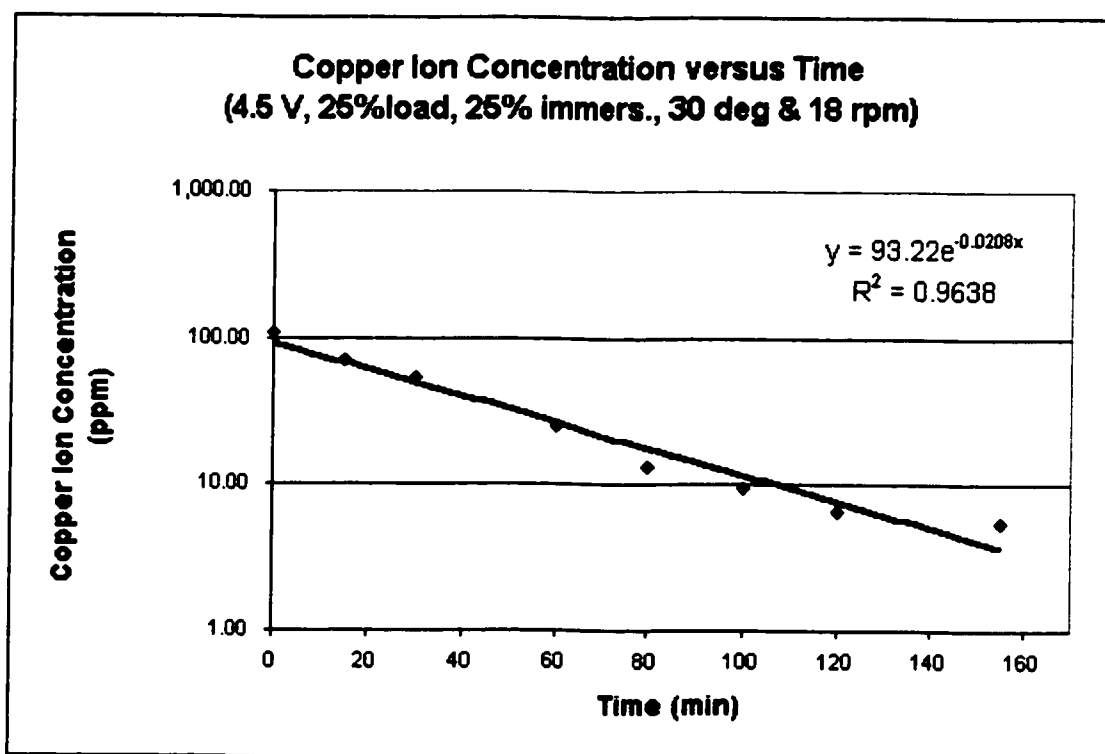


Figure. A-61. Copper ion concentration versus electrolysis time.

Anode Surface Area Effect

Table. A-125. Fixed operation parameters

Voltage (V)	4.52
Current (A)	0.88
Barrel load	50%
Barrel Immersion angle	30
Barrel Immersion percent	50%
Rotating speed (rpm)	18
water volume (lit.)	14
Na ₂ SO ₄ weight (g)	85.53
CuSO ₄ weight (g)	5.32
Temperature (C)	25
Anode Surface area (cm ²)	450

$$(\text{ppm}) = 5.646e0.0871 * (\text{mV})$$

$$\text{area (50\%)} = 0.5905 \text{ m}^2$$

$$V/A = 0.02371 \text{ m}$$

$$k = \begin{matrix} 0.000576 \text{ m/min} \\ 9.6E-06 \text{ m/s} \end{matrix}$$

Table. A-126. Experimental measurements

Time (min)	ppm	mV	I (A)
0	107.41	35.6	0.88
15	41.70	24.7	
30	46.28	25.9	
50	22.32	17.5	
70	15.64	13.4	0.8
90	14.46	12.5	
120	8.90	6.9	
140	3.06	-5.4	0.74
160	1.08	-17.4	

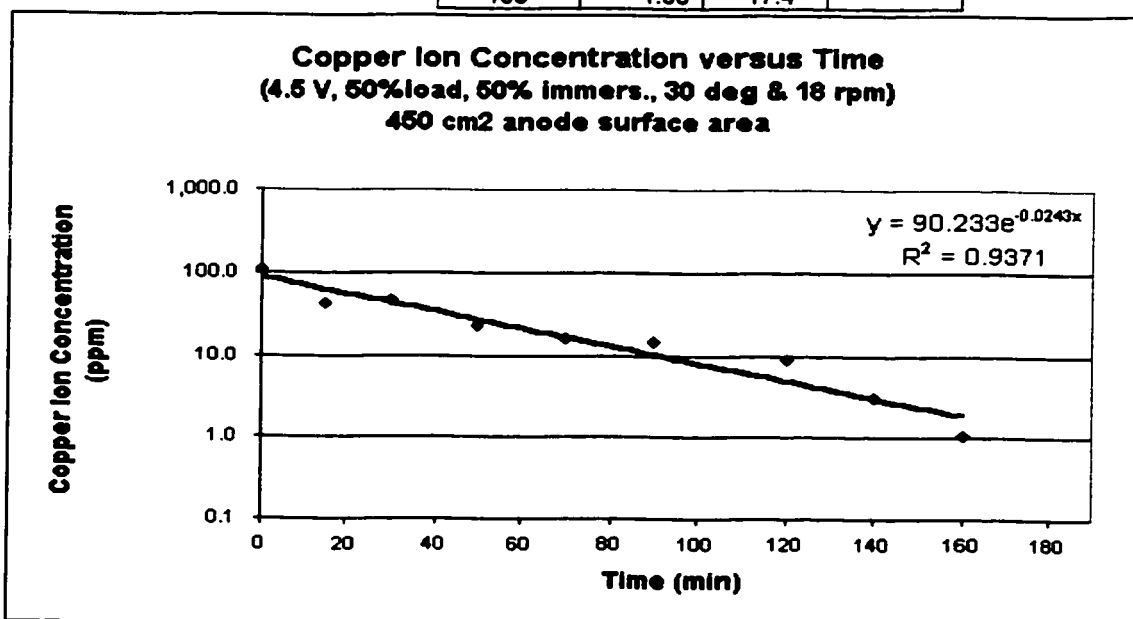


Figure. A-62. Copper ion concentration versus electrolysis time.

Table. A-127. Fixed operation parameters

Voltage (V)	4.51
Current (A)	1.4
Barrel load	50%
Barrel Immersion angle	30
Barrel Immersion percent	50%
Rotating speed (rpm)	18
water volume (lit.)	14
Na ₂ SO ₄ weight (g)	85.52
CuSO ₄ weight (g)	5.32
Anode Surface area (cm ²)	1125

$$(\text{ppm}) = 5.295e0.0849^*(\text{mV})$$

$$\text{area (50\%)} = 0.5905 \text{ m}^2$$

$$V/A = 0.02371 \text{ m}$$

$$k = 0.00083 \text{ m/min}$$

$$1.38E-05 \text{ m/s}$$

Table. A-128. Experimental measurements

Time (min)	ppm	mV	I (A)
0	108.76	35.6	1.4
15	44.22	25	
30	30.18	20.5	
45	22.81	17.2	1.25
65	14.54	11.9	
85	7.25	3.7	1.2
105	3.02	-6.6	
120	1.17	-17.8	1.18
130	0.88	-21.2	

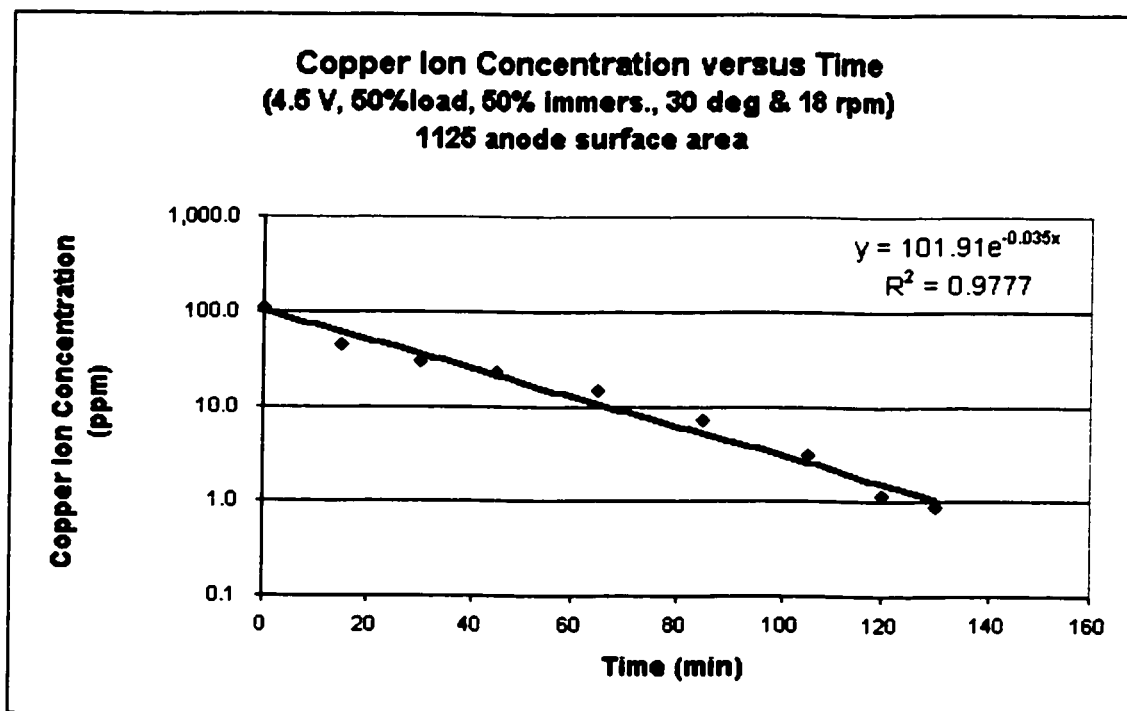


Figure. A-63. Copper ion concentration versus electrolysis time.

Table. A-129. Fixed operation parameters

Voltage (V)	4.51
Current (A)	1.05
Barrel load	50%
Barrel Immersion angle	30
Barrel Immersion percent	50%
Rotating speed (rpm)	18
water volume (lit.)	14
Na2SO4 weight (g)	85.58
CuSO4 weight (g)	5.33
Anode Surface area (cm ²)	675

$$(\text{ppm}) = 5.295e0.0849 \cdot (\text{mV})$$

$$\text{area (50\%)} = 0.5905 \text{ m}^2$$

$$V/A = 0.02371 \text{ m}$$

$$k = 0.000707 \text{ m/min}$$

$$1.18E-05 \text{ m/s}$$

Table. A-130. Experimental measurements

Time (min)	ppm	mV	I (A)
0	116.41	36.4	1.05
15	57.05	28	
30	38.28	23.3	1.05
45	32.58	21.4	
65	18.13	14.5	0.97
85	10.27	7.8	
105	6.12	1.7	0.93
125	2.78	-7.6	
145	1.07	-18.8	0.9

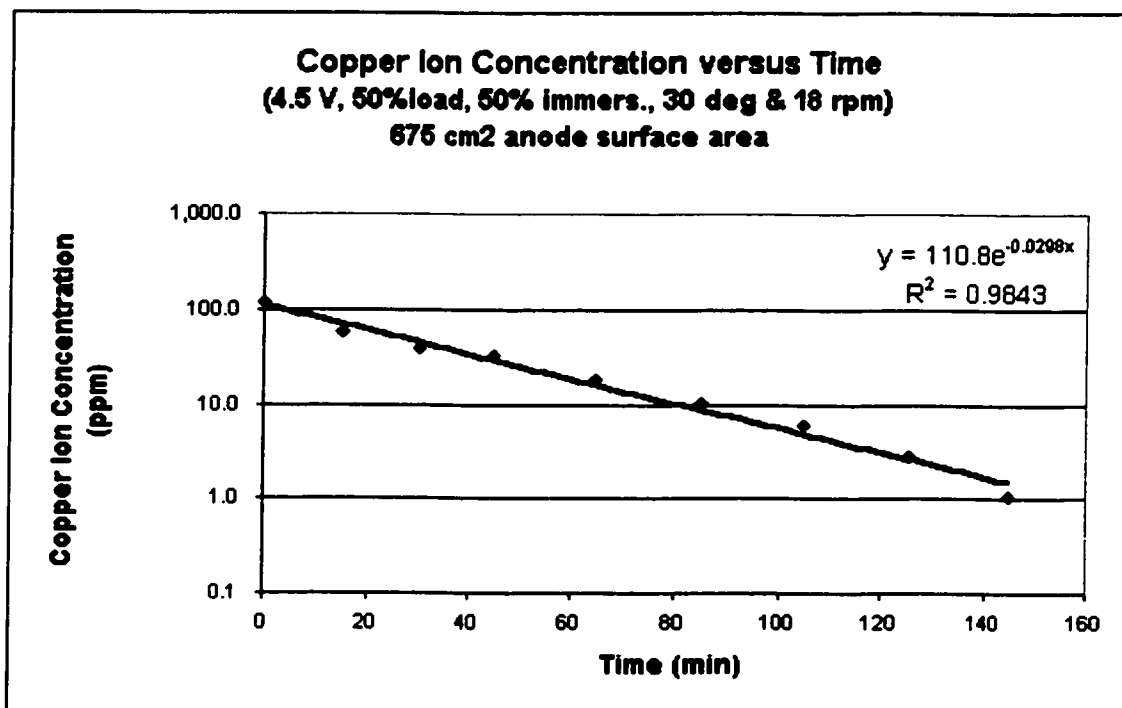


Figure. A-64. Copper ion concentration versus electrolysis time.

Table. A-131. Fixed operation parameters

Voltage (V)	4.5
Current (A)	1.26
Barrel load	50%
Barrel Immersion angle	30
Barrel Immersion percent	50%
Rotating speed (rpm)	18
water volume (lit.)	14
Na ₂ SO ₄ weight (g)	85.52
CuSO ₄ weight (g)	5.32
Temperature (C)	25
Anode Surface area (cm ²)	900

$$(\text{ppm}) = 5.295e0.0849 \cdot (\text{mV})$$

$$\text{area (50\%)} = 0.5905 \text{ m}^2$$

$$V/A = 0.02371 \text{ m}$$

$$k = 0.000825 \text{ m/min}$$

$$1.38E-05 \text{ m/s}$$

Table. A-132. Experimental measurements

Time (min)	ppm	mV	I (A)
0	112.52	36	1.26
15	60.54	28.7	
36	69.94	30.4	
50	49.80	26.4	1.21
70	19.74	15.5	
90	8.45	5.5	1.1
105	4.36	-2.3	
120	2.13	-10.7	1.08
137	0.97	-20	1.1

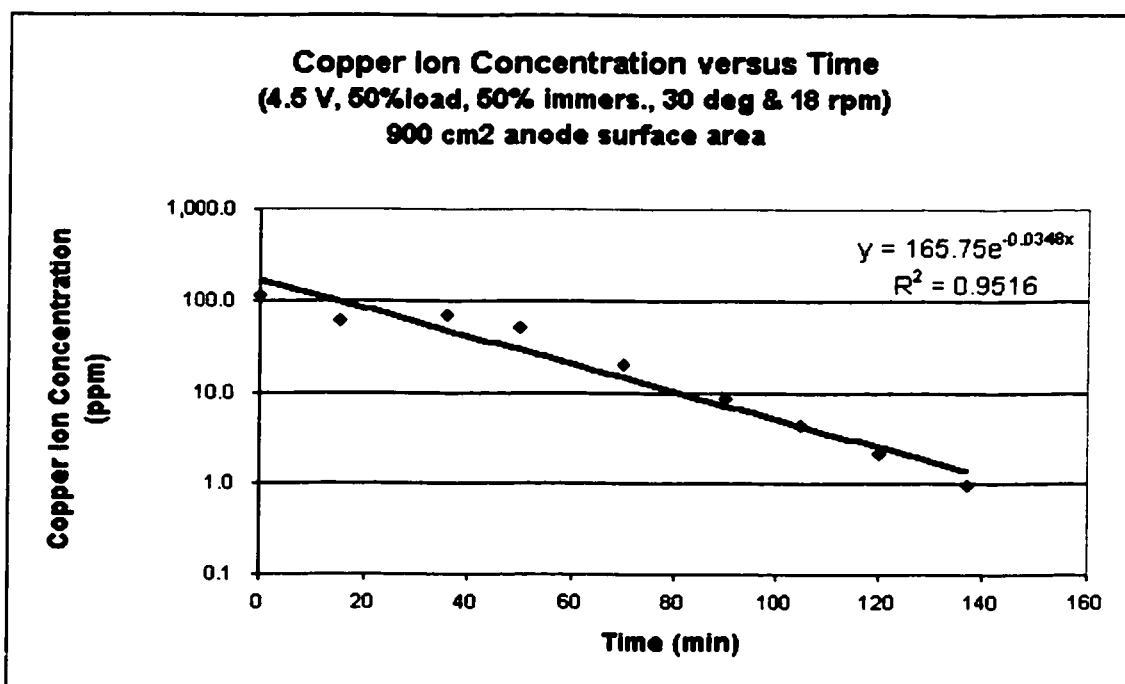


Figure. A-65. Copper ion concentration versus electrolysis time.

NOMENCLATURE

- A total copper particle surface area, m^2
- C copper concentration, mol/m^3
- C_0 initial copper concentration, mol/m^3
- D diffusivity of the copper ion in water, m^2/s
- d_p copper particle diameter, m
- d_b barrel diameter, m
- E anode-cathode cell voltage, V
- F Faraday constant, 96,500 C/equiv
- g gravitational acceleration, $9.8 m/s^2$
- Gr Grashof number, $\frac{g\rho_l(\rho_p - \rho_l)d_p^3}{\mu^2}$, dimensionless
- I cell current, A
- M atomic mass of copper, 63.5 g/mol
- n number of electrons transferred in the cathode deposition reaction, equal to 2 equiv/mol for copper deposition reaction.
- k reaction rate constant (apparent), m/s
- k_m mass transfer coefficient, m/s
- k_t true reaction rate constant, m/s
- Re Reynolds number, $\frac{d_p(d_b\Omega)\rho_l}{\mu}$, dimensionless
- Sc Schmidt number, $\frac{\mu}{\rho_l D}$, dimensionless
- Sh Sherwood number, $\frac{K_m d_p}{D}$, dimensionless
- t time, s

V_{sol}	solution volume, m^3
W	mass of copper removed, kg
α	empirical coefficient, in Eq. (7), dimensionless
β	empirical coefficient, in Eq. (7), dimensionless
γ	empirical coefficient, in Eq. (7), dimensionless
θ	total electrolysis time, s
Ω	barrel rotational speed, rad/s
ρ_l	solution density, kg/m^3
ρ_p	copper particle density, kg/m^3
μ	solution viscosity, kg/ms.

REFERENCES

Bennion, D., and Newman, J., " Electrochemical Removal of Copper Ions from Very Dilute Solutions", *Journal of Applied Electrochemistry*, 2,113,(1972).

Carlo, S., Panizza, M., and Paganelli, P., "Electrochemical Remediation of Copper (II) from an Industrial Effluent: Part I Monopolar Plate Electrodes", *Resources, Conservation and Recycling Journal*, 26, p. 115-124 (1999).

Chin. D.-T."Electrolytic Recovery of Metal from Wastewater". Report to U.S. National Science Foundation, Clarkson University, Potsdam, NewYork, 2000.

Chin, D. -T., and Zhou C.-D., "Copper Recovery and Cyanide Destruction with a Plating Barrel Cathode and a Packed-Bed Anode", *Plating and Surface Finishing*, vol. 80, p.69-77, June (1993).

Chin, D. -T., and Zhou C.-D., "Continuous Electrolytic of Complex Metal Cyanides With a Rotating Barrel Plater as the Cathode and a Packed Bed as the Anode ", *Plating and Surface Finishing*, vol 81, no.6, p.70-78, (1994).

Chin, D. -T., and Zhou C.-D., "Mass Transfer and Particle Motion in a Barrel plater ", *Journal of the Electrochemical Society*. vol 142, no. 6, p 1933-1941,(1995).

"Environmental Protection Rules; Discharge Regulations", *Meteorology and Environmental Protection Administration, Ministry of Defence and Aviation, Jeddah, Saudi Arabia*, 19-21, 1988.

Fleischmann, M., and Oldfield, J., and Timakoon, L., " Electrochemical Removal of Copper Ions by Use of a Fluidized bed Electrode", *Journal of Applied Electrochemistry*, p103-112,(1971a).

Frank, S. Holland." The Development of the Eco-Cell Process", *Chemistry and Industry Journal*, p 453-458., July, 1978.

Hinatsu, J. T., and Foulkes, F. R., " Electrochemical Kinetic Parameters for the Cathodic Deposition of Copper from Dilute Aqueous Acid Sulfate solutions ", *The Canadian Journal of Chem. Eng.*, Vol 69, p 571-576, April (1991).

Lidia, S., Francesco, Z.,and Santosh,N., " Copper Electrodeposition and Oxidation of Complex Cyanide from Wastewater in an Electrochemical Reactor with a Ti/Pt Anode" , *Industry and Engineering Chemistry Research*, 39, p 2132-2139, (2000).

Lobo, V.M." *Physical Sciences Data 41,Handout of Electrolyte Solutions – Part A* ". Elsevier Science Publisher, New York, U.S.A. (1989).

Palmer, S., Breton, M., Nunno,T., and Sullivan, D.," *Metal/Cyanide Contaning Wastes Treatment Technologies*", Noyes Data Corporation, Park Ridge,U.S.A. (1988).

Szpyrkowicz, L., Zilio-Grandi, F., and Kaul, S.," *Electrochemical Treatment of Copper Cyanide Wastewater Using Stainless steel Electrodes*", *Water Science and Technology*, vol.38,no. 6, p 261-268, (1998).

Tison Richard, " *Copper Recovery Using a Tumbled-Bed Electrochemical Reactor.*", *Journal of the Electrochemical society*. vol 128, p 317-322, Feb.,(1981)

Tison, R. P., Howie, B. "Copper Recover from Dilute Solutions Using a Barrel plater ", *Plating and Surface Finishing*, vol. 71, p 54-56, Sep, (1984).

Zhou, C-D," Electrolytic Treatment of Complex Metal Cynides and Mass Transfer study with a plating Barrel," Ph.D. Dissertation, Clarkson University, Postdam, NY, U.S.A., (1993).